

Characterization Well R-15 Completion Report



Los Alamos
NATIONAL LABORATORY

*Los Alamos National Laboratory is operated by the University of California
for the United States Department of Energy under contract W-7405-ENG-36.*

*Produced by the Environmental Restoration Project,
Groundwater Investigations Focus Area*

Cover photo shows a modified Foremost Dual Rotary (DR-24) drill rig. The DR-24 is one of several drill-rig types being used for drilling, well installation, and well development in support of the Los Alamos National Laboratory Hydrogeologic Workplan. The Hydrogeologic Workplan is jointly funded by the Environmental Restoration Project and Defense Programs to characterize groundwater flow beneath the 43-square-mile area of the Laboratory and to assess the impact of Laboratory activities on groundwater quality. The centerpiece of the Hydrogeologic Workplan is the installation of up to 32 deep wells in the regional aquifer.

An Affirmative Action/Equal Opportunity Employer

This report was prepared as an account of work sponsored by an agency of the United States Government. Neither The Regents of the University of California, the United States Government nor any agency thereof, nor any of their employees, makes any warranty, express or implied, or assumes any legal liability or responsibility for the accuracy, completeness, or usefulness of any information, apparatus, product, or process disclosed, or represents that its use would not infringe privately owned rights. Reference herein to any specific commercial product, process, or service by trade name, trademark, manufacturer, or otherwise, does not necessarily constitute or imply its endorsement, recommendation, or favoring by The Regents of the University of California, the United States Government, or any agency thereof. The views and opinions of authors expressed herein do not necessarily state or reflect those of The Regents of the University of California, the United States Government, or any agency thereof. Los Alamos National Laboratory strongly supports academic freedom and a researcher's right to publish; as an institution, however, the Laboratory does not endorse the viewpoint of a publication or guarantee its technical correctness.

***Characterization Well R-15
Completion Report***

Patrick Longmire

David Broxton

William Stone

Brent Newman

Robert Gilkeson

Jon Marin

David Vaniman

Dale Counce

David Rogers

Robert Hull

Steve McLin

Rick Warren

TABLE OF CONTENTS

1.0	INTRODUCTION	1
2.0	SUMMARY OF DRILLING ACTIVITIES	1
2.1	Equipment	1
2.1.1	Phase I Drilling.....	1
2.1.2	Phase II Drilling.....	3
2.2	Schedule	3
2.2.1	Phase I Drilling.....	3
2.2.2	Phase II Drilling.....	3
2.3	Production	4
2.3.1	Phase I Drilling.....	4
2.3.2	Phase II Drilling.....	4
2.3.3	Open-Borehole Drilling	5
2.3.4	Core Drilling	6
2.3.5	Casing Advancement.....	6
2.3.6	Other Drilling Activities.....	8
3.0	GEOLOGY	8
3.1	Stratigraphy and Lithology	8
3.1.1	Alluvium	8
3.1.2	Qbt 1g, Tshirege Member of the Bandelier Tuff and Tsankawi Pumice Bed	15
3.1.3	Volcaniclastic Sediments and Tephra of the Cerro Toledo Interval	15
3.1.4	Otowi Member of Bandelier Tuff	16
3.1.5	Upper Puye Formation.....	16
3.1.6	Late Pliocene Soil	16
3.1.7	Basaltic Rocks of the Cerros del Rio Volcanic Field	16
3.1.8	Lower Puye Formation.....	21
3.2	Axial River Gravels.....	25
3.3	Borehole Geophysics.....	25
3.3.1	Methods	25
3.3.2	Results	26
4.0	HYDROLOGY	30
4.1	Unsaturated Zone	30
4.1.1	Soil-Water Occurrence	30
4.1.2	Soil-Water Movement	32
4.2	Saturated Zones.....	33
4.2.1	Groundwater Occurrence	34
4.2.2	Groundwater Movement	36
5.0	HYDROGEOCHEMISTRY	38
5.1	Geochemistry of Core and Cutting Samples Collected During Phase I Drilling	39
5.1.1	Methods	39
5.1.2	Radionuclides, Percent Organic Carbon, and Inorganic Analytes	40
5.1.3	Stable Isotopes and Distributions of Anions	47
5.2	Hydrogeochemistry of Groundwater Samples	58
5.2.1	Methods	59
5.2.2	Major Ion and Trace Element Chemistry	60
5.2.3	Summary of Groundwater Geochemistry	66

6.0	WASTE MANAGEMENT	67
7.0	SURVEY ACTIVITIES	68
7.1	Geodetic Survey.....	68
7.2	Surface Radiological Survey	68
8.0	WELL DESIGN, CONSTRUCTION, AND DEVELOPMENT	69
8.1	Well Design	69
8.2	Well Construction	69
8.3	Well Development	69
8.4	Pump Installation.....	69
8.5	Wellhead Protection	72
9.0	SITE RESTORATION.....	72
10.0	MODIFICATIONS TO WORK PLANS	72
11.0	IMPLICATIONS FOR CONCEPTUAL GEOLOGIC, HYDROGEOLOGIC, AND GEOCHEMICAL MODELS	79
12.0	RESPONSIBILITIES	82
13.0	REFERENCES	83

Appendixes

Appendix A Lithologic Log

Appendix B Descriptions of Geologic Samples

Appendix C Moisture and Matric-Potential Results

List of Figures

Figure 1.0-1	Locations of R-15, existing water supply wells and test wells, and generalized water-level contours for the regional aquifer	2
Figure 2.3-1	R-15 borehole configuration at total depth.....	7
Figure 3.1-1	West-to-east geologic cross section through wells TW-8, R-15, and R-12	9
Figure 3.1-2	Comparison of actual and predicted geologic contacts in R-15	10
Figure 3.1-3a	Variations in SiO ₂ , K ₂ O/P ₂ O ₅ , Sr, and Mg# in the Cerros del Rio basalts of drill hole R-15	18
Figure 3.1-3b	Variations in SiO ₂ , K ₂ O/P ₂ O ₅ , Sr, and Mg# in the Cerros del Rio basalts of drill holes R-15 and R-12.....	19
Figure 3.1-4	Distributions of sediment-sized fractions for samples from the lower Puye Formation at R-15.....	22
Figure 3.1-5	Variations in SiO ₂ , Fe, Sr, and Cr in two size fractions of the Puye Formation sediments at R-15.....	24
Figure 3.3-1	Natural gamma measurements in borehole R-15.....	27
Figure 3.3-2	Open-borehole natural gamma, conductivity, and resistivity measurements in R-15	28

Figure 3.3-3	Variation of gravimetric moisture content and matric potential with depth in R-15.....	29
Figure 4.1-1	Variations of gravimetric moisture content with depth in R-15, MCM-5.1, and MCM-5.9	31
Figure 4.1-2	Gravimetric moisture and matric potential for Tshirege Member Unit Qbt 1g in borehole R-15	34
Figure 4.2-1	Hydrograph based on transducer data collected from August 31, 1999, to September 7, 1999, for the regional aquifer prior to well completion	36
Figure 5.1-1	Variations in the concentrations of iron, barium, beryllium, chromium, and lead with depth from core samples collected in R-15, Mortandad Canyon	46
Figure 5.1-2	Pore water $\delta^{18}\text{O}$ profile for borehole R-15	48
Figure 5.1-3	Pore water $\delta^{18}\text{O}$ profile for borehole R-15 and MCO-7.2	49
Figure 5.1-4	Pore water fluoride, nitrate, and sulfate concentrations for borehole R-15	50
Figure 5.1-5	Pore water chloride, oxalate, and phosphate concentrations for borehole R-15.....	51
Figure 5.1-6	Pore water nitrate and sulfate concentrations for borehole MCO-7.2	52
Figure 5.1-7	Pore water chloride, fluoride, bromide, and phosphate concentrations for borehole MCO-7.2	53
Figure 5.1-8	Pore water nitrate and perchlorate concentrations for borehole R-15.....	56
Figure 5.1-9	Pore water nitrate and perchlorate concentrations for borehole MCO-7.2.....	57
Figure 8.2-1	As-built well completion diagram of well R-15	70
Figure 8.3-1	Changes in turbidity as a function of time and water removed during pumping.....	71
Figure 8.5-1	Well R-15 wellhead diagram.....	73

List of Tables

Table 2.2-1	Phase I Drilling Shift Information	3
Table 2.2-2	Phase II Drilling Shift Information	4
Table 2.3-1	Preliminary Performance Statistics.....	5
Table 2.3-2	Footage Intervals Drilled with Lubrication Slurry	6
Table 3.1-1	Quantitative X-Ray Diffraction Analyses of Samples from Drill Hole R-15.....	11
Table 3.1-2	Quantitative X-Ray Diffraction Analyses of Puye Size Separates from Drill Hole R-15.....	12
Table 3.1-3	Chemical Analyses of Igneous Lithologies and Cerro Toledo Sediments from Drill Hole R-15.....	13
Table 3.1-4	Chemical Analyses of Puye Formation Size Fractions from Drill Hole R-15	14
Table 3.1-5	Weight Fractions of the >4-mm-, 2- to 4-mm-, and <2-mm- Sediment-Sized Fractions of the Puye Formation at Drill Hole R-15	21
Table 5.1-1	Radionuclide Activities in Samples of Core and Cuttings from Borehole R-15	41
Table 5.1-2	Tritium Activities and Moisture Contents in R-15 Core Samples.....	45
Table 5.1-3	R-15 Anion Pore Water Concentrations	54
Table 5.1-4	MCO-7.2 Anion Pore Water Concentrations	55
Table 5.1-5	Nitrate Pore Water and Cumulative Concentrations for Five Boreholes	58
Table 5.2-1	Field-Measured Parameters for Groundwater Samples Collected at R-15	60

Table 5.2-2	Hydrochemistry of Borehole R-15, Mortandad Canyon.....	61
Table 5.2-3	Tritium Activity in Groundwater Zones at R-15.....	65
Table 5.2-4	Radionuclide Activities in Filtered and Nonfiltered Groundwater Samples from Borehole R-15.....	66
Table 7.1-1	Geodetic Data for Well R-15.....	68
Table 10.0-1	Activities Planned for R-15 Compared with Work Performed.....	74

List of Acronyms and Abbreviations

ASTM	American Society for Testing and Materials
bgs	below ground surface
cpm	counts per minute
cps	counts per second
CVAA	cold vapor atomic absorption
DO	dissolved oxygen
DOC	dissolved organic carbon
DOE	US Department of Energy
DR	dual rotation
EPA	US Environmental Protection Agency
ER	environmental restoration
FSF	field support facility
FY	fiscal year
GFAA	graphite furnace atomic absorption
HE	high explosive
HSA	hollow-stem auger
IC	ion chromatography
ICPES	inductively coupled plasma emission spectroscopy
ICPMS	inductively coupled plasma mass spectrometry
I.D.	inside diameter
IRMS	isotope ratio mass spectrometry
LIKPA	laser-induced kinetic phosphorimetric analysis
LOI	loss on ignition
LSC	liquid scintillation counting
MDA	minimum detectable activity
NGR	natural gamma radiation
NMED	New Mexico Environment Department
NTU	nephelometric turbidity unit
O.D.	outside diameter
PCB	polychlorinated biphenyl

PID	photoionization detector
PPE	personal protective equipment
ppm	parts per million
PVC	polyvinyl chloride
QXRD	quantitative x-ray diffraction
RC	reverse circulation
RCT	radiological control technician
SVOC	semivolatile organic compound
TA	technical area
TD	total depth
TW	test well
UTL	upper tolerance limit
VOC	volatile organic compound
WCSF	waste characterization strategy form
XRF	x-ray fluorescence

Metric to English Conversions

Multiply SI (Metric) Unit	by	To Obtain US Customary Unit
kilometers (km)	0.622	miles (mi)
kilometers (km)	3281	feet (ft)
meters (m)	3.281	feet (ft)
meters (m)	39.37	inches (in.)
centimeters (cm)	0.03281	feet (ft)
centimeters (cm)	0.394	inches (in.)
millimeters (mm)	0.0394	inches (in.)
micrometers or microns (μm)	0.0000394	inches (in.)
square kilometers (km^2)	0.3861	square miles (mi^2)
hectares (ha)	2.5	acres
square meters (m^2)	10.764	square feet (ft^2)
cubic meters (m^3)	35.31	cubic feet (ft^3)
kilograms (kg)	2.2046	pounds (lb)
grams (g)	0.0353	ounces (oz)
grams per cubic centimeter (g/cm^3)	62.422	pounds per cubic foot (lb/ft^3)
milligrams per kilogram (mg/kg)	1	parts per million (ppm)
micrograms per gram ($\mu\text{g/g}$)	1	parts per million (ppm)
liters (L)	0.26	gallons (gal.)
milligrams per liter (mg/L)	1	parts per million (ppm)
degrees Celsius ($^{\circ}\text{C}$)	$9/5 + 32$	degrees Fahrenheit ($^{\circ}\text{F}$)

CHARACTERIZATION WELL R-15 REPORT

by

**Patrick Longmire, David Broxton, William Stone, Brent Newman, Robert Gilkeson, Jon Marin,
David Vaniman, Dale Counce, David Rogers, Robert Hull, Steve McLin, Rick Warren**

ABSTRACT

Characterization well R-15 is located in Mortandad Canyon immediately southeast of the sediment traps within Technical Area (TA) 5, Los Alamos National Laboratory (the Laboratory). This characterization well is the fourth of approximately 32 wells being installed in the regional aquifer as part of the Laboratory's "Hydrogeologic Workplan" (LANL 1998, 59599). R-15 was funded by the Laboratory's Environmental Restoration (ER) Project and is primarily designed to provide geologic, hydrologic, geochemical, and water-level data for potential intermediate-depth perched zones and for the regional saturated zone. Well R-15 is downgradient of multiple contaminant source areas that include release sites in the Mortandad Canyon and possibly upper Sandia Canyon and Los Alamos Canyon watersheds through paleocanyon flow at depth.

R-15 was drilled in two phases; the first phase consisted of using a hollow-stem auger method to drill to a depth of 420 ft within the Otowi Member of the Bandelier Tuff. Phase I was conducted during September 1998. The second phase of drilling commenced in June 1999 using air-rotary methods assisted by the use of drilling mud between the casing and borehole wall. The total depth of the R-15 borehole is 1107 ft. The borehole was backfilled to a depth of 1030 ft and completed with a single-screen well in the Puye Formation.

In descending order, geologic units penetrated in R-15 included alluvium, the Tshirege Member of the Bandelier Tuff, tephra and volcanoclastic sediments of the Cerro Toledo interval, the Otowi Member of the Bandelier Tuff, the fanglomerate facies of the Puye Formation, basaltic rocks of the Cerros del Rio volcanic field, more Puye fanglomerate, and the axial Rio Grande facies of the Puye Formation (Totavi Lentil).

No perched water was encountered in the Cerro Toledo interval or Guaje Pumice Bed. However, a perched zone of saturation was found to occur between the depths of approximately 646 and 740 ft in the Cerros del Rio basalt. A clay-rich zone at the base of the basalt appears to be the perching layer. A slug test of this interval yielded a value for hydraulic conductivity of 2.54×10^{-7} cm/sec, which is at the lower end of the range typical of silt. The top of the regional zone of saturation lies at a depth of 964 ft in the Puye Formation.

A 46-hr aquifer-pumping test was conducted at well R-15 (regional aquifer) on February 19–20, 2000. Water levels were recorded while water was pumped at a constant rate of 11.7 gpm. The screened interval is located between 958.6 and 1020.3 ft below ground surface within the Puye Formation. Drawdown and recovery data were analyzed to determine characteristic values for transmissivity and storage coefficient. Test results suggest that the regional aquifer at well R-15 behaves like a leaky confined aquifer. Overall, an average transmissivity of about $123.4 \text{ ft}^2/\text{day}$ and a storage coefficient of about 0.0025 were determined for the Puye Formation from this pumping test. The corresponding average hydraulic conductivity over the R-15 screened interval is about $2.06 \text{ ft}/\text{day}$, or about $0.00117 \text{ cm}/\text{sec}$.

Twenty-four core samples were analyzed for radionuclides, metals, nonmetals, and percent organic carbon collected during Phase I. Tritium is the only anthropogenic radionuclide present in the core samples analyzed during Phase I investigations. One core sample was collected during Phase II

investigations and was analyzed for radionuclides, metals, and nonmetals. Distributions of nitrate and perchlorate obtained from core leaching tests suggest that these two anions are anthropogenic in origin.

Groundwater samples were collected from a perched zone at a depth of 646 ft and in the regional zone of saturation at depths of 1007 (screening analyses only) and 1100 ft, respectively. A sample of drilling mud was collected from a zone of possible saturation at 482 ft in the upper section of the Puye Formation and analyzed for tritium. The groundwater samples collected from depths of 646 and 1100 ft were chemically characterized for high explosive compounds, major ions, trace elements, dissolved organic carbon, stable isotopes, tritium, and other radionuclides. Analytical methods recommended by both the US Environmental Protection Agency and the Laboratory were followed for groundwater (filtered and nonfiltered) and core samples.

Strontium-90, cesium-137, plutonium-238, plutonium-239,240, and neptunium-237 were not detected in the groundwater samples collected from R-15. Americium-241, however, was detected (0.123 ± 0.052 and 0.207 ± 0.078 pCi/L) in replicate nonfiltered groundwater samples collected from the perched zone. Additional groundwater sampling and analyses are required to verify the preliminary activities of this radionuclide observed at R-15. Activities of uranium-234, uranium-235, and uranium-238 were detected slightly above background in the groundwater samples. Higher activities of the uranium isotopes were measured in the nonfiltered groundwater samples because naturally occurring uranium occurs within the bentonite drilling mud and aquifer materials. Concentrations of total (nonisotopic) dissolved uranium are 1.10 and 1.29 $\mu\text{g/L}$ within the perched zone for the two replicate groundwater samples. Activities of gross alpha, gross beta, and gross gamma in nonfiltered groundwater samples exceed those activities measured in filtered samples. Gross alpha and gross gamma activities are associated with isotopes within the uranium-238, uranium-235, and thorium-232 decay chains, whereas gross beta activities probably are associated with potassium-40 present in the bentonite drilling mud.

Groundwater from the perched zone in R-15 is dominantly a sodium-calcium-bicarbonate type as represented by screening and fixed laboratory samples collected at a depth of 646 ft. This perched groundwater was found to contain 3770 ± 850 pCi/L tritium, 12 parts per billion (ppb) dissolved perchlorate, 11.5 parts per million (ppm) dissolved chloride, 63.9 ppm dissolved sodium, 1.15 ppm dissolved fluoride, 35.4 ppm dissolved sulfate, <0.02 ppm dissolved ammonium, and <0.01 ppm nitrate (as nitrate). This groundwater sample contained bentonite drilling mud, which biased the major ion and trace element chemistry. Concentrations of nonsorbing solutes such as sulfate, nitrate, perchlorate, chloride, fluoride, and tritium of this perched zone are similar to those of the TA- 50 treated discharge water and alluvial groundwater in Mortandad Canyon.

Groundwater near the top of the regional saturated zone (1007 ft) is a sodium-bicarbonate type with a total dissolved solids content of 243 ppm. The major cation and anion chemistry of this water should be similar to groundwater in test well 8 (calcium-sodium-bicarbonate type) 1 km upstream of R-15. However, the bentonite mud used during drilling has biased the major ion chemistry resulting in an increase in sodium concentrations. Activities of tritium were measured in the regional aquifer, using three different analytical-counting methods. Activities of tritium, using a liquid scintillation method, in the regional saturated zone are 220 ± 620 pCi/L with minimum detectable activity of 440 pCi/L. The activity of tritium is 3.19 ± 9.58 pCi/L using direct counting, a more sensitive method (data provided by New Mexico Environment Department's Department of Energy Oversight Bureau; analyses performed by the University of Miami). Activities of tritium are less than detection in the groundwater samples using liquid scintillation counting and direct counting methods. Low activities of tritium (1.12 pCi/L) were detected in the regional aquifer at R-15 at 1100-ft depth using the electrolytic enrichment method at the University of Miami, which is the most sensitive of the three methods used. The concentration of nitrate (as nitrogen) is 1.53 ppm (6.71 ppm nitrate as nitrate), which is elevated above background for the regional groundwater in the Pajarito Plateau area.

1.0 INTRODUCTION

This report describes the drilling, well completion, and testing activities for characterization well R-15. R-15 is located in middle Mortandad Canyon, in Technical Area (TA) 5, within Los Alamos National Laboratory (the Laboratory) (Figure 1.0-1). This well was installed by the Canyons Focus Area of the Environmental Restoration (ER) Project as part of groundwater investigations required by the Mortandad Canyon Work Plan (LANL 1997, 56835). It also satisfies requirements to install a well in the regional aquifer as part of the "Hydrogeologic Workplan" (LANL 1998, 59599) in support of the Laboratory's "Groundwater Protection Management Program Plan" (LANL 1995, 50124).

R-15 primarily is designed to provide water quality, geologic, hydrologic, and geochemical data for potential intermediate-depth perched zones and for the regional aquifer downgradient of potential release sites in Mortandad Canyon watershed and possibly in Sandia Canyon and Los Alamos Canyon watersheds. R-15 is also sited to provide geologic, stratigraphic, hydrologic, and geochemical data that contribute to the understanding of the vadose zone and regional aquifer in this part of the Laboratory. Data collected from R-15 will be used in conjunction with data from other planned characterization boreholes as well as from other data sources to evaluate and update the sitewide hydrologic conceptual model.

Preliminary interpretations are presented for some of the data collected, but discussion of other data is deferred until they can be evaluated in the context of site-wide information collected from other ER Project and hydrogeologic work plan wells. Once all deep groundwater investigations in Mortandad Canyon are completed, the Mortandad Canyon deep groundwater aggregate report will update the geologic and hydrologic conceptual model for the watershed, evaluate potential contaminant transport pathways, and provide an integrated human-health and ecological risk assessment for groundwater use.

Although R-15 is primarily a characterization well, its design also meets the requirements of a monitoring well as defined in Module VIII of the Laboratory's Hazardous Waste Facility Permit. Incorporation of this well into a Laboratory-wide groundwater monitoring program will be evaluated at a later date when the results of this characterization activity are integrated with other groundwater investigations in the "Hydrogeologic Workplan" (LANL 1998, 59599).

2.0 SUMMARY OF DRILLING ACTIVITIES

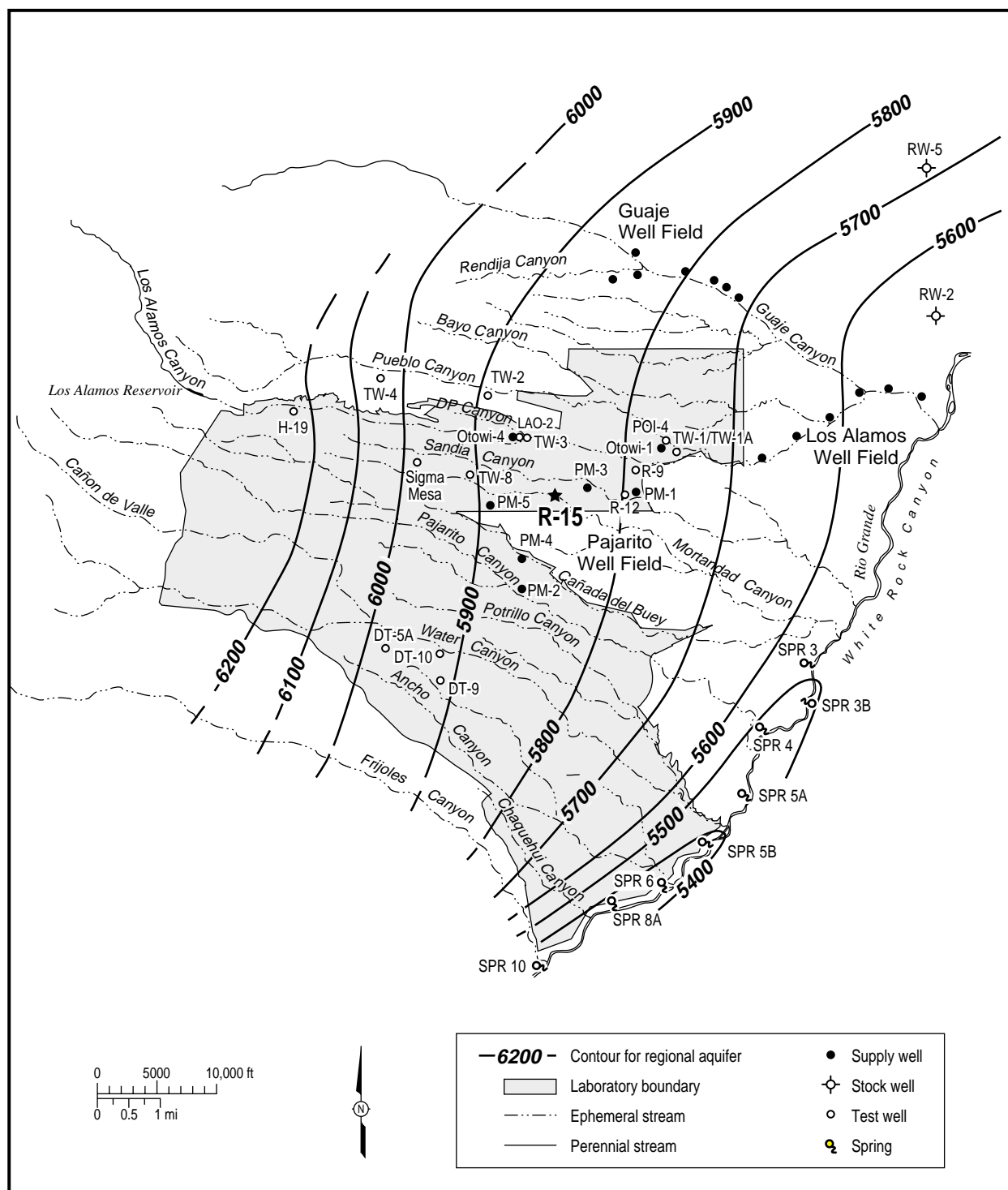
Phase I drilling at R-15 utilized the hollow-stem auger (HSA) drilling technique to drill a total of 420 ft below ground surface (bgs) and install surface casing to a depth of 135 ft bgs. The HSA borehole below the surface casing was back-filled with cuttings and the casing sealed at the surface during Phase I drilling.

R-15 Phase II drilling utilized an air rotary with casing-advance drilling technique to drill to a total borehole depth of 1107 ft. The casing-advance drilling method was assisted by the use of drilling mud behind the casing for lubrication. Installation of a permanent well took place after the borehole was completed.

2.1 Equipment

2.1.1 Phase I Drilling

Phase I drilling at R-15 was conducted by Stewart Brothers Drilling Company using a Failing F-10 drill rig, 4.25-in. inner diameter (I.D.) Truspin™ HSAs, 12-in.-I.D. HSAs, and a Moss™ wireline continuous-core retrieval system.



Source: Purtymun 1984, 6513.

F1.0-1 / R-15 WELL COMPLETION RPT / 062900 / PTM

Figure 1.0-1. Locations of R-15, existing water supply wells and test wells, and generalized water-level contours for the regional aquifer

2.1.2 Phase II Drilling

Phase II drilling at R-15 was performed by Dynatec Drilling Company, Inc. (formerly Tonto Drilling Company), using a customized Foremost™ dual rotation (DR)-24 drill rig (formerly Barber™ drill rig). Dynatec provided three-man drilling crews (double shift), a four-man drilling crew (single shift), crew vehicles, drilling hammers and bits, the Longyear 134-mm core system and dual-wall rod systems, a 1-ton flatbed truck, and a 5-ton boom truck for handling casing, drill pipe, and heavy support apparatus such as hydraulic casing jacks.

The ER Project's field support facility (FSF) provided drill casings, drilling bits, a small front-end loader, the dust suppression system, field support trailers including logging and sampling, water containment tanks, drums for cuttings management, depth-to-water meter, water sampling bailers, and diesel-powered electric generators. The Laboratory's Environmental Technology Group (E-ET) provided onsite water sample testing and filtering apparatus. The Geology and Geochemistry Group (EES-1) provided a core logging microscope. The Water Quality and Hydrology Group (ESH-18) provided a downhole pressure transducer and electronic data logger.

Science and Engineering Associates (SEA) of Santa Fe, New Mexico, provided real-time measurements of moisture and relative humidity of drilling air during air-rotary drilling, and a packer test apparatus for use in saturated intervals.

2.2 Schedule

2.2.1 Phase I Drilling

During Phase I drilling, the Failing F-10 drill rig was mobilized to R-15 on September 10, 1998, and it was demobilized on October 1, 1998. Drilling operations required 16 drilling shifts. Table 2.2-1 compares the actual number of shifts with the number of shifts projected for R-15 Phase I in planning documents.

Table 2.2-1
Phase I Drilling Shift Information

Number of shifts	Field Implementation Plan	Actual
	13 12-hr shifts	16 11-hr shifts

Drilling shifts averaged 11 hr each, depending on production needs.

2.2.2 Phase II Drilling

During Phase II, the DR-24 drill rig was mobilized to R-15 on June 8, 1999, and it was demobilized on September 7, 1999. Drilling operations, including well completion, required 72 drilling shifts. Table 2.2-2 compares the actual number of shifts with the number of shifts projected for R-15 Phase II drilling in planning documents.

Table 2.2-2
Phase II Drilling Shift Information

	Field Implementation Plan	Actual
Number of shifts	62 12-hr shifts	72 12-hr shifts

Drilling shifts averaged 12 hr each, depending on production needs.

2.3 Production

2.3.1 Phase I Drilling

During Phase I drilling, R-15 was continuously cored from the surface to refusal at 420 ft using 4.25-in.-I.D. Truspin™ HSAs with a Moss™ wireline continuous-core retrieval system. Using the in-place 4.25-in. HSA string as a guide, the borehole was reamed by 12-in.-I.D. HSAs from the surface to 125 ft. As the 4.25-in. auger string was withdrawn, the borehole was backfilled with cuttings from 390 to 150 ft. Using a center bit and bentonite slurry, the 12-in. HSAs were advanced from 125 to 135 ft. The additional augering with the 12-in. HSAs brought the bentonite slurry up the borehole annulus and stabilized the borehole wall.

The 12-in. HSAs were removed and seven 16-in.-diameter steel casings were welded together as they were installed from a depth of 135 ft to a stickup of 5 ft above the ground surface. A cement slurry was tremied to 130 ft and rose approximately 10 ft inside and outside the casing. The casing was repeatedly raised and lowered to achieve a homogeneous cement seal. After the lower cement plug cured overnight, the borehole annular space around the casing was cemented to approximately 10 ft bgs.

The total footage drilled in Phase I by the HSA drilling technique was 555 ft. Phase I production statistics are summarized in Table 2.3-1.

2.3.2 Phase II Drilling

Drilling techniques used in Phase II of R-15 consisted of open-borehole drilling, air-rotary coring, and air-rotary under-reamer advance of two different casing strings. Changing drilling systems typically involved tripping-out one system, modifying the drilling head and/or circulation plumbing, and tripping-in another drilling system from the ground surface to the depth of operations. The total Phase II footage drilled by the different drilling techniques and casing sizes was 1181.3 ft. The total footage drilled does not include tripping footage for the various drill systems or casings. The total trip-in footage for Phase I and Phase II drilling was 12,576.0 ft, and the total trip-out footage was 15,051.7 ft. Phase II performance statistics are summarized in Table 2.3-1.

TORKease® polymer and EZ-MUD® bentonite slurries, mixed with community water obtained from Laboratory fire-protection hydrant number 64 located at TA-52, were utilized for 69% of the total borehole depth to lubricate the back side of the casing system during drilling and to prevent binding a casing string to the borehole wall or another casing string. Footage intervals for which lubricating slurry was used are indicated in Table 2.3-2.

Table 2.3-1
Preliminary Performance Statistics

Drilling Types	Phase I			Phase II							Total
	4.25-in.-I.D. HSA Core	12-in. HSA	16-in. Surface Casing	Open Hole System	Air-Rotary Core	13-5/8-in. Casing ^a	11-3/4-in. Casing ^a	7-in. Dual Wall Rods	4 1/2-in. Dual Wall Rods	B Rods	
Total footage drilled (ft)	420 ^b	135	— ^c	125.0	11.5 ^b	629.3	415.5	—	—	—	1,736.3 ^b
Total footage rate (ft/hr) ^d	18	12.4	—	20.9	0.5	25.8	22.2	—	—	—	—
Bandelier Tuff ^e footage (ft)	420	135	—	—	—	342.0	0	—	—	—	—
Bandelier Tuff ^e rate (ft/hr) ^d	18	12.4	—	—	—	21.9	NA	—	—	—	—
Basalt ^f footage (ft)	—	—	—	125.0	5.3	249.0	44	—	—	—	—
Basalt ^f rate (ft/hr) ^d	—	—	—	20.9	—	11.3	6.0	—	—	—	—
Puye ^g clastics footage (ft)	—	—	—	—	6.2	23.0	361.0	—	—	—	—
Puye ^g clastics rate (ft/hr) ^d	—	—	—	—	—	12.1	20.4	—	—	—	—
Cement footage (ft)	—	—	—	—	—	15.3	10.5	—	—	—	—
Cement rate (ft/hr)	—	—	—	—	—	4.5	2.3	—	—	—	—
Trip-in footage (ft)	405	—	135	—	740	130.0	1232.0	6162.0	2717.0	1055.0	12,576.0
Trip-in rate (ft/hr) ^d	49.1	—	33.8	—	161.5	104.0	106.4	391.2	429.30	—	—
Trip-out footage (ft)	835	135	—	—	751.5	735.6	1650.0	7103.0	2787.0	1055.0	15,051.7
Trip-out rate (ft/hr) ^d	97.5	54.0	—	—	300.4	—	—	316.6	428.8	—	—
Pull back footage (ft)	—	135	—	—	130.0	360.0	—	—	—	—	—
Permanent cement seal	—	—	1	—	—	—	—	—	—	—	—
Temporary casing seal (#)	—	—	—	—	—	2	—	—	—	—	—
Life-of-hole casing TD (ft)	—	—	135	—	—	735.6	1107.0	—	—	—	—

^a Holte 3-wing under-reamers for 13-5/8-in. and 11-3/4-in. casings, and Mitsubishi 2-wing under-reamer for 9-5/8-in. casing, using 7-in. reverse circulation (RC) rods.

^b Total depth (TD) of borehole is 1107 ft. Total cored footage (431.5 ft) is 39% of total borehole footage (1107 ft).

^c A dash in the table means "not applicable."

^d Rates are weighted averages over footages drilled or tripped, including breaks but excluding repairs and change out of tools.

^e Bandelier Tuff footage and rates include Cerro Toledo interval.

^f Basalt footage and rates include Cerros del Rio basalt and Santa Fe Group basalt.

^g Puye Formation footage and rates include old alluvium.

2.3.3 Open-Borehole Drilling

Phase I operations utilized the HSA drilling method. During Phase II drilling, open-borehole drilling was used to explore deeper sections of bedrock before coring or casing advancement. Dynatec drilled 125.0 ft of open borehole in basaltic rocks at an average rate of 20.9 ft/hr using a reverse circulation (RC) 44 (4 7/8-in.-I.D.) percussion hammer. Open-borehole drilling in the poorly consolidated sedimentary strata of the Puye Formation was not attempted because of concerns about borehole stability.

Table 2.3-2
Footage Intervals Drilled with Lubrication Slurry

Drilling Technique/Tools	Dry Footage Intervals (ft)	Footage Intervals with Lubrication Slurry (ft)
HSA/4.25-in.-I.D.	0–420	
HSA/12-in.-I.D.	0–125	
HSA/12-in.-I.D.		125–135
Air rotary/13 5/8-in. casing		135–420
Air rotary /13 5/8-in. casing	420–452	
Air rotary /13 5/8-in. casing		452–492
Air rotary /11 3/4-in. casing	492–538	
Air rotary /13 5/8-in. casing		538–610
Air rotary /Open-hole RC 44 hammer	610–740	
Air rotary /134 mm core	740–751.5	
Air rotary /11 3/4-in. casing	735–736.5	
Air rotary /11 3/4-in. casing		738–1107

2.3.4 Core Drilling

Core was collected in R-15 to provide undisturbed samples for geological, geochemical, contaminant, and hydrological characterization. In addition, core was used to identify perching layers beneath perched groundwater and to provide information for placing casing seals.

During Phase I drilling, continuous HSA core was collected from the surface to auger refusal at 420 ft. Average core recovery was 95%. During Phase II drilling, 11.5 ft of air-rotary core was collected from 420 to 1107 ft. The total amount of core collected during Phase I and Phase II drilling was 431.5 ft of core, or 39% of total borehole depth.

In R-15, average core recovery was 93.4% from 431.5 total ft cored in all intervals. Of the 431.5 ft cored, 420 ft were produced from the Bandelier Tuff at an average rate of 18 ft/hr and an average recovery of 95%; 5.3 ft were produced from basaltic rocks at an average rate of 1.0 ft/hr and average recovery of 47.2%; 6.2 ft were produced from sedimentary rocks at an average rate of 4.6 ft/hr and average recovery of 22.6%.

The HSA drilling method was set up for core retrieval during Phase I drilling. During Phase II drilling, a Longyear 134-mm coring system was used by converting the top head drive and circulation system of the Foremost™ DR-24 drill rig to operate the coring tools.

2.3.5 Casing Advancement

After the 16-in.-diameter surface casing was installed in Phase I drilling, multiple telescoped casing strings were installed during Phase II to advance the borehole and to prevent borehole collapse, maintain circulation of drilling fluids, and prevent perched water from communicating downhole as the borehole advanced (Figure 2.3-1). The multiple telescoped casings used during Phase II are retractable. Table 2.3-1 lists the casings and rates of advancement in different lithologic materials in R-15.

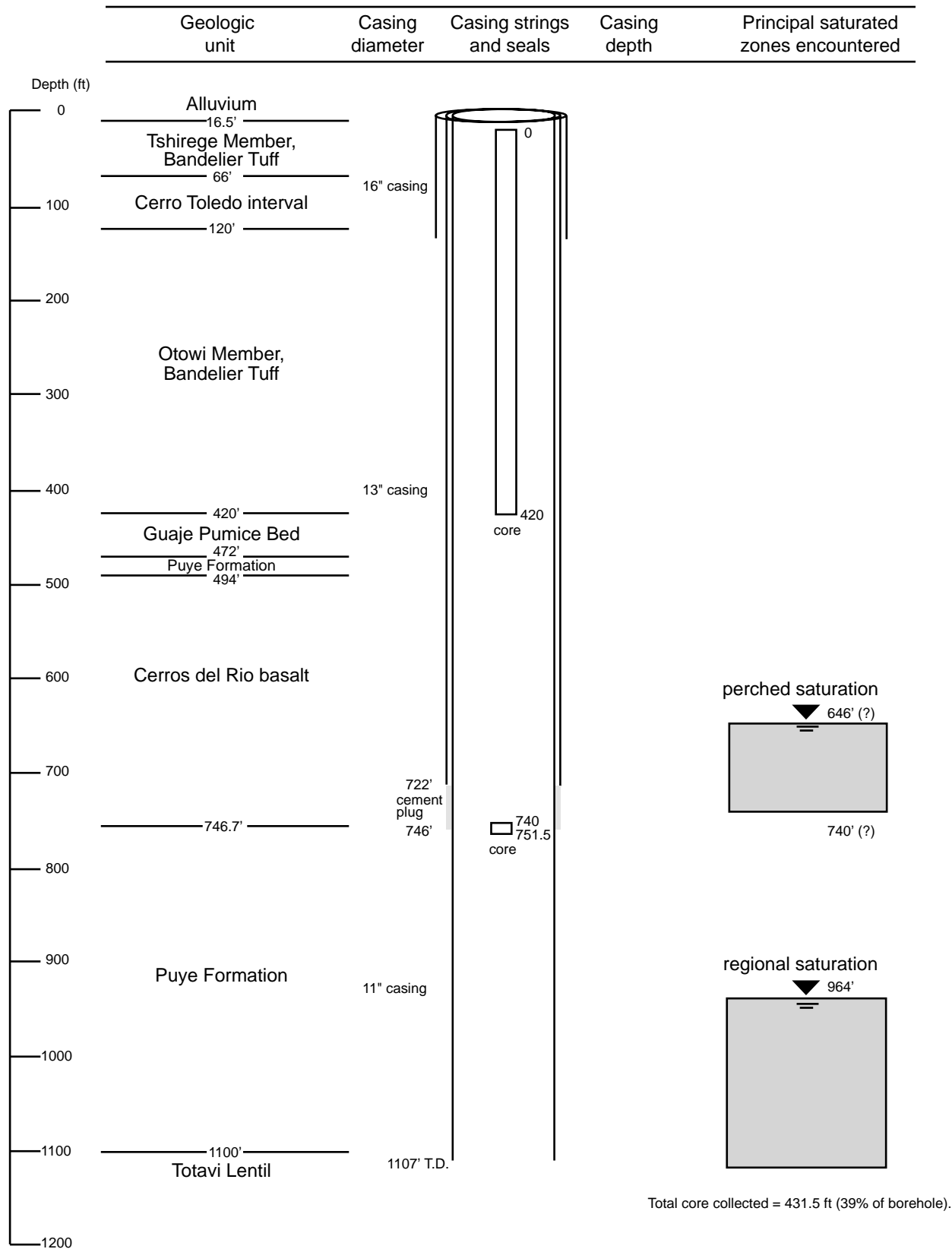


Figure 2.3-1. R-15 borehole configuration at total depth

2.3.6 Other Drilling Activities

Other drilling activities included conditioning and reaming the borehole with various casing strings to prevent locking up with other casings or the borehole wall. Activities such as cleaning clay cake from drill bits, casing, and air-circulation equipment during drilling of clay-rich rock units were minimized by injecting water, TORKease, EZ-MUD, and bentonite slurries during drilling to lubricate the casing system. Well completion involved installing a "B"-sized core rod string as a tremie line to deliver annular materials to the bottom of the borehole.

3.0 GEOLOGY

Geologic studies at R-15 can be viewed in the context of nearby drill-hole studies as shown in Figure 3.1-1. Based on the information from these drill holes and then-current geologic interpretation, the predicted geology at R-15, compared with the geology actually encountered, is shown in Figure 3.1-2. This comparison illustrates the impact of new data from R-15 on current understanding of site geology in this area.

3.1 Stratigraphy and Lithology

The principal geologic units encountered in R-15, in descending order, consist of alluvium; unit Qbt 1g of the Tshirege Member of the Bandelier Tuff, including the Tsankawi Pumice Bed; tephra and volcanoclastic sediments of the Cerro Toledo interval; the Otowi Member of the Bandelier Tuff, including the Guaje Pumice Bed; sediments of the Puye Formation; a thin late-Pliocene soil; basalts of the Cerros del Rio volcanic field; a sequence of Puye Formation sediments ranging from coarse fanglomerate to sandstones with pumice beds; and axial Rio Grande deposits (Totavi Lentil of Griggs 1964, 8795). These units and subunits within them are described in the lithologic log of Appendix A. Samples of representative lithologies were collected for further analysis; a listing and description of each of these samples is given in the geologic sample descriptions of Appendix B. All of the samples listed in Appendix B include descriptions obtained either by binocular microscope or by petrographic microscope using thin sections. A subset of these samples was analyzed by quantitative x-ray diffraction (QXRD); results of these analyses are listed in Tables 3.1-1 and 3.1-2 and are discussed throughout this section. Samples of representative volcanic and sedimentary lithologies were analyzed by x-ray fluorescence (XRF) for major and trace elements with results listed in Tables 3.1-3 and 3.1-4. The XRF data are referred to in relevant subsections of the text below.

Before R-15 was drilled, the lithologies predicted to occur at the site included intermediate-composition (latitic) lava (Tt2) and a lower Cerros del Rio basalt (Tb3) within the Puye Formation. These lavas were not encountered in R-15 (Figure 3.1-2). The absence of these lavas indicates a simpler depositional history for the Puye Formation in this part of the Laboratory. This new information will help in constraining the occurrence of lavas intercalated within the Puye Formation.

3.1.1 Alluvium (0- to 16.5-ft depth)

The alluvium at R-15 is pumiceous and contains abundant 1- to 2-mm crystals of quartz and chatoyant sanidine derived from exposures of the Bandelier Tuff. The alluvium consists predominantly of detritus from the Bandelier Tuff. No samples of the alluvium were collected for detailed characterization.

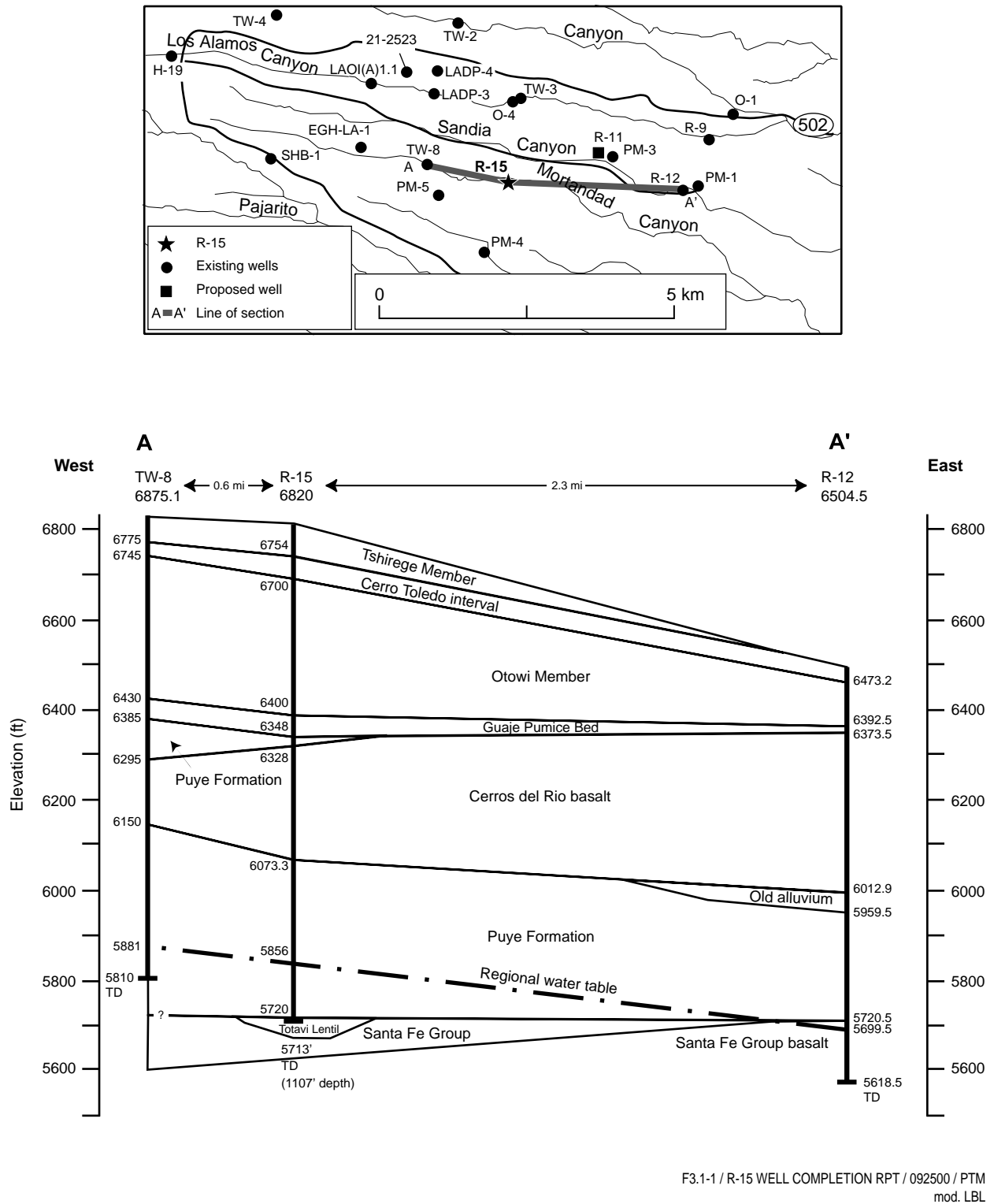
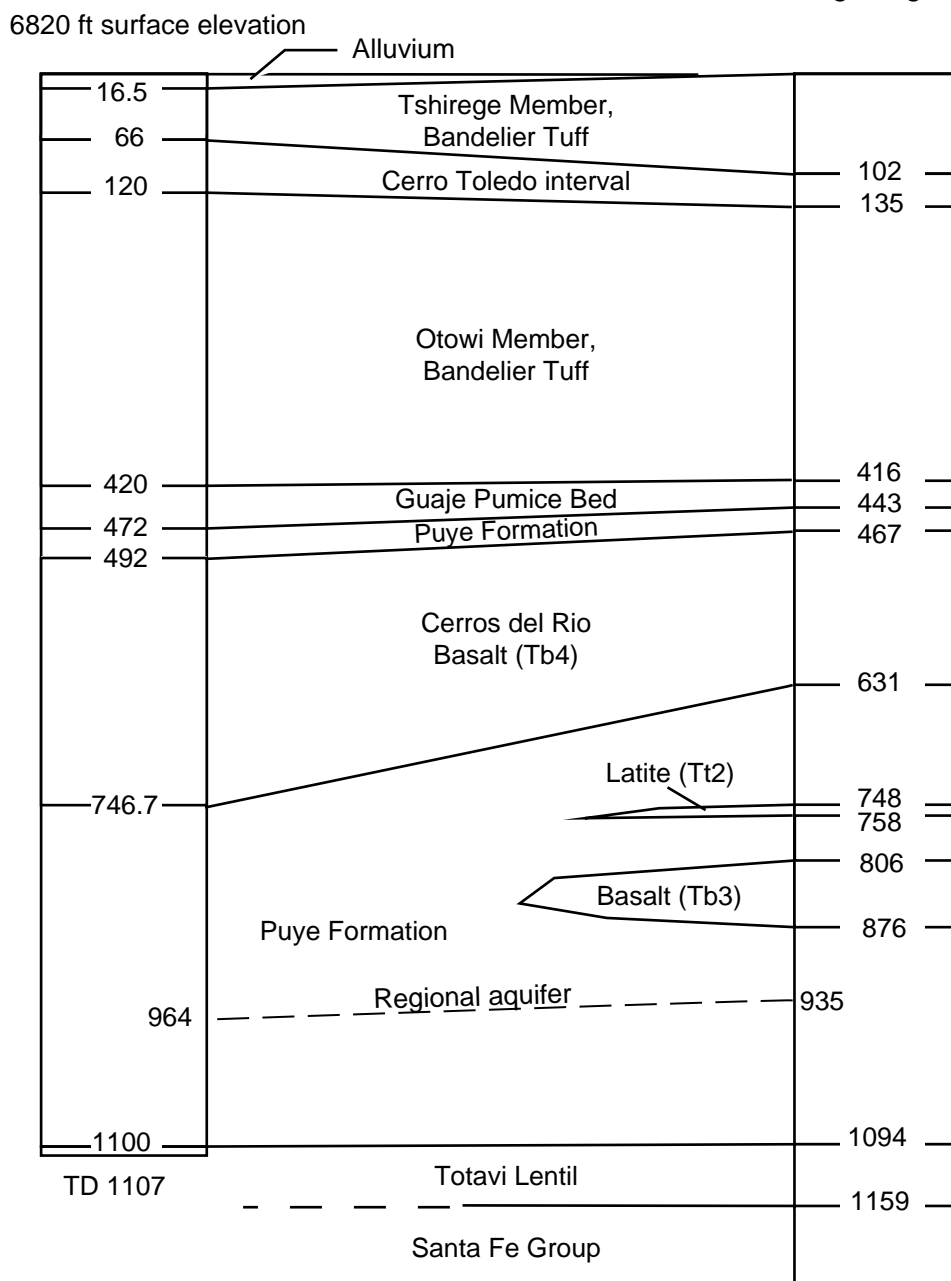


Figure 3.1-1. West-to-east geologic cross section through wells TW-8, R-15, and R-12

R-15 actual geology

R-15 predicted geology
from 3-D geologic model



Notes: 1. All depths in feet.
2. TD = total depth.

F3.1-2 / R-15 WELL COMPLETION RPT / 092500 / PTM
mod. LBL

Figure 3.1-2. Comparison of actual and predicted geologic contacts in R-15

Table 3.1-1
Quantitative X-Ray Diffraction Analyses of Samples from Drill Hole R-15

Sample, Unit, and Sample Type	Smectite	Kaolinite	Mica	Quartz	Cristobalite	Tridymite	Pyroxene	Olivine	Feldspar	Glass	Amphibole	Hematite	Magnetite	Total
R15-64.5, Otowi, core	— ^a	3	—	16	—	—	—	—	26	55	—	—	—	100
R15-69.5, Cerro Toledo, core	18 ^b	—	—	16	1	—	—	—	15	50	tr ^c	0.5	—	100
R15-74.5P7, Cerro Toledo, core	7 ^b	—	—	—	—	—	—	—	2.5	91	—	—	—	100
R15-532D, Cerros del Rio basalt, cuttings	15	1.2	—	—	—	—	20	2.3	59	—	—	0.8	3.5	101.8
R15-562D, Cerros del Rio basalt, cuttings	—	—	—	—	—	—	21	6.2	67	—	—	1.9	4.3	100.4
R15-577D, Cerros del Rio basalt, cuttings	14	2.1	—	—	—	—	24	2.2	56	—	tr	0.3	1.6	100.2
R15-610D, Cerros del Rio basalt, cuttings	—	—	—	—	—	—	22	6.6	67	—	—	0.8	2.9	99.3
R15-705D, Cerros del Rio basalt, cuttings	—	—	—	—	—	—	23	8.9	62	—	—	0.6	5.1	99.6
R15-740D, Cerros del Rio basalt, cuttings	—	—	—	—	—	—	27	13	54	—	tr	0.8	4.1	98.9
R15-740D, sandy fracture fill in basalt, cuttings	9	—	—	—	—	—	21	8.3	58	—	tr	0.5	2.9	99.7
R15-743.4, Cerros del Rio basalt, core	—	—	tr	—	—	—	23	12	57	—	—	1.5	6.8	100.3
R15-746, silty sand, cuttings	13	0.3	—	25	4	3	6	1.8	46	—	—	0.5	1.2	100.8

Notes: 1. Analytical errors (2σ) are ~5% of the amount reported for abundances >10%, ~10% of the amount reported for abundances <10%.

2. All values reported in weight percent.

^a A dash in the table means that the phase was not detected.

^b Clay composed principally of poorly crystalline smectite with possible admixed kaolinite, illite, and/or chlorite.

^c tr = trace (detected at <0.5 wt %).

Table 3.1-2
Quantitative X-Ray Diffraction Analyses of Puye Size Separates from Drill Hole R-15

Sample Depth (ft) and Size Range	Smectite	Kaolinite	Clinoptilolite	Mica	Quartz	Cristobalite	Tridymite	Feldspar	Glass	Hematite	Magnetite	Total
Coarse Fanglomerates												
772, >2 mm	2.5	—*	—	0.8	0.3	8.1	13.8	55.0	16.7	0.3	3.5	101.1
772, <2 mm	3.3	—	—	0.5	0.1	6.6	13.4	56.9	17.0	0.7	2.8	101.4
787, >2 mm	1.8	—	—	0.6	0.5	8.7	10.2	60.3	15.8	0.6	2.6	101.2
787, <2 mm	2.8	—	—	1.0	0.4	8.0	10.9	58.6	14.4	1.1	1.8	99.1
879, >2 mm	1.5	—	—	1.0	0.9	10.1	10.8	58.4	15.2	0.6	2.1	100.7
879, <2 mm	2.0	—	—	1.7	5.0	9.1	9.7	52.0	15.2	0.7	1.7	97.1
965, >2 mm	0.0	—	—	3.0	1.7	11.9	11.2	63.8	8.3	1.0	2.2	103.1
965, <2 mm	1.2	—	—	1.4	5.3	10.2	8.9	59.8	10.0	0.6	2.3	99.7
Pumiceous Sandstone												
979, >2 mm	1.8	—	—	1.1	1.6	10.0	9.2	53.3	21.3	0.8	1.5	100.7
979, <2 mm	1.6	—	—	0.7	3.7	7.9	8.6	48.6	26.4	0.5	1.8	99.8
Finer-Grained Sediments												
1037, >2 mm	3.0	—	—	0.7	1.4	4.5	2.0	37.6	48.3	0.3	1.1	99.0
1037, <2 mm	2.9	—	—	0.8	2.8	3.1	2.0	33.8	52.7	0.3	0.6	99.0
1099, >2 mm	4.0	0.6	—	1.2	10.9	5.0	2.0	48.4	22.9	1.2	2.6	98.8
1099, <2 mm	9.2	0.2	—	0.8	9.3	3.9	2.0	39.5	33.4	0.5	0.3	99.1
Totavi												
1103, >2 mm	8.0	—	—	3.0	6.8	5.0	3.0	58.8	12.8	0.6	1.3	99.3
1103, <2 mm	5.0	—	0.5	1.7	19.0	4.3	2.5	51.6	13.6	0.4	1.5	100.1

Notes: 1. Analytical errors (2σ) are ~5% of the amount reported for abundances >10%, ~10% of the amount reported for abundances <10%.

2. All values reported in weight percent.

3. Data provide comparison results for mineralogy in sediment fines ("very coarse sand" and finer, <2 mm grain size) and in coarser sediment constituents ("granule" and coarser, >2 mm grain size).

* A dash in the table means that the phase was not detected (detection limit ~0.1%).

Table 3.1-3
Chemical Analyses of Igneous Lithologies and Cerro Toledo Sediments from Drill Hole R-15

Sample No.	R15-64.5	R15-69.5	R15-74.5P7	R15-532D	R15-562D	R15-577D	R15-610D	R15-660D	R15-705D	R15-740	R15-787	R15-1009	R15-1067
Stratigraphic Unit	Tshirege unit Qbt 1g	Cerro Toledo	Cerro Toledo	Cerros del Rio basalt	Cerros del Rio basalt	Cerros del Rio basalt	Cerros del Rio basalt	Cerros del Rio basalt	Cerros del Rio basalt	Cerros del Rio basalt	Dacitic lava	Rhyolitic pumice	Rhyolitic pumice
Sample Type	core	core	core	cuttings	cuttings	cuttings	cuttings	cuttings	cuttings	core	cuttings	cuttings	cuttings
Alteration	unaltered	clay	clay	clay	unaltered	clay	unaltered	unaltered	unaltered	unaltered	unaltered	unaltered	unaltered
SiO ₂ %	76.0	72.3	72.0	50.5	51.6	50.5	51.1	49.2	50.7	48.0	65.7	73.0	73.5
TiO ₂ %	0.07	0.34	0.15	1.47	1.49	1.43	1.45	1.66	1.67	1.75	0.56	0.12	0.11
Al ₂ O ₃ %	12.6	14.6	14.5	16.3	16.2	15.9	16.0	16.1	15.9	15.5	14.7	11.8	12.3
FeO %	NA ^a	NA	NA	NA	NA	NA	NA	6.42	NA	7.18	1.66	NA	NA
Fe ₂ O ₃ % ^b	1.57	2.35	1.39	11.16	11.43	11.40	11.60	3.70	11.09	3.18	2.33	0.73	0.66
MnO %	0.09	0.10	0.06	0.13	0.16	0.16	0.16	0.16	0.17	0.17	0.07	0.07	0.06
MgO %	<0.11	0.39	0.16	6.69	6.45	7.11	6.65	6.18	6.80	8.22	1.96	0.19	0.12
CaO %	0.29	0.59	0.48	8.91	9.05	8.63	9.04	9.15	9.17	8.91	3.62	0.34	0.35
Na ₂ O %	3.68	2.32	2.49	3.32	3.46	3.15	3.49	3.60	3.51	3.55	4.24	2.39	2.70
K ₂ O %	4.51	3.59	5.29	1.01	1.06	1.01	1.05	1.46	1.47	1.51	2.89	5.93	5.63
P ₂ O ₅ %	<0.01	0.02	0.01	0.37	0.35	0.35	0.35	0.61	0.58	0.63	0.32	0.01	0.01
Total %	98.79	96.57	96.59	99.83	101.32	99.65	100.95	98.18	101.08	98.52	98.12	94.65	95.39
LOI ^c %	2.40	4.44	4.62	1.09	-0.20	1.09	-0.37	0.72	-0.20	-0.37	0.89	4.36	4.25
V ppm	<10	20	ND	193	193	188	198	199	209	191	56	<10	<10
Cr ppm	<8	15	10	201	189	201	198	213	213	242	34	25	42
Ni ppm	<10	ND	ND	86	85	89	93	133	112	159	24	19	<10
Zn ppm	<10	108	76	100	99	94	100	69	100	98	58	<10	<10
Rb ppm	218	172	144	11	21	18	16	23	23	22	50	116	110
Sr ppm	14	91	25	454	482	437	493	650	687	765	585	17	20
Y ppm	95	102	35	20	25	22	21	32	36	14	14	<6	49
Zr ppm	222	334	174	156	159	147	148	198	199	203	177	84	83
Nb ppm	114	86	65	21	20	19	21	41	23	29	18	35	44
Ba ppm	66	244	170	471	513	513	475	633	727	728	1277	518	466

Note: Values and analytical errors are reported in percent or parts per million by weight. Analytical errors (2σ) are SiO₂, 0.7; TiO₂, 0.01; Al₂O₃, 0.2; FeO and Fe₂O₃, 0.06; MnO, 0.01; MgO, 0.08; Nb, 7.0; CaO, 0.1; Na₂O, 0.1; K₂O, 0.05; P₂O₅, 0.01; V, 10; Cr, 8; Ni, 10; Zn, 12; Rb, 5; Sr, 25; Y, 6; Zr, 30; and Ba, 50.

^a NA = not analyzed.

^b All iron reported as Fe₂O₃ unless ferrous/ferric ratio was determined by digestion/titration.

^c LOI = loss on ignition; negative values indicate oxidation of ferrous iron during ignition.

Table 3.1-4
Chemical Analyses of Puye Formation Size Fractions from Drill Hole R-15

Sample	R15-772 coarse fanglomerate		R15-787 coarse fanglomerate		R15-879 coarse fanglomerate		R15-965 coarse fanglomerate		R15-979 pumiceous sandstone		R15-1037 finer-grained sediment		R15-1099 finer-grained sediment		R15-1103 axial river gravel (Totavi Lentil)	
Size	>2 mm	<2 mm	>2 mm	<2 mm	>2 mm	<2 mm	>2 mm	<2 mm	>2 mm	<2 mm	>2 mm	<2 mm	>2 mm	<2 mm	>2 mm	<2 mm
SiO ₂ %	67.0	65.2	66.8	67.5	70.1	71.8	68.8	69.3	68.5	69.2	68.7	70.1	69.0	70.4	65.8	69.6
TiO ₂ %	0.53	0.52	0.51	0.50	0.40	0.39	0.41	0.40	0.43	0.50	0.44	0.32	0.51	0.36	0.54	0.479
Al ₂ O ₃ %	14.9	14.3	14.8	14.7	14.4	14.1	14.2	14.2	14.2	13.7	13.9	13.2	13.6	13.2	14.8	13.5
Fe ₂ O ₃ % ^a	3.93	3.95	3.90	3.74	2.97	2.81	3.02	2.84	2.87	3.10	2.82	2.05	3.02	2.23	4.52	3.41
MnO %	0.06	0.07	0.06	0.06	0.05	0.05	0.06	0.05	0.06	0.07	0.07	0.07	0.07	0.07	0.09	0.05
MgO %	1.71	1.75	1.73	1.67	1.26	1.25	1.52	1.43	1.22	1.27	1.08	0.83	1.25	0.95	1.45	1.05
CaO %	3.51	4.45	3.22	3.12	2.39	2.30	2.46	2.46	2.29	2.41	2.24	1.66	1.70	1.58	3.42	2.77
Na ₂ O %	4.05	3.76	3.88	4.06	3.92	3.64	3.87	3.74	3.83	3.66	3.53	3.40	3.53	3.00	3.53	3.20
K ₂ O %	3.10	3.11	3.21	3.25	3.88	3.68	3.83	3.63	3.99	3.82	3.89	4.22	3.85	3.99	3.76	3.38
P ₂ O ₅ %	0.23	0.22	0.22	0.20	0.14	0.13	0.18	0.13	0.15	0.16	0.13	0.12	0.17	0.13	0.23	0.16
Total %	99.00	97.35	98.30	98.87	99.43	100.16	98.37	98.22	97.54	97.82	96.78	95.93	96.70	95.87	98.13	97.54
LOI ^b %	0.52	1.21	0.44	0.51	0.51	0.64	0.44	0.59	1.65	1.02	2.07	2.64	1.81	2.83	0.98	1.18
V ppm	55	58	53	43	32	23	41	35	43	46	41	31	53	31	71	56
Cr ppm	33	36	36	39	45	38	49	47	38	28	13	24	21	24	42	15
Ni ppm	32	20	21	19	36	25	36	37	16	20	<10	11	<10	<10	<10	<10
Zn ppm	49	50	41	47	38	30	43	35	34	37	40	38	39	39	50	33
Rb ppm	54	66	66	72	104	97	107	93	95	84	86	90	94	91	84	80
Sr ppm	495	470	473	458	312	304	309	337	326	321	306	220	316	240	602	526
Y ppm	19	12	25	16	16	8	18	22	17	16	21	25	23	19	21	19
Zr ppm	171	168	166	176	151	140	157	141	145	148	143	122	150	131	180	170
Nb ppm	20	25	20	21	36	16	36	31	23	28	27	22	33	25	19	13
Ba ppm	1165	1156	1146	1155	850	826	832	800	854	924	784	861	755	928	1057	943

Note: Analytical errors (2σ) are listed in Table 3.1-3.

^a All iron reported as Fe₂O₃.

^b LOI = loss on ignition.

3.1.2 Qbt 1g, Tshirege Member of the Bandelier Tuff (16.5- to 65-ft depth) and Tsankawi Pumice Bed (65- to 66-ft depth)

The vitric lower portion (Qbt 1g; Broxton and Reneau 1996, 55429) of the Tshirege Member of the Bandelier Tuff is the bedrock unit immediately underlying alluvium at R-15. The devitrified upper part of Qbt 1 has been eroded away. A sample from the lower part of this ash flow, at 64.5-ft depth, is typical of the Tshirege Member in high feldspar plus quartz phenocryst abundance (~40 wt %) with trace amounts of amphibole in vitric nonwelded pumice. X-ray diffraction analysis (Table 3.1-1) indicates a minor amount of alteration to kaolinite (~3%) in the principally vitric matrix. Chemical data (Table 3.1-3) show a major-element composition similar to the overlying vapor-phase altered Qbt 2 of the Tshirege Formation (Broxton et al. 1995, 50121), with the exception of some trace elements. The concentrations of four trace elements are significantly elevated in Qbt 1g (data from R-15) relative to Qbt 2 (data from Pajarito Mesa: Broxton et al. 1995, 50121). These trace elements are zinc (112 ppm in Qbt 1g vs. 60–80 ppm in Qbt 2), rubidium (218 ppm vs. 132–141 ppm), yttrium (94 ppm vs. 36–56 ppm), and niobium (114 ppm vs. 65–72 ppm).

The loss-on-ignition value (water) for the Qbt 1g sample at 64.5-ft depth is 2.40% (Table 3.1-3). This value, in a sample with 55% glass and minimal clay, indicates a glass water content of ~5 wt %. Such high water contents show that the glass within Qbt 1g is perlitic. The perlitic nature of this nonwelded vitric sample may be related to the high gravimetric moisture content at this depth (23%; Appendix C of this document) compared with the upper portions of Qbt 1g at R-15 (5% to 17% gravimetric moisture).

3.1.3 Volcaniclastic Sediments and Tephra of the Cerro Toledo Interval (66- to 120-ft depth)

The Cerro Toledo interval at R-15 consists of dry, pumiceous, mafic-rich sand and gravel from 66- to 95-ft depth. Below 95 ft the Cerro Toledo interval consists of moist to fully saturated sands and gravels (95- to 105-ft depth), of moist red-brown clay-rich silt (105- to 110-ft depth), and of moist fine- to medium-grained, well-sorted, clean sand (110- to 120-ft depth). Two samples from the Cerro Toledo interval at R-15 were examined in detail, one from a pumiceous sandstone (at 69.5-ft depth) and one from a pumice fall (at 74.5-ft depth). These two samples correspond with a transition in measured gravimetric moisture content from 28 wt % (at 69.5 ft) to 38 wt % (at 74.5 ft; Appendix C of this document).

The pumiceous sandstone at 69.5-ft depth is a very friable, light brown sandstone with white aphyric and vitric pumice up to 5 mm in size and dark brownish-black, irregular 1.5 mm patches of iron- or manganese-oxide staining in a fine-grained sandstone matrix. Clay alteration occurs in the pumice as well as in the sandstone matrix. Sand grains are mostly 0.1 to 0.2 mm in diameter, in abundant clay matrix. The sand grains consist of quartz, volcanic glass, feldspars (both sanidine and plagioclase) and rarer mafic grains (including pyroxene, biotite, amphibole, and olivine). X-ray diffraction analysis (Table 3.1-1) shows that this sample is 50 wt % glass, ~30 wt % crystalline sand detritus (subequal amounts of quartz and feldspar), and ~18 wt % poorly crystalline clays (smectite with possible kaolinite, illite, and/or chlorite). Chemical analysis (Table 3.1-3) shows moderately high contents of iron (reported as Fe_2O_3 , 2.35 wt %), vanadium (20 ppm), and chromium (15 ppm), reflecting the relatively abundant mafic mineral detritus.

The pumice fall at 74.5-ft depth consists of pinkish-gray vitric aphyric pumice 1 to 2 cm in size. Pale yellow-brown clay lines or fills many vesicles in the pumice rims but not in the pumice interiors. The pumice contains some clusters of shattered feldspar, up to 2 mm in size, with interpenetrate twinning. The x-ray diffraction analysis of this sample (Table 3.1-1) shows it to be >90 wt % glass, indicating very limited alteration. The clay that does occur (6.5 wt % of a poorly-crystalline smectite with possible kaolinite, illite, and/or chlorite, as in the overlying sample at 69.5 ft) is sedimented within voids or on pumice rims and does not appear to be a direct alteration of the host pumice. The textural and x-ray diffraction evidence

suggest that the clay was transported into the pumice fall, perhaps from the overlying pumiceous sandstone.

3.1.4 Otowi Member of Bandelier Tuff (ash flow from 120- to 420-ft depth; Guaje Pumice Bed from 420- to 472-ft depth)

At R-15 the Otowi Member of the Bandelier Tuff consists of iron- or manganese-oxide stained, slightly indurated vitric ash-flow tuff in the upper 29 ft (120- to 149-ft depth). This upper portion of the Otowi Member contains relatively coarse pumice (up to 8 cm) and abundant lithic fragments of intermediate-composition Tschicoma lavas (up to 5 vol % of the ash flow). Below 149 ft, the main body of the Otowi ash flow (271 ft thick) is massive, vitric, and nonwelded with pumice sizes typically less than 5 cm and containing ~1 vol % of xenoliths from the Tschicoma Formation. The underlying Guaje Pumice Bed is 52 ft thick at R-15 (420- to 472-ft depth). No samples of these units were selected for more detailed characterization.

3.1.5 Upper Puye Formation (472- to 492-ft depth)

The total thickness of the Puye Formation, including intercalated Cerros del Rio basalts and axial gravels of the Totavi, is over 635 ft at R-15 (from 472-ft depth to total depth [TD] at 1107 ft). A thin sequence of Puye Formation fanglomerates (20 ft) lies at the top of the section above a Pliocene soil and basalts of the Cerros del Rio volcanic field. The thin upper Puye Formation is a fanglomerate made up of Tschicoma Formation volcanic clasts. No samples of this thin upper Puye sediment were selected for more detailed characterization.

3.1.6 Late Pliocene Soil (492- to 497-ft depth)

A clay-rich late Pliocene soil overlies the Cerros del Rio basalts in R-15. From 492 to 494 ft the soil consists of a clay- and silt-rich matrix with clasts of weathered Cerros del Rio basalt. From 494 to 497 ft this interval consists of clays mixed with oxidized basalt. The lower three feet of clay plus basalt may represent flow-top weathering before the stabilization of the overlying soil. No samples of these deposits were selected for more detailed characterization.

3.1.7 Basaltic Rocks of the Cerros del Rio Volcanic Field (497- to 746.7-ft depth)

Late Pliocene basaltic rocks of the Cerros del Rio volcanic field in R-15 consist of vesicular to massive basalt flows separated by zones of basaltic breccia. X-ray diffraction analyses of seven samples of the Cerros del Rio basalt from R-15 are listed in Table 3.1-1, and chemical analyses of seven samples are listed in Table 3.1-3. In previous studies of samples from characterization wells R-9 and R-12 (Broxton et al. 2000, 66599; 66601), the Cerros del Rio basalts were subdivided into a four-part stratigraphy of upper tholeiite, lower tholeiite, upper alkalic basalt, and lower alkalic basalt. Sampling of the Cerros del Rio basalt at R-15 suggests a similar transition from tholeiitic to alkalic basalt with depth, but the compositional trends with depth are not as regular as those recognized in R-9 and R-12.

Examination of cuttings obtained at R-15 suggests aphanitic transitions between more massive ophitic flow interiors. The principal textures encountered include an aphanitic sequence from 497- to 537-ft depth, an ophitic olivine-pyroxene porphyritic sequence from 537- to 570-ft depth, another aphanitic sequence from 570- to 580-ft depth, and another ophitic olivine-pyroxene porphyritic sequence from 580- to 643-ft depth. These oscillations between fine and coarse crystallization texture suggest two principal upper flow units with a contact between the two in the interval between 570- to 580-ft depth. The ophitic sequence from 580- to 643-ft depth is underlain by a thick zone of clay-coated and subrounded basalt fragments (possible older alluvium) from 643 to 677 ft. Although likely reworked, this interval is tentatively

correlated with the upper alkalic basalt at R-9 and R-12. This apparently reworked interval correlates with a high natural gamma signal in the core as logged through casing (see Figure 3.3-1). Below this interval of clay-coated and rounded basalt fragments is another ophitic sequence from 677- to 700-ft depth overlying a basal aphanitic sequence from 700- to 745-ft depth and 1.7 ft of a silty sand (745- to 746.7-ft depth). These features suggest a provisional stratigraphy of two upper flows (~497- to 575-ft depth and ~575- to 643-ft depth), a complex transition sequence with abundant alteration from 643- to 677-ft depth, and a lower flow sequence from 677- to 745-ft depth, above a silty sand that contains basaltic fragments. X-ray diffraction data (Table 3.1-1) and chemical data (Table 3.1-3) help in illustrating the similarities and differences between these units as well as providing a basis for comparison with data from other drill holes. In this section, the data from the Cerros del Rio basalt at R-12 are used as a basis for comparison.

Figure 3.1-3a illustrates four parameters of basalt composition that aid in defining the Cerros del Rio basalt stratigraphy in R-15. The parameters shown include silica content, K_2O/P_2O_5 ratio, Mg# [representing the cation ratio $Mg/(Mg+Fe)$], and Sr content. Clay-altered basalt samples at R-15 are designated by distinctive symbols (♦) to separate them from those samples that contain no clay (●). Increasing SiO_2 content and decreasing Mg# are indices of magma evolution through olivine fractionation. Higher K_2O/P_2O_5 values reflect increasing basalt contamination by assimilation of high-K, low-P crustal rocks. Higher Sr contents are characteristic of more alkalic basalt compositions.

In Figure 3.1-3b the same parameters are used to compare the Cerros del Rio basalt samples in R-15 with those from drill hole R-12. To compare the basalts from these two drill holes, the data are overlaid relative to their elevation above sea level. The section of Cerros del Rio basalts at R-12 is thicker than that at R-15, but the same general trends are seen in both drill holes. However, the trends of variation with depth are not as regular in R-15 as in R-12 and the more alkalic compositions at R-12 (specifically in the lower alkalic basalt) are not present at R-15. Some of this variation is likely attributable to source-to-toe zonation in flows, as well as to effects of clay alteration in some of the R-15 basalt samples.

3.1.7.1 Upper Tholeiite (497- to ~575-ft depth)

The interval from 497- to ~575-ft depth in R-15 consists of tholeiitic basalt with variable clay alteration. A sample analyzed from 532-ft depth contains ~16 wt % clay (predominantly smectite with a small amount of kaolinite; Table 3.1-1). This sample can be compared with another at 562-ft depth that has no clay alteration in the basalt matrix (although binocular microscope examination of uncleaned cuttings shows rare grayish-pink clay lining some vesicles; Appendix B). The two samples differ principally in the lower olivine and feldspar content of the clay-altered basalt (Table 3.1-1), suggesting that olivine and feldspar are the primary phases most affected by clay alteration.

Chemical differences (Table 3.1-3) are not as prominent, but the clay alteration does result in modest differences. This effect is seen in Figure 3.1-3a, where the clay-altered sample is higher in K_2O/P_2O_5 ratio, higher in Mg#, and lower in Sr content. However, comparison of the chemical data between unaltered and altered basalts shows that the differences are minor.

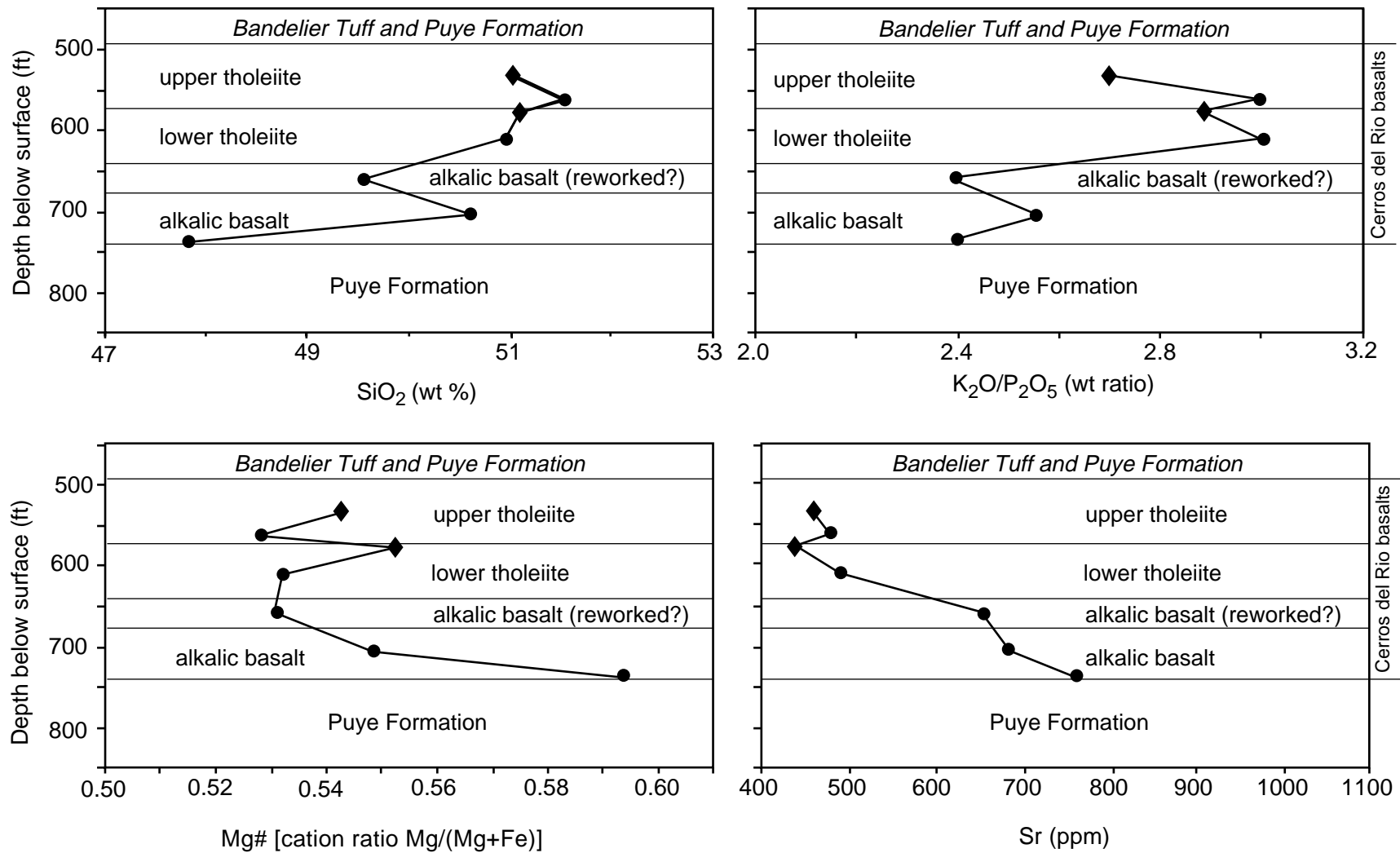
3.1.7.2 Lower Tholeiite (~575- to 643-ft depth)

Two samples of the lower tholeiite were examined in detail, an altered sample from 577-ft depth and an unaltered sample from 610-ft depth. As in the upper tholeiite, the shallower sample is altered to ~16 wt % clay (smectite with minor kaolinite) and differs from the unaltered basalt principally by having a lower olivine and feldspar content (Table 3.1-1), suggesting again that the abundances of these two phases diminish through clay alteration. The chemical differences between the altered and unaltered tholeiites are similar to those between the altered and unaltered samples from the upper tholeiite (Figure 3.1-3a).

December 2000

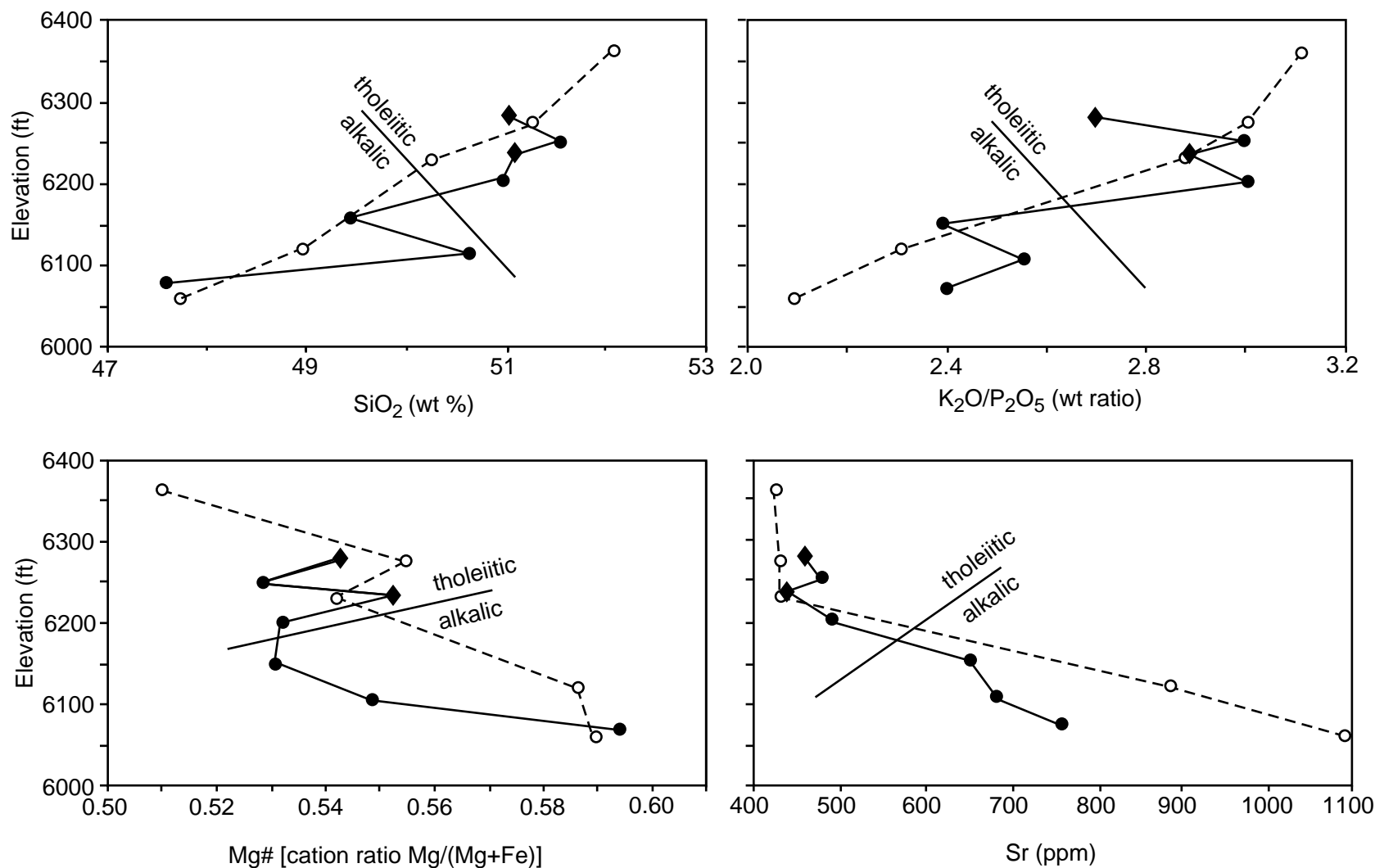
18

ER2000-0308



F3.1-3a / R-15 WELL COMPLETION RPT / 072100 / PTM

Figure 3.1-3a. Variations in SiO₂, K₂O/P₂O₅, Sr, and Mg# [cation ratio of Mg/(Mg+Fe)] in the Cerros del Rio basalts of drill hole R-15. Different symbols are used for the R-15 data from clay-altered (♦) and unaltered (●) basalts.



F3.1-3b / R-15 WELL COMPLETION RPT / 081700 / PTM

Figure 3.1-3b. Variations in SiO_2 , $\text{K}_2\text{O}/\text{P}_2\text{O}_5$, Sr , and Mg\# [cation ratio of $\text{Mg}/(\text{Mg}+\text{Fe})$] in the Cerros del Rio basalts of drill holes R-15 and R-12. Different symbols are used for the R-15 data from clay-altered (♦) and unaltered (●) basalts. The data from R-15 are overlain on comparable data from the Cerros del Rio basalts at R-12, normalized to elevation above sea level (open symbols and dashed lines illustrate the data from R-12).

A thin section of the unaltered sample at 610-ft depth shows ~5 wt % olivine phenocrysts up to 2 mm in size and plagioclase laths and blocks to 1 mm, grading downward into the groundmass size range. Maximum symmetrical extinction angles on albite twins in the plagioclase grains indicate core compositions of approximately anorthite-55. Some fragments from this sample of drill cuttings have olivine phenocrysts that are markedly altered to iddingsite.

3.1.7.3 Fragmented Alkalic Basalt (643- to 677-ft depth)

Binocular microscope examination of samples from this interval shows relatively uniform, 1–2 cm subrounded basalt fragments with clay coatings approximately 1 mm thick. Although bentonite mud was used in drilling R-15, it is not believed that the clay coatings on these basalt fragments represent clays introduced during drilling. Thin-section examination of a sample from 660-ft depth shows that the clasts are coated by a highly adhesive layer of at least two generations of clay-rich silt, including detritus of basalt powder and eolian mica. No similar clay coatings occur in other intervals drilled in the same manner. The supplied bentonite in all other intervals was also readily dispersed in washing of cuttings. For these reasons it is considered unlikely that the clays so tightly bonded to the basalt fragments in this interval could have been introduced during drilling. Evidence of fragment roundness and clay coating support an assignment of “older alluvium” to this interval, but the uniformity of clast composition is inconsistent with such an assignment. The chemical composition of the basalt sample from 660 ft, cleaned of surface silt, is consistent with a lava similar to the upper part of the alkalic trend in R-12 (e.g., Sr data in Figure 3.1-3b).

3.1.7.4 Alkalic Basalt (677- to 745-ft depth) and Basal Silty Sand (745- to 746.7-ft depth)

The alkalic basalt at 677 to 745 ft is represented by samples from 705-, 740-, and 743.4-ft depth. Cuttings at 705-ft depth consist of dark gray to brownish black, medium- to very coarse-grained basalt with phenocrysts of abundant light green olivine to 2 mm and scarce to common plagioclase to 1 mm. Orange-pink clay coats a few fragments and occurs as massive vesicle fillings up to 5 mm thick, but was cleaned from the fragments analyzed by x-ray diffraction (Table 3.1-1). A thin section of the sample at 705 ft shows ~3% olivine phenocrysts up to 2 mm in size, but most olivine is intergranular and occurs in the sample groundmass. Maximum symmetrical extinction angles on plagioclase albite twins indicate core compositions of approximately anorthite-50. X-ray diffraction data from the sample at 705-ft depth (Table 3.1-1) show higher olivine content (8.9%) than in the overlying tholeiitic basalts (6.2–6.6% in the unaltered samples). The chemical analysis of the sample at 705-ft depth (Table 3.1-3) shows the higher K_2O plus Na_2O and higher Sr content indicative of alkalic basalt. The parameters plotted in Figure 3.1-3b suggest that the sample at 705-ft depth may be correlated with the alkalic basalt series at R-12 but if so it has lower SiO_2 , higher K_2O/P_2O_5 , lower Mg#, and lower Sr content. All of these differences are features that tend to make the sample at 705-ft depth transitional between the tholeiitic and alkalic samples from R-12.

The R-15 Cerros del Rio basalt samples at 740-ft and 743.4-ft depth have mineralogical compositions (Table 3.1-1) and the XRF-analyzed sample has a chemical composition (Table 3.1-3) more mafic than the samples at 705 ft and above. The two samples from 740 to 743.4 ft have 12.3 wt % to 12.8 wt % olivine in contrast to the 8.9 wt % olivine content of the sample from 705 ft. Higher olivine content correlates with higher Mg# and, in the Cerros del Rio basalts analyzed from this region, a more alkalic character. Chemical analysis of the sample from 740 ft verifies this, but the sample has relatively high Mg# (0.59) but lower Sr content than the lowest alkalic basalt in R-12. Despite the difference in maximum Sr content, the overall trends and petrographic character in the basalts at R-15 and R-12 are very similar and justify correlation of the Cerros del Rio basalt units between these drill holes.

The thin, silty sand below the basalt at 645- to 746.7-ft depth contains millimeter-to-centimeter basalt fragments. These fragments include basalt, visible in the sand fraction and detected in QXRD (Table 3.1-1). The abundant quartz, however, indicates a mixed provenance.

3.1.8 Lower Puye Formation (746.7- to 1107-ft depth; TD)

The Puye Formation beneath the Cerros del Rio basalts consists of coarse fanglomerate to a depth of 973 ft, a sequence of pumiceous sandstones from 973 to ~1005 ft, finer-grained sediments and pumice beds from ~1005 to 1100 ft, and axial river gravels (Totavi Lentil of Griggs 1964, 8795) from 1100 ft to TD (1107 ft).

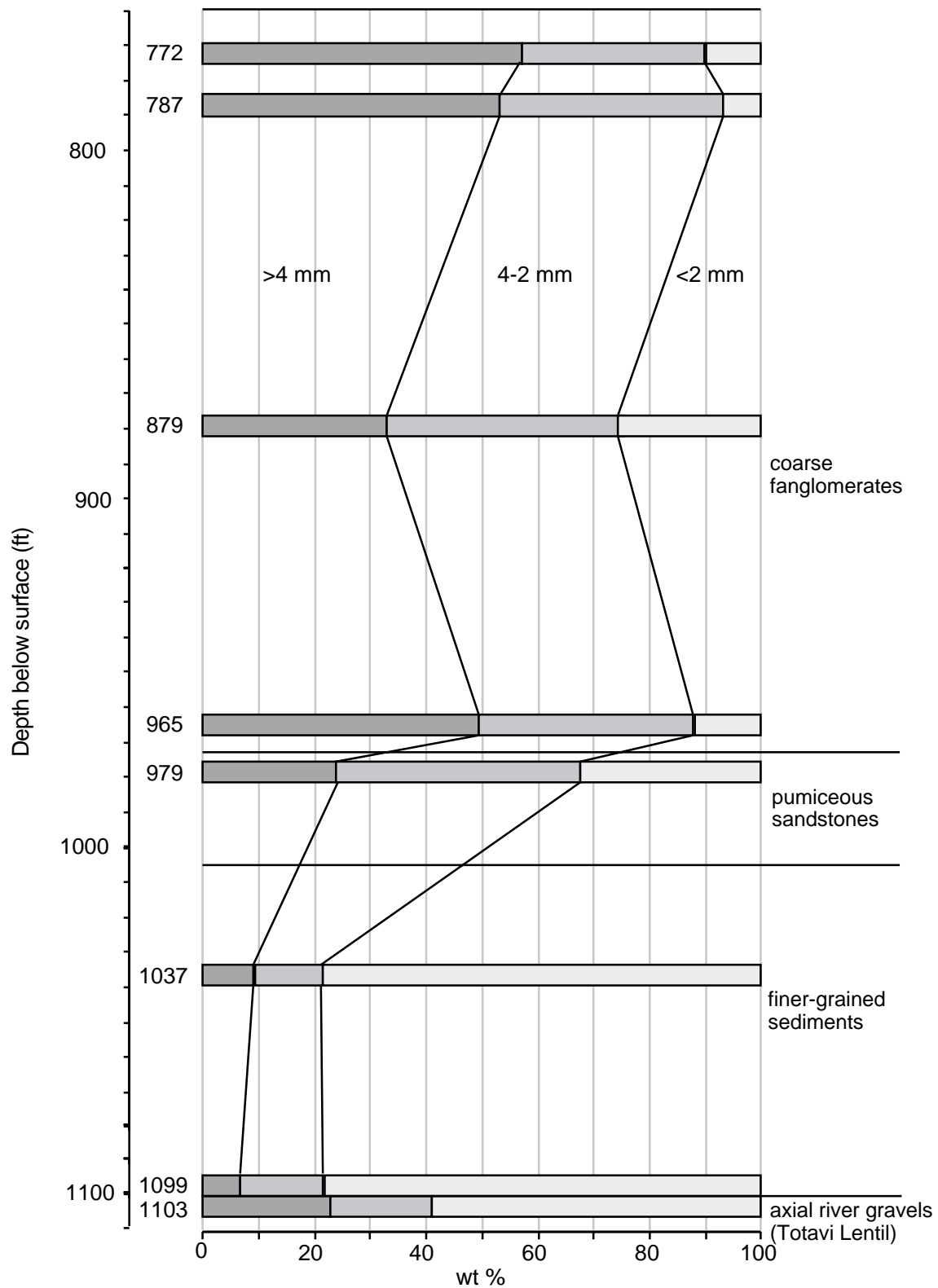
The stratigraphic subdivision of the lower Puye Formation at R-15 into upper coarse fanglomerate, pumiceous sandstone, and a lower fine-grained series with pumice beds is closely similar to the Puye Formation stratigraphy observed in R-9 and R-12. This similarity indicates that these subdivisions of Puye Formation stratigraphy can be extended between the three drill holes, over a distance of more than two miles. However, there are two prominent differences between the Puye Formation at wells R-9 and R-12 and the Puye Formation at R-15. First, all of the volcanic glass in the lower Puye Formation at R-9 and R-12 has been completely altered to smectite. In R-15 the volcanic glass throughout the Puye Formation remains vitric. Second, axial river gravels were not encountered in either R-9 or R-12, whereas river gravels containing fragments of quartzite and plutonic rocks were encountered in R-15.

Because clay alteration is extremely limited in the Puye Formation at R-15, it is possible to evaluate the contributions of different size fractions to the Puye Formation at this site. To obtain these data several representative Puye Formation samples from R-15 were sieved into >4-mm-, 2- to 4-mm-, and <2-mm-sized fractions and weighed. The results of this analysis are provided in Table 3.1-5 and summarized in Figure 3.1-4. Determinations of finer-sized data were not attempted because of the likely loss of clay and some silt during drilling; coarser-sized fraction determinations would approach the range where drilling effects result in extensive size reduction.

Table 3.1-5
Weight Fractions (%) of the >4-mm-, 2- to 4-mm-, and <2-mm-
Sediment-Sized Fractions of the Puye Formation at Drill Hole R-15

Sample Depth	>4 mm	2 to 4 mm	<2 mm
767–772 ft	57	33	10
782–787 ft	53	39	8
877–879 ft	33	41	26
963–965 ft	49	39	12
977–979 ft	24	43	33
1035–1037 ft	9	12	79
1097–1099 ft	7	15	78
1101–1103 ft	23	18	59

For chemical and mineralogical analysis, the >4-mm- and 2- to 4-mm-sized fractions obtained from the Puye sediments were combined but analyzed separately from the <2-mm-sized fractions. These data are compiled in Tables 3.1-2 and 3.1-4. Representative chemical parameters (SiO_2 , Fe_2O_3 , Cr, and Sr) are plotted for the >2-mm- and <2-mm-sized fractions in Figure 3.1-4. Chemical data were also obtained for clasts of a unique pyroxene-rich red-and-black flow-banded lava from 787-ft depth, and for two slightly reworked pumice units at 1009-ft and 1067-ft depth. These data are included in Table 3.1-3.



F3.1-4 / R-15 WELL COMPLETION RPT / 071700 / PTM

Figure 3.1-4. Distributions of sediment-sized fractions (weight percent) for samples from the lower Puye Formation at R-15. Depths for the bottom of each cuttings run analyzed are shown for each sieved and weighed sample.

3.1.8.1 Coarse Fanglomerates (746.7- to 973-ft depth)

Coarse fanglomerates, with clasts of Tschicoma Formation lavas, occur from 746.7 to 973 ft at R-15. Lithic clasts range in size to at least 4–5 cm; larger clasts are likely to occur but are fragmented by drilling. The >4 mm clast constituent typically forms ~50 wt % of the sediment and the finer fraction, <2 mm, seldom forms more than ~10 wt %. In addition to the characteristic Tschicoma Formation dacitic to rhyodacitic lavas, clasts of a distinctive red/black dacite with strong flow-banding occur at 782- to 787-ft and at 877- to 879-ft depth. This lithology is a crystal-rich lava with phenocrysts of plagioclase, orthopyroxene, clinopyroxene, and possible relict amphibole. Multiple generations of clinopyroxene indicate disequilibrium that may be related to admixture of more than one lava in the generation of the red and black banding. The sand component in the sediments at 782- to 787-ft and 877- to 879-ft depth is relatively minor in contrast to gravels and cobbles. Sands (<2 mm) at 877- to 879-ft depth and 963- to 965-ft depth are relatively quartz-rich. Below 919-ft depth, the sand component is less abundant and the variability among Tschicoma lithologies represented diminishes. It is in this lower section that quartz-biotite-clinopyroxene dacites predominate. However, the chemical data suggest that a distinctive rise in silica content of the volcanic clasts occurs between 782- to 787-ft and 877- to 879-ft depth (Figure 3.1-5).

The regional water level at R-15 is at 964-ft depth, which is 9 ft into the lower part of the coarse fanglomerates. The Puye Formation from this depth down is thus fully saturated yet essentially unaltered. This is unlike the Puye Formation occurrences at R-9 and R-12, which are unsaturated yet contain no original glass as a result of clay alteration.

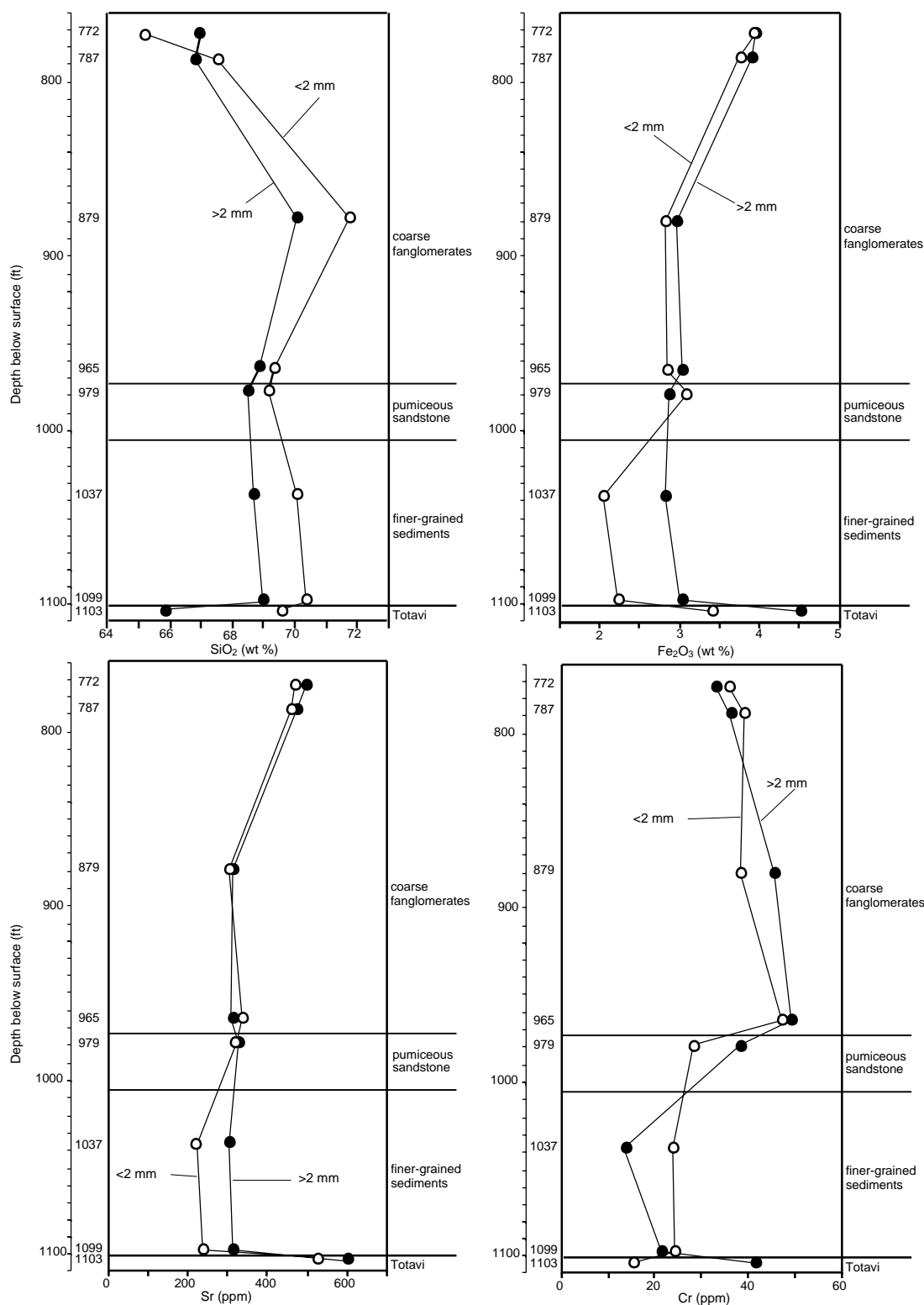
3.1.8.2 Pumiceous Sandstones (973- to ~1005-ft depth)

From 973-ft depth to the bottom of the Puye Formation, the >4 mm clast constituents form <30 wt % of the sediments, the <2 mm constituents increase in abundance, and glass abundance increases (Table 3.1-2) relative to the upper Puye Formation. However, in the pumiceous sandstones from 973- to ~1005-ft depth the <2-mm-sized fraction does not predominate to the extent observed below ~1005-ft depth. The pumiceous sandstones include some rounded and frosted quartz grains, indicating significant transport. Rhyolitic and basaltic clasts occur along with the more common clasts of intermediate-composition Tschicoma Formation lavas. A thin section of the sample from 977- to 979-ft depth contains vitric aphyric pumice and a devitrified quartz-sanidine-plagioclase porphyritic pumice as well as intermediate lavas and minor basalt.

3.1.8.3 Finer-Grained Sediments and Pumice Beds (~1005- to 1100-ft depth)

The Puye Formation sediments below 1005 ft at R-15 are sand-dominated, with relatively few clasts of >2 mm (Figure 3.1-4). Included in the lower Puye Formation are two thin beds of slightly reworked pumice, one at 1007- to 1009-ft depth and another at 1065 to 1067 ft; chemical analyses of these tephra deposits are listed in Table 3.1-3. Compared to the Tshirege Member sample in this table the tephra deposits in the Puye are notably lower in Fe, Na, Rb, Zr, and Nb but enriched in K and Ba.

Clasts in the sediments other than the pumice beds include rhyolitic lithologies, intermediate lavas, and rare basalt. Included with these clasts is one occurrence of fused sandstone, possibly contact-metamorphosed, at 1045- to 1047-ft depth. The base of the subunit, at 1099- to 1100-ft depth, includes fragments of cemented sandstone. Clay alteration is highest of all Puye samples at this depth, but still <10% (Table 3.1-2). Thin sections of the finer-grained sediments include a variety of intermediate lavas with variable amounts of aphyric pumice. Clasts in thin section consist of a altered and unaltered volcanic lithologies with lesser amounts of well-cemented sandstone (Appendix B).



F3.1-5 / R-15 WELL COMPLETION RPT / 072100 /PTM

Figure 3.1-5. Variations in SiO₂, Fe (reported as Fe₂O₃), Sr, and Cr in two size fractions (>2 mm and <2 mm) of the Puye Formation sediments at R-15. Depths listed are the bottoms of the cuttings run for each sample. Data used to generate this figure are provided in Table 3.1-4.

Chemical differences between the >2-mm- and <2-mm-sized fractions are more pronounced in the finer-grained sediments than in the coarse fanglomerates. The <2 mm fraction of the finer-grained sediment fraction is more siliceous and lower in iron and strontium (Figure 3.1-5).

3.2 Axial River Gravels (Totavi Lentil of Griggs 1964, 8795) (1100- to 1107-ft depth)

The lowermost samples in R-15 consist of well-rounded gravels in a sand matrix. The well-rounded form of the gravels and the occurrence of up to 10% quartzite plus fragments of plutonic rocks indicate that these riverine deposits represent sediments deposited by the ancestral Rio Grande (Totavi Lentil of Griggs 1964, 8795). These sediments include silicified or chloritized volcanic detritus, as well as intermediate volcanic detritus from the Tschicoma Formation. Gravels and cobbles to 5 cm provide much of this source-lithology information, yet the <2-mm-sized fraction still predominates (Figure 3.1-4). These deposits are principally sands, although the sands include indicators of distinctive provenance such as grains of rose quartz that are not found in the overlying Puye Formation sediments. The sand-sized (<2 mm) fraction contains ~19% quartz by weight (Table 3.1-2). The quartz-rich nature of the sands is revealed in the higher silica and lower iron and chromium content of the <2-mm fraction (Figure 3.1-5).

3.3 Borehole Geophysics

3.3.1 Methods

The borehole geophysical methods that were used during the drilling of borehole R-15 include natural gamma radiation (NGR or gamma) measurements, and electrical resistivity (and therefore conductivity) measurements. Resistivity and gamma measurements were made from surface to 360 ft in open hole (uncased), and deeper gamma measurements were made inside the drill casing.

Gamma measurements record total gamma radiation in the borehole. For rocks not contaminated by radionuclides, potassium-40 and daughter products of the uranium and thorium decay series are the main naturally occurring gamma-emitting radioisotopes. Gamma measurements in boreholes are used for stratigraphic correlation and for identification of rocks and sediments that have a high clay content. Uranium and thorium are concentrated in clay by the process of adsorption and ion exchange. Basalt generally has much lower natural radioactivity than rhyolite (Brookins 1984, 12453).

Borehole resistivity measurements are a record of the composite electrical resistivity (or its inverse, conductivity) of the rocks and their pore fluids that surround the borehole. Most minerals are poor conductors of electricity, so the conductivity of rocks is chiefly due to the presence of continuous fluids in the pore spaces. Rocks with pores filled with high ionic-strength water are better conductors than rocks with pores filled with low ionic-strength water.

Electrical resistivity is measured using an induction tool. A magnetic field produced by the tool induces electrical currents in the surrounding formation. The current strength is proportional to the electrical conductivity of the surrounding rocks. Measurement of resistivity works well in boreholes that are filled with a nonconducting substance like air or fresh water. The induction tool used in R-15 has a radius of investigation of from 10 to 28 cm and a vertical resolution of 65 cm. The measurement point is 91 cm (36 in.) from the top of the probe.

3.3.2 Results

Measurements with the gamma probe in R-15 were taken three times during drilling of the borehole. The gamma logs along with stratigraphic contacts and drill casing depths are shown in Figure 3.3-1. In this display the original log readings were smoothed several times with 7- and 21-point moving average filters. The first gamma log was run from the surface to a depth of 360 ft inside the open borehole. The second gamma log was run from the surface to a depth of 740 ft inside the 16-in. surface casing and the 13.63-in.-diameter drill casing. The third run was made through the surface casing and the 13.63-in. and 11.88-in. drill casings.

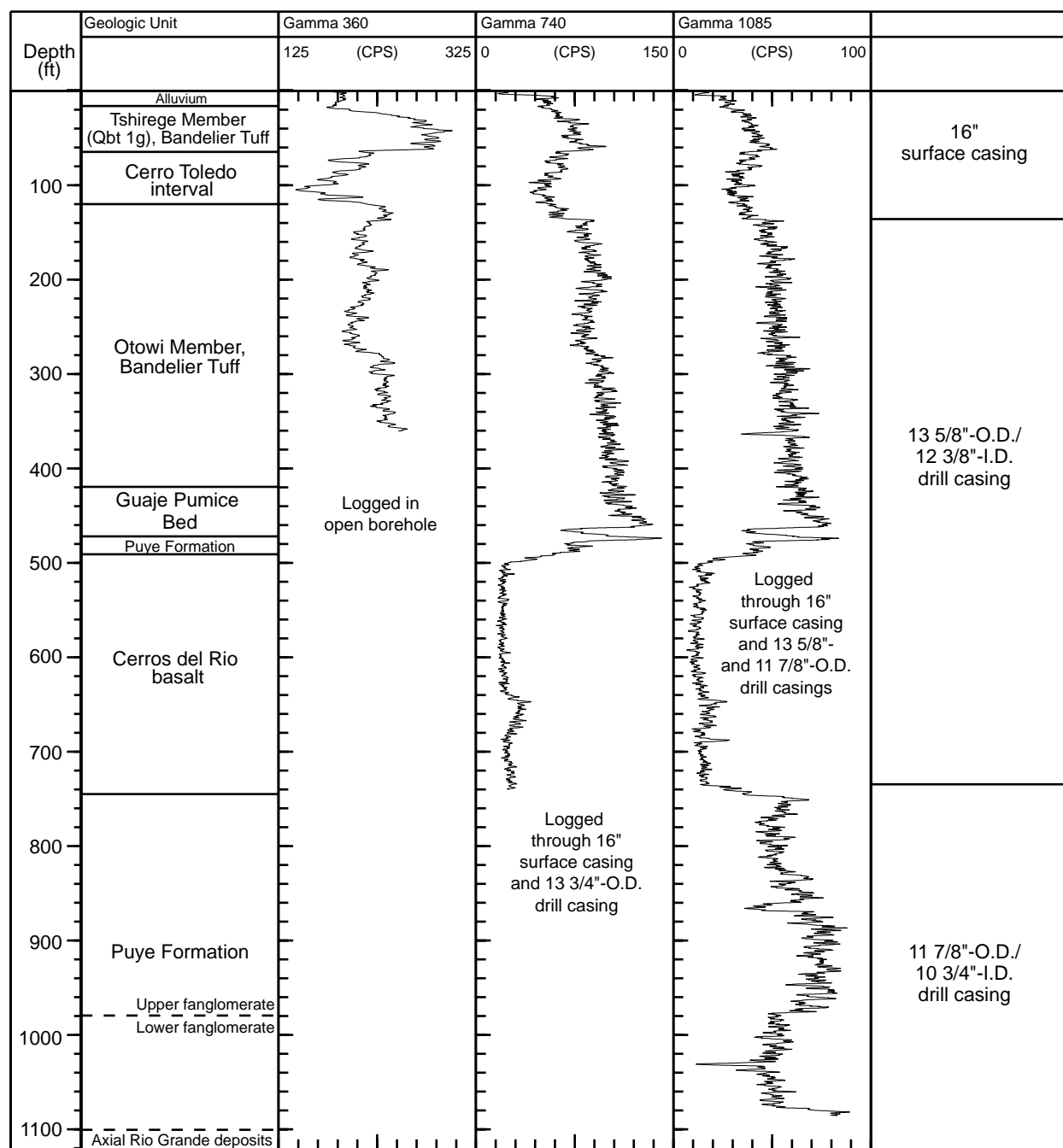
The gamma logs run through casings show a decrease in gamma counts due to absorption by the casings. Strong changes in gamma readings occur at the end of casing strings. Comparison of the 360 ft and 740-ft log at the base of the 16-in. surface casing shows that the small zone of higher gamma counts in the upper 15 ft of the Otowi Member is obscured in the deeper log by the base of the surface casing. Inspection of the 1085-ft log at the base of the 13.63-in. casing at 740 ft shows a sharp increase in gamma counts. The increase may be due to a reduction in gamma absorption below 740 ft because measurement occurs through only one casing string, in addition to change in lithology from lower radioactivity basalt to higher radioactivity Puye Formation.

Electrical resistivity was measured in the open hole above a depth of 360 ft and is shown along with the gamma log run to this depth in Figure 3.3-2. In this display the original log readings were smoothed several times with 7- and 21-point moving average filters. The conductivity log shows six maxima between the surface and 120-ft depth. In general the shallowest four maxima correspond to peaks observed in the gravimetric moisture content (Figure 3.3-3). However, the conductivity maxima are deeper than the corresponding moisture content maxima by about 3 ft or more. This may be due to the fact that the measuring point on the resistivity tool is 3 ft below the top of the probe so that there is a datum shift between the log and moisture content data. The conductivity maxima at 100 and 110 ft correspond to the lower portion of a broad moisture content maximum in the lower Cerro Toledo interval, and to a smaller moisture maximum near the base of that unit. The gradual increase of conductivity with depth in the Otowi Member corresponds to a gradual increase in moisture content in the same interval.

Most major lithologic contacts can be discerned from the gamma log. At the top of Qbt 1g gamma counts rise compared to the overlying alluvium. Gamma readings fall within the Cerro Toledo interval and rise again within the Otowi Member. Several zones on the gamma log within the Otowi Member might correspond to lithologic zones such as flow boundaries in that unit: gamma values fall off below 140 ft, rise again at 180 ft, reach a low at 240 ft, and show a significant increase below 280 ft.

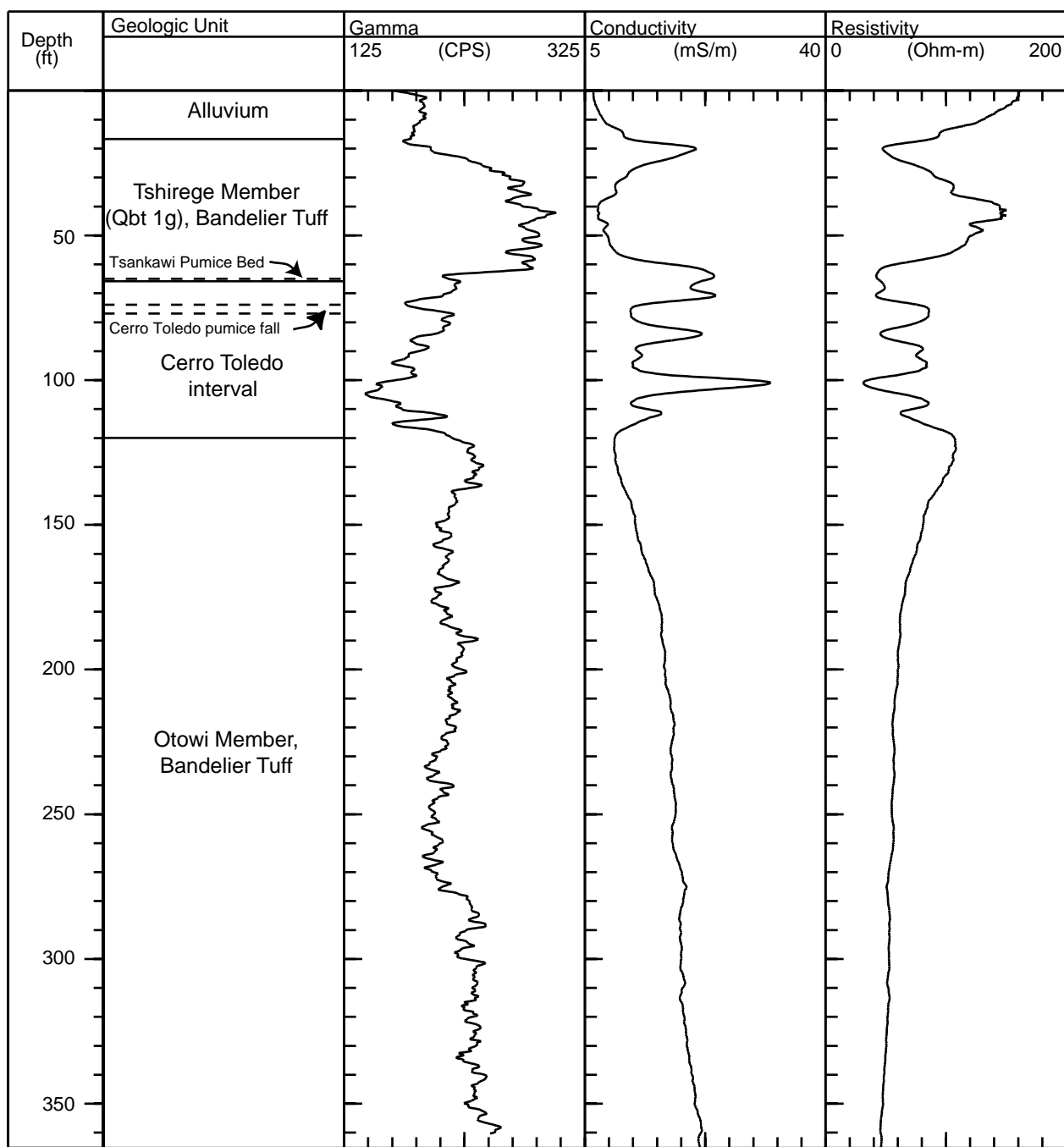
While the top of the Guaje Pumice Bed is picked at 420 ft, the gamma log shows no corresponding change. Instead, the gamma counts rise at 440 ft. In R-12 (Broxton et al. 2000, 66601) the Guaje Pumice Bed shows a strong increase in gamma readings compared to the overlying Otowi Member and underlying basalt. This gamma high in the Guaje Pumice Bed in R-12 has a blocky appearance with a sharp transition at the top and base of the unit. In R-15, the gamma log is ragged: gamma counts fall within the base of the Guaje Pumice Bed at 460 ft and rise at the top of the Puye Formation at 472 ft. The zone from 464 ft to 472 ft corresponds to a lithic-rich pumiceous lithology that is uncommon in the Guaje Pumice Bed.

Below about 490 ft, gamma counts fall off strongly, corresponding to the Cerros del Rio basalt. A rise in gamma at about 643 to 677 ft corresponds to a zone of vesicular basalt and possible old alluvium, which may be a basalt interbed or rubbleized flow (see Section 3.1.7.3). Below the base of the basalt at approximately 745 ft the gamma radioactivity rises within the Puye upper fanglomerate. A decrease in gamma at 865 ft followed by a rise suggests the presence of a separate unit within the upper fanglomerate. The Puye lower fanglomerate below 973 ft is marked by a decrease in gamma counts. A strong decrease in gamma at 1030 ft may indicate another lithology within this unit.



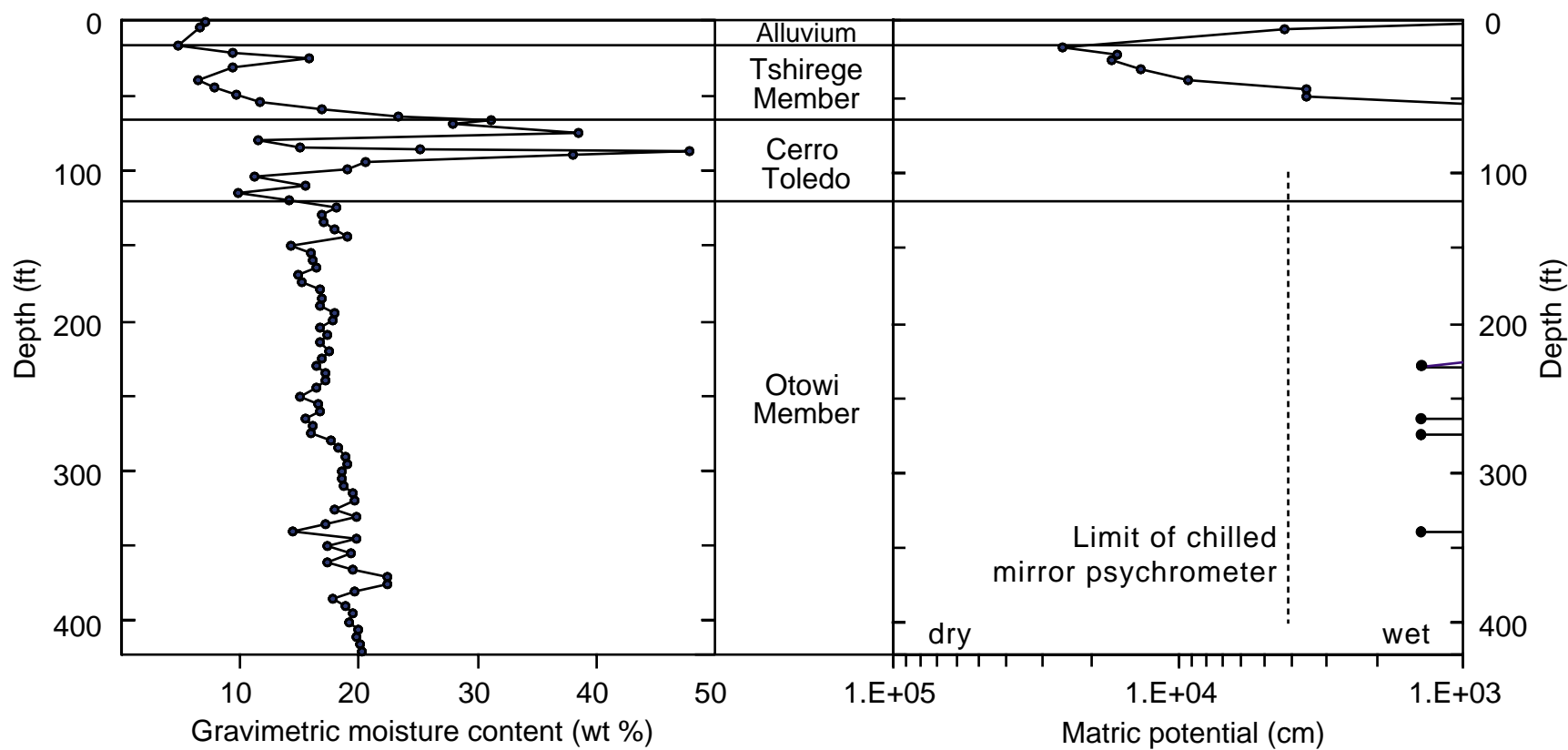
F3.2-1 / R-15 WELL COMPLETION RPT / 072100 / PTM

Figure 3.3-1. Natural gamma measurements in borehole R-15



F3.2-2 / R-15 WELL COMPLETION RPT / 091599 / PTM

Figure 3.3-2. Open-borehole natural gamma, conductivity, and resistivity measurements in R-15



F3.3-3 / R-15 WELL COMPLETION RPT / 070600 / PTM

Figure 3.3-3. Variation of gravimetric moisture content and matric potential with depth in R-15

4.0 HYDROLOGY

4.1 Unsaturated Zone

This section discusses the occurrence and movement of water in the unsaturated zone at R-15.

4.1.1 Soil-Water Occurrence

4.1.1.1 Methods

For the upper 420 ft, moisture content was determined from core samples recovered by HSA. After core was screened for radioactivity, samples were immediately placed in preweighed and prelabeled jars with tightly fitting lids. The moisture content was determined gravimetrically by drying the samples in an oven in accordance with American Society for Testing and Materials (ASTM) method D2216-90. Samples collected for moisture content are listed with the analytical results in Appendix C. Moisture content is given as the ratio of the weight of water to the weight of the dry sample.

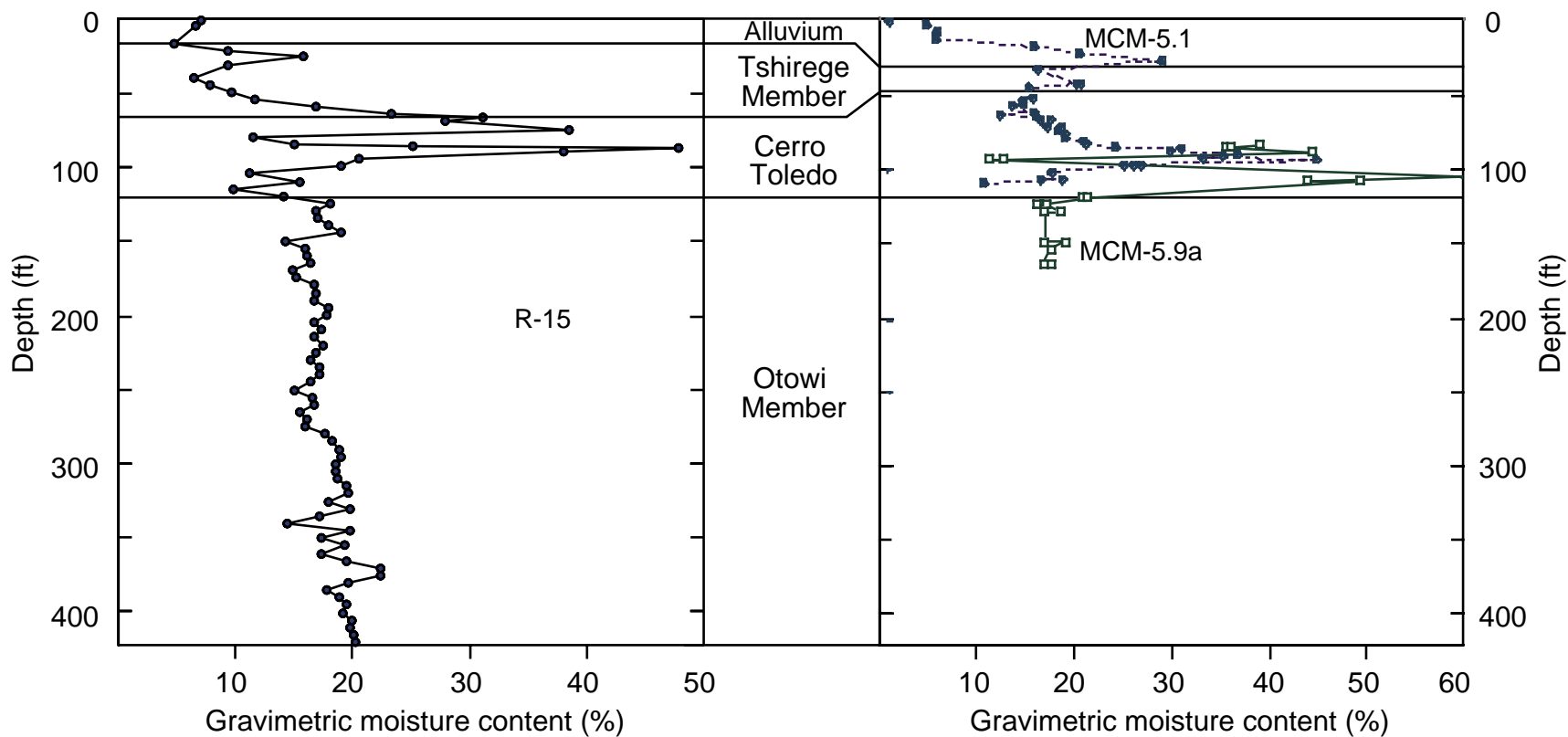
4.1.1.2 Moisture Content

Moisture content in the alluvium is about 7 wt % gravimetric (Figure 3.3-3). In Qbt 1g just below the alluvium at a depth of 24 ft, the moisture content has a maximum value of 15.8 wt %. Below this maximum, moisture in Qbt 1g reaches a minimum of 6.5 wt % at 39 ft, then rises through Qbt 1g to a second maximum within the Cerro Toledo interval. Moisture content reaches 38.5 wt % at 74.3 ft, the depth of a pumice fall in the Cerro Toledo interval. This moisture value may correspond to a volumetric moisture content of about 46 wt % to 50 wt %, assuming bulk densities of 1.2 to 1.3 g/cm³ (Rogers and Gallaher 1995, 49824). The rock may be saturated or nearly at saturation at this depth because these estimated volumetric moisture contents are in the range of the rock porosity. Porosity for Qbt 1g, the Tsankawi Pumice Bed, and Cerro Toledo interval ranges from 35 wt % to 65 wt % with median values of about 47 wt % to 50 wt % (Rogers and Gallaher 1995, 49824).

In sediments of the Cerro Toledo interval, moisture content shows minima of about 10 wt % above and below a third maximum of 48 wt % at 87 ft. This moisture value also probably indicates saturation, corresponding to a volumetric moisture content in the range 57 wt % to 62 wt %, assuming bulk densities of 1.2 to 1.3 g/cm³. The location of these maxima may correspond to variations in grain size within sediments of the Cerro Toledo interval. No free water was observed in the borehole or in core retrieved from the Cerro Toledo interval during drilling by the HSA method.

In the Otowi Member, moisture content generally increases with depth although there is moderate fluctuation in this pattern. At the top of the Otowi Member, from 124 to 144 ft, moisture content is between 17 wt % and 19 wt %. At 159 ft, moisture content is 16 wt % and generally rises to 20 wt % at 419 ft.

Two other Mortandad Canyon wells show shallow moisture content profiles similar to that found in R-15. Well MCM 5.1 is located about 2800 ft upstream from R-15. MCM 5.9A is located 600 ft downstream from MCM 5.1 and about 2200 ft upstream from R-15. The stratigraphy of these wells was reinterpreted for the Mortandad Canyon work plan (LANL 1997, 56835), changing the reported thicknesses of the Cerro Toledo interval and Qbt 1g from earlier work (Purtymun 1995, 45344). The contacts for the base of the alluvium and Qbt 1g in Figure 4.1-1 are from MCM 5.1. The contact for the base of the Cerro Toledo interval is from MCM 5.9A. The basal Cerro Toledo interval contact in MCM 5.9A is probably high compared to its depth in MCM 5.1. The canyon floor falls faster in elevation between the wells than does the base of the Cerro Toledo interval, according to cross sections in the Mortandad Canyon work plan (LANL 1997, 56835).



F4.1-1 / R-15 WELL COMPLETION RPT / 091599 / PTM

Figure 4.1-1. Variations of gravimetric moisture content with depth in R-15, MCM-5.1, and MCM-5.9

Like R-15, MCM 5.1 has several gravimetric moisture content maxima (calculated from volumetric moisture content and bulk density data in Rogers and Gallaher [1995, 49824]) in the shallowest 100 ft of the well. The moisture maxima apparently are associated with similar stratigraphic horizons in the two wells. Although the shallower maximum in R-15 lies in the upper part of Qbt 1g, in MCM 5.1 the maximum is at the base of the alluvium (depth of 30 ft) and extends into Qbt 1g. A second maximum in R-15 begins at the base of Qbt 1g and extends into sediments of the Cerro Toledo interval, with a third maximum in the Cerro Toledo interval, about 20 ft below the top of the Tsankawi pumice. The second moisture content maximum in MCM 5.1 lies entirely within the Cerro Toledo interval, at about 50 ft below the top of the combined Cerro Toledo interval and Tsankawi units (depth of 100 ft).

MCM 5.9A also shows a significant moisture maximum (calculated from volumetric moisture content and bulk density data in Rogers and Gallaher [1995, 49824]) within the lower portion of the Cerro Toledo interval (Figure 4.1-1). Otowi Member gravimetric moisture contents in MCM 5.9A are similar to those found in R-15. Moisture contents in MCM 5.9A near the top of the Otowi Member at 120 ft are 21 wt %, falling to 16 wt % at 125 ft. As depth increases to 165 ft, moisture content fluctuates between 17 wt % and 19 wt %.

A pattern of downward increasing moisture similar to that found in R-15 for the Otowi Member was reported for core samples collected in LADP-3 in Los Alamos Canyon (Broxton et al. 1995, 50119), and R-12 in Sandia Canyon (Broxton et al. 2000, 66601). In R-12, gravimetric moisture contents in the Otowi Member ash-flow tuffs systematically increase with depth from 6 wt % near the top to 20 wt % near the base of the unit. In LADP-3, gravimetric moisture contents for the Otowi Member range from 10 wt % to 23 wt %, although in the upper part moisture first decreases with depth.

4.1.2 Soil-Water Movement

4.1.2.1 Methods

When the pores in a rock are not filled with water, the hydrostatic pressure (or matric potential in unsaturated rock) is less than atmospheric pressure. The pressure potential is negative, meaning that work is required to remove water from the rock. The energy making up matric potential arises from capillary forces holding water in the pores, and adsorption that holds water to particle surfaces. Figure 3.3-3 shows the absolute value of the matric potential.

Water potential was measured using a chilled-mirror water activity meter as described by Gee et al. (1992, 58717). Samples were doubly sealed in ziplock bags and wrapped in packing tape immediately following screening of core or cuttings for radioactivity. With some exceptions, storage time ranged from 8 to 12 days; storage time for two samples (R15-389.5 and -394.2) was 18 days; storage time for five samples (R15-399.6 through -419.2) was 17 days. Measurements were made in duplicate within 10 min after water was added to plastic vials with tight-fitting lids; the vials were directly inserted into the water activity meter. Core was crushed into millimeter-sized fragments as quickly as possible after the seal was broken in order to load the vials.

Repeat measurements demonstrated that samples produced the same results as long as the measurements were made less than three hours after loading the vials and securing the lids. All analytical runs were bracketed by measurements of standards, which demonstrate a 2σ reproducibility of 0.0026 for 114 analyses of the matric potential of distilled water. This is close to the instrumental precision stated in Gee et al. (1992, 58717) of 0.003 water activity units (-0.4 millipascals [Mpa] or -4080 cm H₂O). Data listed in Appendix C for matric potential analyses represent the average of two measurements made on a sample.

The chilled mirror psychrometer (or water activity meter) measures matric potential in very dry soils or rocks. The meter measures water activity, which can be converted to matric potential. The units of matric potential may be given as pressure in pascals (Pa), or as the height of an equivalent column of water, in centimeters ($10,200 \text{ cm H}_2\text{O} = 1 \text{ MPa}$). The limit for the meter is in soils drier than 0.003 water activity units (-0.4 MPa or $-4080 \text{ cm H}_2\text{O}$) (Gee et al. 1992, 58717). This value is shown on the accompanying plots as the limit of the chilled mirror psychrometer. As a result of measurement uncertainty, some measurements near a water activity of 1 (that is, near saturation and outside the instrument's working range) produce water activity measurements greater than unity.

Despite the limitation of the water activity meter for measuring matric potential in the driest rocks, the method has advantages. Where the water activity meter works it is inexpensive, and gives more detailed vertical information than would laboratory measurements on the available core samples. In dry rock such as that encountered at characterization well R-25, the profile from the water activity meter provides a picture of vertical matric potential fluctuations over a 350-ft depth that would not otherwise be apparent. In selected cases in each well, laboratory measurements will be made over a wider range of moisture content using core samples preserved for that purpose.

4.1.2.2 Matric Potential

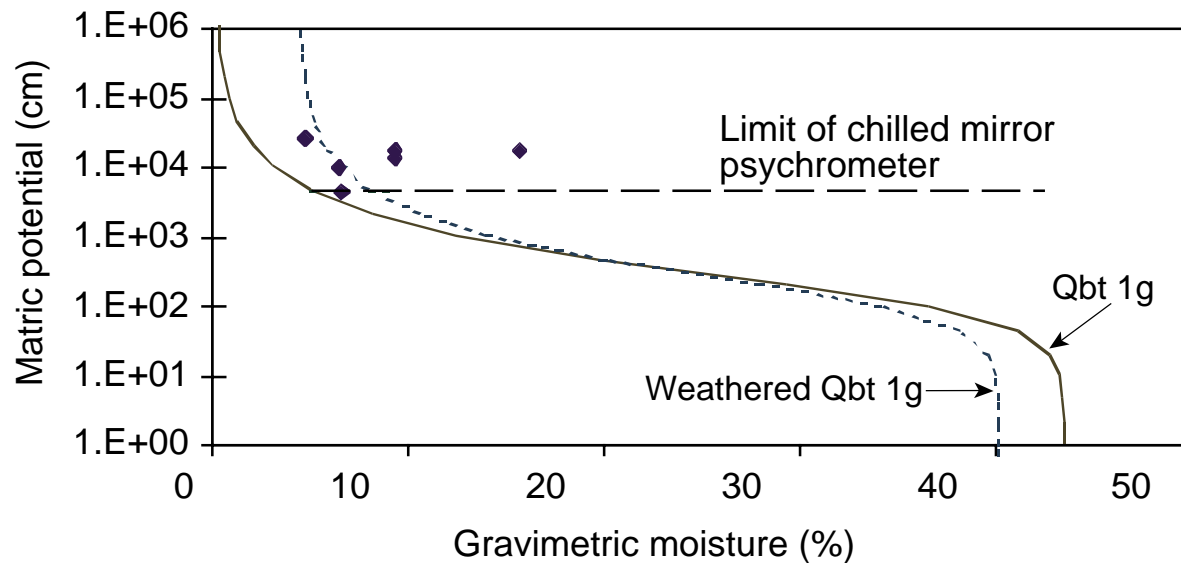
A profile of matric potential versus depth appears next to the moisture content data in Figure 3.3-3. The axis of the matric potential plot is reversed so that drier values appear to the left on the plot, corresponding to the direction of drier values of moisture content data. In general, the dry values of matric potential correspond to the dry moisture-content measurements. The exact correspondence of matric potential and moisture content depends on rock texture and reflects factors like porosity and pore size distribution. The only core samples that showed matric potential measurements within the working range of the water activity meter were six samples of Qbt 1g. These samples generally have gravimetric moisture contents below 10%.

A second method of displaying the matric potential data is shown in Figure 4.1-2. This display represents the drier portion of a moisture-retention curve. The moisture-retention curve relates the soil moisture content of unsaturated soils and rocks to the energy state of the soil water. The water content (or gravimetric moisture content) reported here equals the mass of water divided by the dry mass of solids in a sample; to convert to volumetric moisture content, water content is multiplied by the dry bulk density of the sample.

Two average moisture-retention curves determined from cores by Rogers and Gallaher (1995, 49824) are shown in Figure 4.1-2. The curves are for Qbt 1g and a unit in Mortandad Canyon described by Purtymun (1995, 45344) as weathered Qbt 1g. The moisture-content curves were converted from volumetric moisture content to water content using the median dry bulk density for the units: 1.17 g/cm^3 for Qbt 1g and 1.19 g/cm^3 for weathered Qbt 1g. Half the observed data from R-15 are in agreement with the drier region of these curves, while the other three values fall at higher matric potential than suggested for their moisture contents.

4.2 Saturated Zones

Up to five saturated zones were projected to occur at R-15: four perched water bodies and the regional zone of saturation. Perched saturation was expected in the Cerro Toledo interval, the Guaje Pumice Bed, the Cerros del Rio basalt and the upper part of the Puye Formation, in descending order. Regional saturation was predicted to be encountered in the lower part of the Puye Formation and continue into the underlying Santa Fe Group.



F4.1-2 / R-15 WELL COMPLETION RPT / 091599 / PTM

Figure 4.1-2. Gravimetric moisture and matric potential for Tshirege Member Unit Qbt 1g in borehole R-15

4.2.1 Groundwater Occurrence

No perched saturation was found in the Cerro Toledo interval or the Guaje Pumice Bed. First water encountered was that found to be perched in the Cerros del Rio basalt. Regional saturation was in the Puye Formation.

4.2.1.1 First Saturation

The first water encountered at R-15 was that in a perched zone of saturation in the Cerros del Rio basalt. The first indication of saturation was the appearance of water in the open borehole after one shift of drilling with the RC 44 (4 7/8-in.-I.D.) air hammer from 680 to 740 ft. The borehole was dry at 680 ft at the beginning of the drilling shift. The water was first detected at a depth of 655.6 ft by electric probe 2.5 hr after the air-hammer drill system was tripped out from a depth of 740 ft. There were 130 ft of open borehole below the 13-in. casing at the time the air hammer was tripped out. No saturation was apparent to the driller or in the drill cuttings during drilling for the 680- to 740-ft interval. After 14.75 hr, the water-level depth was measured to be 646.4 ft (Figure 2.3-1), with 130 ft of open hole at the time of this measurement.

Following sampling of water in the open borehole, the 13-in. drill casing was advanced from 610 to 740 ft using TORKease and EZ-MUD mixtures to lubricate the casing. Although the circulation materials generally obscured where groundwater was being produced, the driller identified a zone at 707 to 717 ft, which seemed to yield more water than zones above or below. If the top of the perched saturation was indeed at a depth of 707 to 717 ft, a water-level rise of 61 to 71 ft is indicated. This apparent water-level rise does not necessarily signify confined conditions. It is more likely due to the lag time for groundwater to fill the hole, because of low production through the walls of the 4 7/8-in. open hole. Additionally, water is assumed to reside within fractures in the basalt. These fractures may be saturated to the static water level of 646.4 ft, but possibly were not intersected by the R-15 borehole until greater depths.

After the 4 7/8-in. pilot borehole was redrilled to a depth of 740 ft with the 13-in. casing-advance system and drilling equipment was removed, water-level depth was repeatedly measured by electric probe to be 723 ft. At a depth of 751.5 ft, with no open borehole, a water-level reading of 729 ft was obtained. This 6-ft lower water level is probably due at least in part to the greater borehole depth.

This groundwater is interpreted to be perched for three reasons. First, it lies well above the projected depth for the regional zone of saturation (964 ft). Second, perching could readily be provided by the interval of clay-rich flow-base rubble and underlying clay-rich silty sand (lying at a depth of approximately 740 to 746.7 ft) that occurs at the base of the Cerros del Rio basalt (see Table 3.1-1). Third, when the underlying Puye Formation was drilled with air, the hole was noted to be dry.

4.2.1.2 Deep Saturation

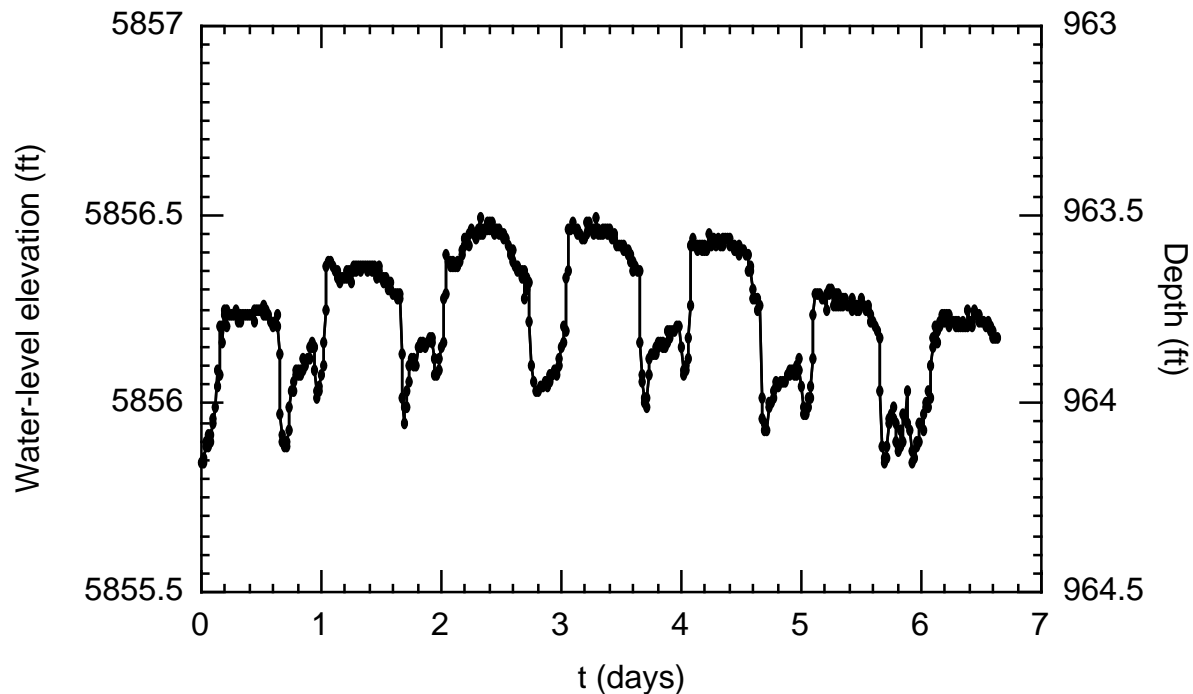
Groundwater believed to be associated with the regional zone of saturation was encountered in the lower part of the Puye Formation while drilling mud was used as a lubricant behind the casing. Observations by the driller suggest deep groundwater was encountered by a depth of 1007 ft, but possibly as shallow as 965 ft. The initial measurement of water-level depth associated with the top of the deep saturation at R-15 was 970 ft, taken when total depth was 1087 ft, with no open borehole, more than 13 hr after any drilling activity. This is very close to the projected depth for the regional water level of 960 ft. Saturation continued to total depth of 1107 ft. Data from a transducer left in the hole for approximately 7 days (August 31, 1999, to September 6, 1999) after the drill casing was pulled back to 1027-ft depth and the borehole was backfilled with sand capped by bentonite to a depth of 1039 ft indicate the water level remained fairly constant at a depth of 964 ft or an elevation of 5856 ft (Figure 4.2-1).

Regional saturation occurs at a shallower elevation than at R-9 (5694.8 ft) and R-12 (5699.5 ft), located approximately 1.3 mi to the northeast and 1.1 mi to the east of R-15, respectively. The elevation of the water table in R-15 is approximately 26 ft lower than the static water level in nearby TW-8 (depth to groundwater is 996 ft at an elevation of 5882 ft). This saturated zone is believed to be associated with the regional aquifer because its elevation is consistent with that found in nearby supply wells PM-1 and PM-3, and in TW-3 and TW-8.

The top of the regional zone of saturation occurs just above the contact between the upper and central fanglomerate of the Puye Formation. Saturation extends downward into axial Rio Grande deposits of the Totavi Lentic (see Section 3.1.8). Above 973 ft, the Puye Formation consists of fairly coarse gravel (up to cobble size) as is typical of the fanglomerate facies. Below that, and extending to a depth of 1100 ft, the Puye Formation is a coarse tuffaceous sand, with granules and minor pebbles of pumice.

4.2.1.3 Other Possible Saturation

Near-saturated conditions are believed to occur in the Cerro Toledo interval at depths of 74.3 and 87 ft, based on observed moisture contents and estimated rock porosities (see Section 4.1.1.2). However, no free groundwater was produced in these zones, which were drilled dry by HSA. Two other zones of possible saturation were identified in addition to those described in Sections 4.2.1.1 and 4.2.1.2. The occurrence of saturated conditions in these zones is uncertain because they did not produce clearly identifiable groundwater.



Note: Water levels are based on surface elevation of 6818 ft.

F4.2-1 / R-15 WELL COMPLETION RPT / 091599 / PTM

Figure 4.2-1. Hydrograph based on transducer data collected from August 31, 1999, to September 7, 1999, for the regional aquifer prior to well completion

A small zone of saturation may occur in the uppermost deposits of the Puye Formation, based on the driller's observation of increased fluidity of the mud used to lubricate the backside of the drill casing. However, saturated conditions were not found when use of drilling mud was halted. A sample of the drilling mud collected from a depth of 482 ft within this zone contains 57 pCi/L of tritium (see Table 5.2-3), an activity that is higher than expected for drilling mud made up with regional aquifer water but lower than tritium activities commonly found in Mortandad Canyon alluvial groundwater.

4.2.2 Groundwater Movement

Groundwater movement involves both a direction and a rate. Although data for evaluating horizontal flow direction is not provided by a single well, vertical direction can be determined by analysis of head distribution along the borehole, especially if casing is advanced during drilling. A general idea of potential flow rate is provided by the hydraulic conductivity of a saturated material; more specific measures of potential flow rate (e.g., Darcy flux and seepage velocity) require knowledge of that and other hydrologic properties. Measurements of hydraulic conductivity are obtained by field or laboratory tests, as discussed in Section 4.2.2.2.

4.2.2.1 Vertical Head Distribution

The sense of the vertical gradient, that is, whether water movement is up or down, is best determined by examining water levels measured at different borehole depths with a minimum of open borehole. If

water-level depth increases with borehole depth, the gradient is downward. If water-level depth decreases with borehole depth, the gradient is upward.

Too few static water-level measurements were made to determine the direction of the vertical gradient at R-15 with any certainty. However, two readings associated with the deep saturation probably represent static conditions for the respective depths at which they were measured and thus give some sense of vertical head distribution. When the casing was screwed into the soft clay-rich material in the Puye Formation at the bottom of the borehole at a depth of 1087 ft (after the transducer had been removed and 13 hr and 40 min had passed since any drilling activity), water-level depth was measured to be 970 ft for a head value of 5850 ft (using a ground-surface elevation at R-15 of 6820 ft). Transducer data collected over a 7-day period after the borehole was backfilled with 12 ft of open hole at a depth of 1039 ft give an average water-level depth of 964 ft for a head of 5856 ft (Figure 4.2-1). As groundwater moves from higher to lower head, these readings tend to support a downward vertical gradient. However, the depths for the two readings are closely spaced and the shallower head is a composite value, representing a 12-ft interval. It is possible that there is little or no vertical gradient in the regional zone of saturation at this location and flow is predominantly horizontal or nearly so. The occurrence of perched water in the basalt above suggests that the vertical gradient in that portion of the borehole is downward.

4.2.2.2 Hydraulic Properties

Both field and laboratory measurements provide data on the hydraulic properties of saturated materials. Field measurements are made in conjunction with slug or pumping tests. Laboratory tests may be performed on core samples collected from the borehole.

As slug and packer tests can be made only when drilling equipment is out of the hole, optimum use is made of such opportunities. Thus, a two-test strategy was initiated at R-15 as the standard protocol when sufficient perched water was encountered to permit sampling. Immediately after water is collected for chemical analysis (representing a slug of water removed), water level is measured and a transducer is emplaced to monitor its recovery. Following that, the transducer is withdrawn and a single-packer device is deployed for an injection/pressure test of the open-borehole interval or the material immediately beneath the bottom of the casing if the material would collapse in an open borehole. Results from the two tests of hydraulic conductivity of the saturated medium then can be compared.

The order of field testing the upper saturated zone at R-15 was reversed from that described above as the transducer was not emplaced immediately after bailing for water samples. An injection/pressure test of the clay-rich rock perching the water in the basalt by means of a single-packer device was planned to follow the collection of water samples for chemical analysis. For this, the 13-in. casing was drilled into the clay-rich rocks at 740-ft depth. However, the test was canceled due to a malfunction of the packer equipment, caused by an electrical short in the wiring.

After the packer device was removed from the borehole, a slug test was performed. Groundwater was removed from the well by bailing and water-level recovery was analyzed. Water-level data were collected using a transducer over a period of 1.5 days (2200 min). A value for hydraulic conductivity of $2.547\text{E-}07$ cm/sec was obtained using the Bouwer-Rice unconfined method of analysis (Bouwer and Rice 1976, 64056). This value falls at the lower end of the range of hydraulic conductivities reported as typical for silt (Freeze and Cherry 1979, 64057). The perching horizon includes both clay-rich basaltic rubble and clay-rich silty sand. The slug test confirms that these are low-conductivity materials.

The test is believed to have been valid, but was not ideal. As it took about 35 min to bail water from the casing, the slug was not removed instantaneously. Then it took another 5 to 10 min to emplace the transducer, so early-time data were missed. This could have been avoided if the transducer were already in the hole when it was bailed. However, it was feared, and reasonably so, that the lines for the bailer and transducer would become entangled. Nonetheless, the test provided a reasonable measure of the hydraulic nature of the perching horizon.

A single-packer test was also planned for the deep zone of saturation at a depth of 1087 ft. However, efforts to remedy the wiring problem discovered during testing of the perching medium were apparently ineffective and the attempt to test the deep saturated medium was also unsuccessful.

A 46-hr aquifer-pumping test was conducted at well R-15 on February 19–20, 2000. Water levels were recorded in R-15 while water was pumped at a constant rate of 11.7 gpm. Once the pump was turned off, water level recovery was recorded for an additional 24-hr. R-15 is completed into the regional aquifer and has a 60-ft screen. This screened interval is located 960–1020 ft bgs within the Puye Formation. Drawdown and recovery data were analyzed to determine characteristic values for transmissivity and storage coefficient. These results suggest that the regional aquifer at well R-15 behaves like a leaky-confined aquifer. Overall, an average transmissivity of about 123.4 ft²/day and a storage coefficient of about 0.0025 were determined for the Puye Formation from this pumping test. The corresponding average hydraulic conductivity over the R-15 screened interval is about 2.06 ft/day, or about 0.00117 cm/sec.

Details of the tests described will be presented in a separate document being prepared by ESH-18. Values presented here for hydraulic properties are preliminary and may be modified after further analysis.

5.0 HYDROGEOCHEMISTRY

The Laboratory has collected and analyzed surface water and groundwater samples within Mortandad Canyon since the early 1960s. Known groundwater contaminants within Mortandad Canyon west of R-15 include americium-241; cesium-137; plutonium-238; plutonium-239,240; strontium-90; tritium; uranium-235; uranium-238; nitrate, chloride, sulfate, and other inorganic solutes (Environmental Surveillance and Compliance Programs 1997, 56684; Rogers 1998, 59169; LANL 1997, 56835). Tritium activities up to 1,000,000 pCi/L have been observed in alluvial groundwater within Mortandad Canyon in the past.

Movement of groundwater within the Guaje Pumice Bed may be controlled by a northwest-southeast-trending paleodrainage (Broxton and Reneau 1996, 55429) that may serve as a conduit for contaminants discharged to Los Alamos Canyon and Sandia Canyon to the north of Mortandad Canyon. Contaminants of concern in Sandia Canyon include tritium and nitrate (Environmental Surveillance and Compliance Programs 1997, 56684). For several decades treated sewage has been discharged from the TA-3 sanitary system into upper Sandia Canyon. Surface water samples collected in upper Sandia Canyon suggest that this discharge may have contained tritium until the early 1980s (Rogers 1998, 59169). Tritium activities up to 18,000 pCi/L have been observed at surface water sampling station SCS-2 (Rogers 1998, 59169).

Known groundwater contaminants in upper Los Alamos Canyon include americium-241; cesium-137; plutonium-238; plutonium-239,240; strontium-90; tritium; uranium-235; and uranium-238 (LANL 1995, 50290).

5.1 Geochemistry of Core and Cutting Samples Collected During Phase I Drilling

Samples of core and cuttings were collected from R-15 and analyzed for metals and radionuclides for characterization purposes. Results of chemical and radiochemical analyses are used to determine both naturally occurring elements and contaminant distributions within R-15. Organic compounds were not identified as contaminants of concern at R-15, based on recent sediment and water sampling (MCO-3) conducted by the Laboratory in Mortandad Canyon (Environmental Surveillance and Compliance Programs 1997, 56684). Organic compounds, however, were analyzed using the core samples and consistent with previous sampling in Mortandad Canyon. No anthropogenic (manmade) organic compounds are present in R-15 core samples.

5.1.1 Methods

Twenty-four samples of core and cuttings were collected from the vadose zone for geochemical and contaminant characterization conducted during Phase I drilling. One core sample was collected from a perching layer within the Cerros del Rio basalt during phase II drilling. Core and cutting samples were collected from the following depth intervals: 0 to 17.0 ft, 17.5 to 20.0 ft, 25.0 to 25.3 ft, 40.0 to 41.5 ft, 63.3 to 64.3 ft, 65.0 to 65.8 ft, 68.3 to 69.3 ft, 75.8 to 76.6 ft, 87.0 to 87.4 ft, 90.8 to 91.6 ft, 100.0 to 101.3 ft, 105.0 to 105.8 ft, 112.5 to 114.5 ft, 115.0 to 115.8 ft, 120.0 to 120.8 ft, 148.3 to 149.3 ft, 150.0 to 150.8 ft, 170.0 to 170.8 ft, 230.0 to 231.3 ft, 270.0 to 272.5 ft, 325.0 to 327.5 ft, 380.0 to 384.0 ft (duplicate), 415.0 to 419.0 ft, and 740.0-751.5 ft. Approximately 500 to 1000 g of core or cuttings samples were placed in appropriate sample jars in protective plastic bags before they were shipped to analytical laboratories.

Samples of core and cuttings were analyzed using US Environmental Protection Agency (EPA)-approved analytical methods. Solid samples were partially digested using hot HNO_3 (EPA SW-846 Method 3050) before metal analyses. Samples of core and cuttings were shipped to Paragon Analytics, Inc., in Fort Collins, Colorado, for metal and radionuclide analyses. Analyses of aluminum, antimony, arsenic, barium, beryllium, cadmium, calcium, chromium, cobalt, copper, iron, lead, magnesium, manganese, molybdenum, nickel, potassium, selenium, silver, sodium, thallium, vanadium, and zinc were determined by inductively coupled plasma emission spectroscopy (ICPES). Mercury was analyzed by cold vapor atomic absorption (CVAA). Core samples were washed with deionized water for 24 hr before anion analyses. Concentrations of bromide, chloride, fluoride, nitrate, and sulfate were determined by ion chromatography (IC). Total cyanide content was determined by colorimetry. The precision limits for major anions and trace elements were generally less than $\pm 10\%$.

Radionuclide activities in core samples were determined by alpha spectrometry (americium-241; plutonium-238; plutonium-239,240; uranium-234; uranium-235; and uranium-238); gamma spectrometry (cesium-137 and gamma-emitting isotopes); gas proportional counting (strontium-90); and liquid scintillation (tritium) at Paragon Analytics, Inc., and direct counting at the University of Miami. Sample duplicates were collected and analyzed in accordance with EPA procedures.

The following equation was used to convert the activity of tritium present in the pore water from picocuries per gram to picocuries per liter:

$$\text{pCi/L} = (\text{pCi/g})(1 \text{ g H}_2\text{O}/1 \text{ ml H}_2\text{O})(\theta/1 - \theta)(10^3 \text{ ml/L})$$

where θ = gravimetric moisture content and the density of the pore water is assumed to be equal to 1.

Gravimetric moisture contents were measured at EES-1.

Field screening for volatile organic compounds (VOCs) was conducted using a photoionization detector (PID) instrument. No VOCs were detected with the field instrument.

ER Project personnel have performed data quality validation on chemical and radiochemical analytical results for core and cutting samples collected from R-15. There are no serious deficiencies associated with the analytical results. Samples were partly digested and analyzed within required holding times. A complete, detailed data validation was conducted on these core samples in early fiscal year (FY) 2000.

5.1.2 Radionuclides, Percent Organic Carbon, and Inorganic Analytes

Table 5.1-1 provides radionuclide activities in core and cuttings from R-15. Isotopes of uranium (uranium-234, uranium-235, and uranium-238), tritium, gross alpha, gross beta, and gross gamma are detected at activities greater than their minimum detectable activities (MDAs) in the core samples. Activities of gross alpha, gross beta, and gross gamma in samples of core and cuttings are greater than 1 pCi/g, where measurable, and vary with depth (Table 5.1-1). Presence of tritium in the core samples is a result of aqueous-phase and/or vapor-phase transport through the vadose zone within the Bandelier Tuff. Fourteen additional core samples were analyzed for tritium and analytical results are provided in Table 5.1-2. Increasing activities of tritium generally correlate with increasing moisture contents of the core and cutting samples, which may reflect the occurrence of buried soils and alteration zones within the Bandelier Tuff and Cerro Toledo interval.

Activities of isotopic uranium are higher in samples collected from the Bandelier Tuff, reflecting the high total uranium in this unit (Otowi Member) (Ryti et al. 1998, 58093). Lower activities of uranium-234, uranium-235, and uranium-238 generally were found in samples collected from the Cerro Toledo interval. Activities of total isotopic uranium do not appear to be elevated above Laboratory background for the Bandelier Tuff.

Activities of americium-241; cesium-137; plutonium-238; plutonium-239,240; and strontium-90 are less than detection in most of the samples of core and cuttings, indicating that no Laboratory-derived contamination from these isotopes is detectable in these core samples collected from R-15 during Phase I drilling. Americium-241, however, was detected in the core sample collected from the basalt rubble in the perching layer at an activity of 0.0355 ± 0.0184 pCi/L (2σ error) (MDA equal to 0.014 pCi/g). This perching layer is clay-rich (smectite) and americium adsorbs strongly onto solids with high surface areas such as clay minerals and hydrous iron oxides (Langmuir 1997, 56037).

Organic carbon contents of the samples were the highest within the alluvium and in the upper portion of Qbt 1g of the Bandelier Tuff, ranging from 0.07 to 0.14 wt %. These values may represent recycling of solid organic matter within the alluvium and Qbt 1g. Organic carbon contents of the remaining samples were less than 0.05 wt %, indicating small amounts of solid organic carbon are present within the lower section of Qbt 1g and the Otowi Member of the Bandelier Tuff and Cerro Toledo interval.

Table 5.1-1
Radionuclide Activities in Samples of Core and Cuttings from Borehole R-15

Depth (ft)	0–17.0	17.5–20.0	25.0–25.7	40.0–41.5	63.3–64.3	65.0–65.8	68.3–69.3
Geologic Unit	Alluvium	Bandelier Tuff ^a	Bandelier Tuff ^a	Bandelier Tuff ^a	Bandelier Tuff ^a	Bandelier Tuff ^a	Bandelier Tuff ^a
Strontium-90^b	0.14 ± 0.34	-0.17 ± 0.31	0.13 ± 0.33	0.14 ± 0.32	0.17 ± 0.31	0.02 ± 0.31	0.08 ± 0.30
Cesium-137	-0.023 ± 0.070	0.027 ± 0.064	0.016 ± 0.088	0.004 ± 0.075	0.057 ± 0.097	-0.00 ± 0.11	-0.03 ± 0.11
Plutonium-238	0.0059 ± 0.0080	0.0012 ± 0.0066	0.0054 ± 0.0100	0.0018 ± 0.0072	-0.0025 ± 0.0068	-0.0162 ± 0.0116	0.0027 ± 0.0072
MDA^c	0.013	0.012	0.021	0.018	0.017	0.039	0.016
Plutonium-239,240	0.0036 ± 0.0074	0.0054 ± 0.0072	0.0004 ± 0.0084	0.0036 ± 0.0074	0.0042 ± 0.0068	-0.0022 ± 0.0092	0.0000 ± 0.0072
MDA	0.013	0.012	0.022	0.013	0.0062	0.027	0.0067
Americium-241	0.0060 ± 0.0080	0.0113 ± 0.0136	0.0299 ± 0.0172	-0.0080 ± 0.0128	0.0097 ± 0.0104	0.035 ± 0.020	0.0146 ± 0.0140
MDA	0.014	0.025	0.014	0.039	0.016	0.019	0.020
Uranium-234	0.775 ± 0.124	0.719 ± 0.114	1.359 ± 0.192	2.24 ± 0.30	2.70 ± 0.36	1.198 ± 0.170	2.00 ± 0.26
MDA	0.019	0.019	0.018	0.0067	0.0069	0.012	0.014
Uranium-235	0.040 ± 0.022	0.071 ± 0.028	0.119 ± 0.036	0.106 ± 0.032	0.134 ± 0.038	0.080 ± 0.028	0.118 ± 0.036
MDA	0.027	0.025	0.018	0.018	0.023	0.012	0.018
Uranium-238	0.761 ± 0.122	0.791 ± 0.122	1.53 ± 0.22	2.09 ± 0.28	2.88 ± 0.38	1.306 ± 0.184	2.05 ± 0.28
MDA	0.023	0.015	0.0068	0.016	0.022	0.015	0.018
Gross Alpha	2.91 ± 0.79	2.13 ± 0.75	Not analyzed	3.78 ± 0.93	2.85 ± 0.79	9.1 ± 2.0	10.3 ± 1.9
Gross Beta	1.63 ± 0.62	2.43 ± 0.69	Not analyzed	2.23 ± 0.68	1.79 ± 0.66	4.68 ± 0.96	4.96 ± 0.97
Gross Gamma	10.75 ± 1.40	10.54 ± 1.38	Not analyzed	18.12 ± 2.34	19.61 ± 2.52	13.11 ± 1.72	17.79 ± 1.32
MDA	0.32	0.37		0.55	0.43	0.51	0.63
Tritium	0.12 ± 0.03	0.48 ± 0.07	Not analyzed	0.22 ± 0.04	8.6 ± 1.1	12.3 ± 1.6	14.6 ± 1.9
Organic Carbon (wt %)	0.13	0.14	0.07	<0.05	<0.05	<0.05	<0.05

Notes: 1. Activities are reported in picocuries per gram.

2. Error of two standard deviations is reported.

Table 5.1-1 (continued)

Depth (ft)	75.8–76.6	87.0–87.4	90.8–91.6	100.0–101.3	105.0–105.8	112.5–114.5
Geologic Unit	Bandelier Tuff ^a	Cerro Toledo interval	Cerro Toledo interval	Cerro Toledo interval	Cerro Toledo interval	Cerro Toledo interval
Strontium-90 ^b	0.01 ± 0.30	0.02 ± 0.28	0.12 ± 0.27	-0.07 ± 0.27	-0.05 ± 0.28	0.09 ± 0.26
Cesium-137	-0.008 ± 0.056	0.02± 0.12	0.07± 0.12	-0.013± 0.053	-0.005± 0.046	-0.040 ± 0.071
Plutonium-238	-0.0042 ± 0.0096	0.0005 ± 0.0098	0.0040± 0.0082	-0.0008± 0.0068	0.0102 ± 0.0122	0.0032 ± 0.0064
MDA ^e	0.031	0.026	0.015	0.013	0.023	0.012
Plutonium-239,240	0.0073 ± 0.0108	-0.0015 ± 0.0078	0.042 ± 0.022	0.0013 ± 0.0068	-0.0053 ± 0.0072	0.0150 ± 0.0112
MDA	0.021	0.022	0.015	0.013	0.023	0.012
Americium-241	0.0061 ± 0.0136	0.0221 ± 0.0154	0.025 ± 0.024	0.0139 ± 0.0140	0.0091 ± 0.0110	0.0054 ± 0.0088
MDA	0.030	0.015	0.046	0.023	0.019	0.018
Uranium-234	1.65 ± 0.22	1.45 ± 0.20	1.58 ± 0.22	0.953 ± 0.146	0.891 ± 0.136	1.49 ± 0.20
MDA	0.026	0.024	0.016	0.019	0.023	0.021
Uranium-235	0.073 ± 0.028	0.102 ± 0.032	0.095 ± 0.032	0.060 ± 0.026	0.047 ± 0.022	0.077 ± 0.030
MDA	0.019	0.018	0.016	0.021	0.021	0.027
Uranium-238	1.70 ± 0.24	1.48 ± 0.20	1.74 ± 0.24	1.190 ± 0.174	0.874 ± 0.132	1.54 ± 0.22
MDA	0.019	0.021	0.020	0.017	0.021	0.023
Gross Alpha	5.2 ± 1.2	Not analyzed	3.71 ± 0.92	1.71 ± 0.62	4.8 ± 1.2	0.91 ± 0.45
Gross Beta	3.09 ± 0.75	Not analyzed	2.68 ± 0.70	1.61 ± 0.58	3.90 ± 0.85	1.17 ± 0.52
Gross Gamma	13.54 ± 1.76	Not analyzed	15.34 ± 2.00	10.22 ± 1.34	9.21 ± 1.20	12.05 ± 1.56
MDA	0.48		0.54	0.37	0.36	0.37
Tritium	11.7 ± 1.5	Not analyzed	12.5 ± 1.7	3.74 ± 0.50	8.6 ± 1.1	4.90 ± 0.65
Organic Carbon (wt %)	<0.05	<0.05	<0.05	<0.05	<0.05	<0.05

Notes: 1. Activities are reported in picocuries per gram.

2. Error of two standard deviations is reported.

Table 5.1-1 (continued)

Depth (ft)	115.0–115.8	120.0–120.8	148.3–149.3	150.0–150.8	170.0–170.8	230.0–231.3
Geologic Unit	Cerro Toledo interval	Bandelier Tuff ^d	Bandelier Tuff ^d	Bandelier Tuff ^d	Bandelier Tuff ^d	Bandelier Tuff ^d
Strontium-90 ^b	-0.16 ± 0.28	-0.19 ± 0.26	-0.17 ± 0.26	-0.04 ± 0.27	-0.06 ± 0.42	0.16 ± 0.44
Cesium-137	-0.019± 0.055	0.05 ± 0.12	0.00± 0.11	0.027± 0.084	-0.031± 0.064	-0.066± 0.084
Plutonium-238	-0.0018± 0.0072	-0.0203 ± 0.0100	0.0050 ± 0.0082	0.0010± 0.0078	0.0041± 0.0084	-0.0015 ± 0.0100
MDA ^c	0.016	0.039	0.016	0.021	0.018	0.029
Plutonium-239,240	0.0045 ± 0.0072	-0.0035 ± 0.0078	0.0000 ± 0.0074	0.0029 ± 0.0078	0.0059 ± 0.0080	-0.0034 ± 0.0078
MDA	0.0068	0.026	0.0068	0.017	0.013	0.025
Americium-241	0.0182 ± 0.0160	0.0124 ± 0.0136	0.0298 ± 0.0178	0.0040 ± 0.0082	0.0106 ± 0.0114	0.0127 ± 0.0132
MDA	0.025	0.024	0.017	0.015	0.018	0.021
Uranium-234	0.891 ± 0.136	1.78 ± 0.24	1.96 ± 0.26	1.86 ± 0.26	1.83 ± 0.24	1.73 ± 0.24
MDA	0.020	0.021	0.0067	0.0071	0.013	0.014
Uranium-235	0.059 ± 0.026	0.135 ± 0.038	0.111 ± 0.034	0.067 ± 0.028	0.115 ± 0.034	0.087 ± 0.030
MDA	0.027	0.017	0.018	0.024	0.013	0.019
Uranium-238	0.872 ± 0.134	1.83 ± 0.24	1.90 ± 0.26	1.92 ± 0.26	1.91 ± 0.26	1.77 ± 0.24
MDA	0.016	0.0070	0.032	0.019	0.015	0.019
Gross Alpha	3.59 ± 0.95	2.73 ± 0.81	0.71 ± 0.43	0.98 ± 0.54	0.87 ± 0.56	0.87 ± 0.50
Gross Beta	3.11 ± 0.76	2.26 ± 0.68	1.37 ± 0.56	1.28 ± 0.59	1.62 ± 0.61	1.40 ± 0.57
Gross Gamma	9.75 ± 1.28	15.36 ± 2.00	14.73 ± 1.92	15.82 ± 2.06	14.60 ± 1.88	14.36 ± 1.86
MDA	0.37	0.57	0.52	0.51	0.51	0.46
Tritium	6.59 ± 0.88	7.23 ± 0.96	17.0 ± 2.2	14.6 ± 1.9	21.2 ± 2.8	2.65 ± 0.35
Organic Carbon (wt %)	<0.05	<0.05	<0.05	<0.05	<0.05	<0.05

Notes: 1. Activities are reported in picocuries per gram.

2. Error of two standard deviations is reported.

Table 5.1-1 (continued)

Depth (ft)	270.0–272.5	325.0–327.5	380.0–382.0	380.0–382.0	415.0–419.0	740.0–751.5
Geologic Unit	Bandelier Tuff ^d	Bandelier Tuff ^d	Bandelier Tuff ^b	Bandelier Tuff ^b	Bandelier Tuff ^b	Basalt perching layer ^b
Strontium-90 ^b	0.06 ± 0.38	0.20 ± 0.48	0.24 ± 0.44	0.10 ± 0.42	0.18 ± 0.44	Not analyzed
Cesium-137	0.067 ± 0.084	-0.018 ± 0.066	0.015 ± 0.086	-0.025± 0.074	-0.055± 0.081	-0.038± 0.071
Plutonium-238	-0.0010 ± 0.0082	-0.0009 ± 0.0070	-0.0008 ± 0.0068	0.0075 ± 0.0108	0.0033± 0.0088	0.0025± 0.0068
MDA ^c	0.015	0.013	0.013	0.021	0.021	0.015
Plutonium-239,240	0.0040 ± 0.0082	0.0013 ± 0.0070	0.0013 ± 0.0068	0.0033 ± 0.0090	0.0047 ± 0.0102	0.0033 ± 0.0068
MDA	0.015	0.013	0.013	0.0021	0.023	0.013
Americium-241	0.0155 ± 0.0164	-0.0040 ± 0.0092	0.0169 ± 0.0160	-0.0005 ± 0.0108	0.0157 ± 0.0192	0.0355 ± 0.0184
MDA	0.028	0.030	0.026	0.030	0.037	0.014
Uranium-234	1.81 ± 0.24	1.375 ± 0.196	2.85 ± 0.36	2.66 ± 0.34	2.91 ± 0.38	1.088 ± 0.162
MDA	0.027	0.026	0.017	0.020	0.014	0.025
Uranium-235	0.104 ± 0.034	0.061 ± 0.026	0.106 ± 0.034	0.132 ± 0.038	0.115 ± 0.036	0.064 ± 0.026
MDA	0.017	0.017	0.017	0.021	0.019	0.022
Uranium-238	1.80 ± 0.24	1.345 ± 0.192	2.81 ± 0.36	2.76 ± 0.36	2.91 ± 0.38	1.115 ± 0.163
MDA	0.019	0.023	0.021	0.018	0.019	0.022
Gross Alpha	1.42 ± 0.57	1.26 ± 0.61	1.70 ± 0.64	1.32 ± 0.63	1.38 ± 0.60	8.2 ± 1.9
Gross Beta	0.47 ± 0.48	1.77 ± 0.62	1.30 ± 0.57	1.03 ± 0.57	1.35 ± 0.57	4.16 ± 0.93
Gross Gamma	13.83 ± 1.80	14.80 ± 0.52	17.67 ± 0.70	16.74 ± 0.64	17.68 ± 0.62	Not analyzed
MDA	0.53	0.63	0.85	0.79	0.75	
Tritium	4.96 ± 0.66	17.1 ± 2.2	26.5 ± 3.4	28.3 ± 3.7	0.25 ± 0.05	0.495 ± 0.086
Organic Carbon (wt %)	<0.05	<0.05	<0.05	<0.05	<0.05	Not analyzed

Notes: 1. Activities are reported in picocuries per gram.

2. Error of two standard deviations is reported.

^a Bandelier Tuff–Tshirege Member.

^b Radionuclides and parameters analyzed by Paragon Analytics, Inc.

^c MDA = minimum detectable activity.

^d Bandelier Tuff–Otowi Member.

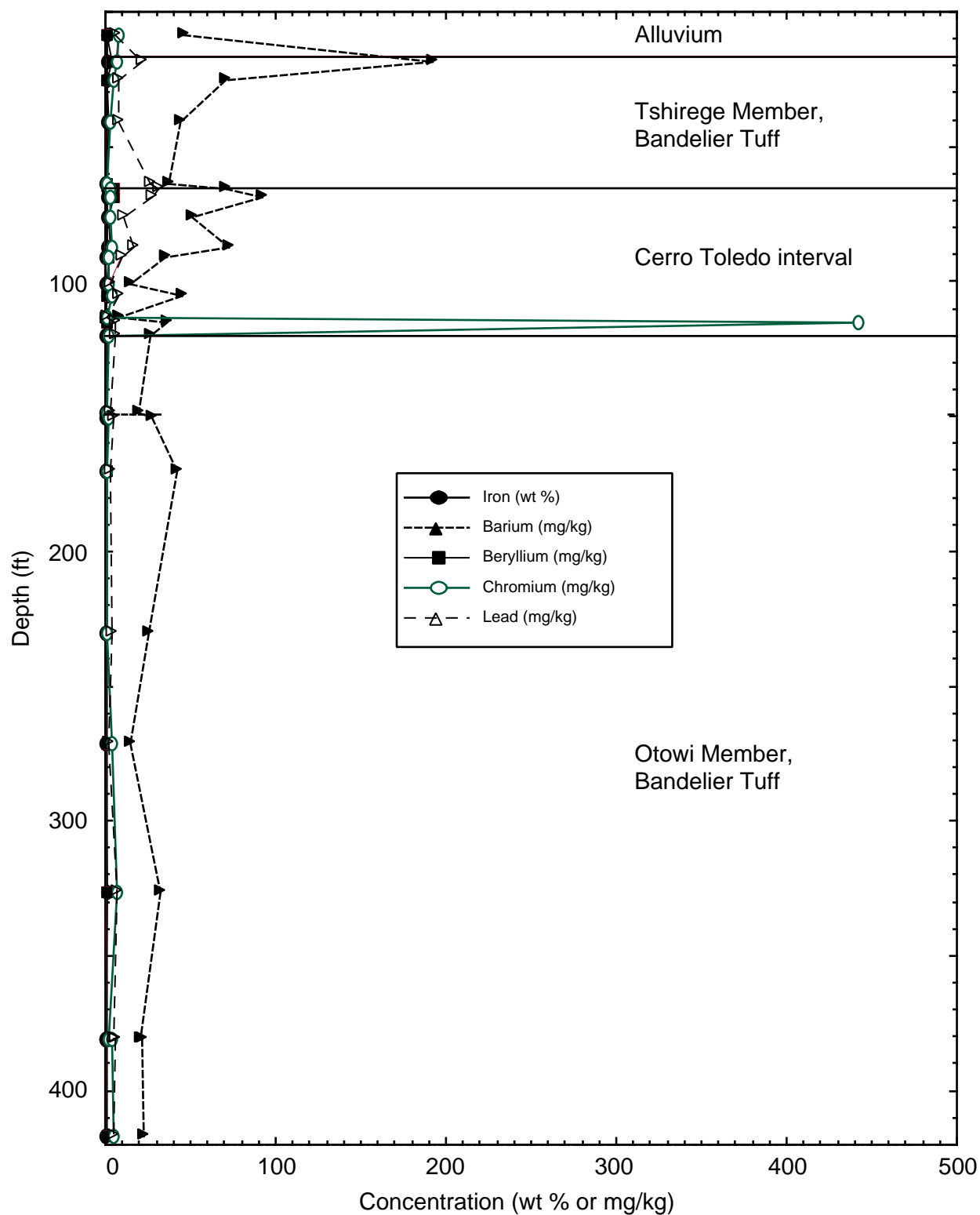
^e ICPMS = inductively coupled plasma mass spectrometry.

^f MDC = minimum detectable concentration.

Table 5.1-2
Tritium Activities and Moisture Contents in R-15 Core Samples

Depth (ft)	Tritium Activity		Moisture Content (wt %)	Hydrogeologic Unit
	(pCi/g)	(pCi/L)		
22.3	0.665	69.2	9.42	Tshirege Member
39.8	0.077	5.3	6.49	Tshirege Member
59.8	11.64	2374	16.94	Tshirege Member
69.8	7.78	3021	27.97	Cerro Toledo interval
84.8	6.39	1132	15.05	Cerro Toledo interval
104.8	3.99	502	11.18	Cerro Toledo interval
114.8	5.7	621	9.82	Cerro Toledo interval
144.8	12.11	2852	19.06	Otowi Member
169.8	18.3	3199	14.88	Otowi Member
229.8	2.88	567	14.46	Otowi Member
269.8	4.97	952	16.08	Otowi Member
319.8	21.8	5338	19.67	Otowi Member
379.8	22.2	5405	19.58	Otowi Member
414.8	0.216	54.3	20.08	Otowi Member

Concentrations of antimony, mercury, selenium, silver, and thallium in the solid samples are less than detection using ICPEES and CVAA methods. Distributions of iron, barium, beryllium, chromium, and lead within the alluvium, Bandelier Tuff, and Cerro Toledo interval at R-15 are shown in Figure 5.1-1. These elements generally are present above analytical detection limits, whereas antimony, arsenic, cadmium, cobalt, copper, iron, lead, mercury, manganese, nickel, selenium, silver, thallium, and vanadium are either not present (U value) or less than quantitation limits (B value). In general, concentrations of most of these elements are less than Laboratory background upper tolerance limits (UTLs) for the Bandelier Tuff. Concentrations of aluminum, barium, chromium, and iron, however, exceed the Laboratory's background UTL values, for the Bandelier Tuff in the R-15 core samples. This probably is due to the presence of clay minerals and hydrous iron oxides at the alluvium/Qbt 1g and Qbt 1g/Tsankawi contacts and within oxidized alteration zones within the Bandelier Tuff and Cerro Toledo interval. These solid phases were visually identified in the field characterized by clay nodules and iron staining. The XRD analyses (Table 3.1-1) show that these clay minerals are illites and smectites with minor amounts of kaolinite. Many transition metals, including cobalt, chromium, zinc, copper, manganese, nickel, and iron, occur naturally within hydrogeologic materials including the Bandelier Tuff, and they can become concentrated or redistributed on solid surfaces through adsorption processes (Langmuir 1997, 56037). Distributions of aluminum, arsenic, barium, calcium, chromium, iron, lead, manganese, and zinc at R-15 may be the result of natural processes, including chemical alteration (hydrolysis) of glass within the Bandelier Tuff. Groundwater zones were not encountered in the Bandelier Tuff at R-15, which, if present, can transport contaminants through the subsurface.



F5.1-1 / R-15 WELL COMPLETION RPT / 072100 / PTM

Figure 5.1-1. Variations in the concentrations of iron, barium, beryllium, chromium, and lead with depth from core samples collected in R-15, Mortandad Canyon

5.1.3 Stable Isotopes and Distributions of Anions

5.1.3.1 Methods

Core samples collected from R-15 were analyzed for stable isotopes and several anions, including bromide, chloride, fluoride, nitrate, nitrite, oxalate, perchlorate, phosphate, and sulfate. The stable isotope analyses ($\delta^{18}\text{O}$, δD) were performed on moisture-protected samples using the vacuum distillation method of Shurbaji and Campbell (1997, 64063) and the $\delta^{18}\text{O}$ and δD extraction methods of Socki et al. (1992, 64064) and Kendall and Coplen (1985, 64061), respectively. The analytical precision for the $\delta^{18}\text{O}$ and δD analyses by mass spectrometry was better than $\pm 0.2\text{‰}$ and $\pm 4\text{‰}$, respectively.

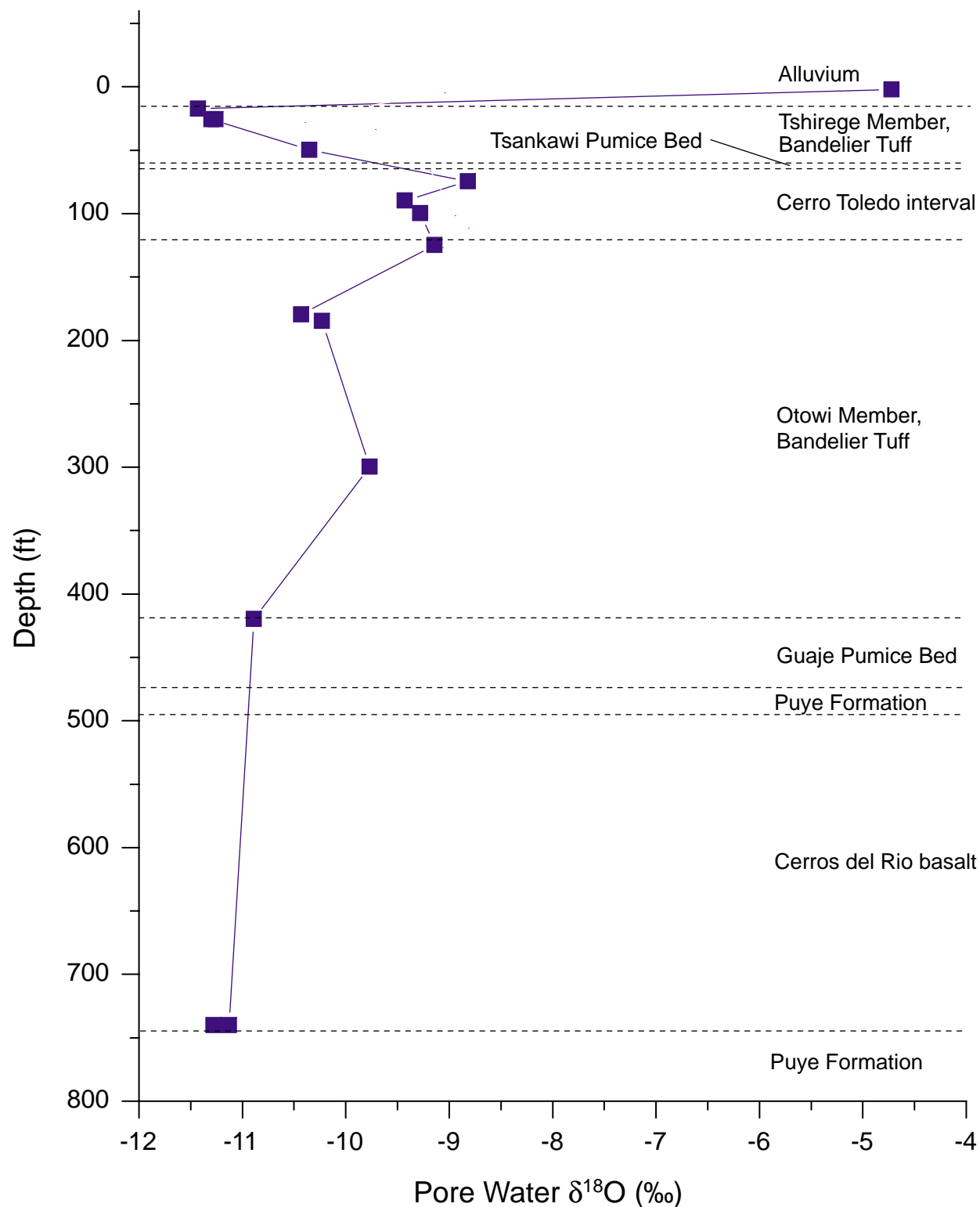
Pore water anion concentrations were calculated using leachate concentrations, gravimetric moisture contents, and bulk densities. Moisture content data are reported in Section 4.1.2. Bulk density has not been measured on the R-15 or MCO-7.2 samples; therefore estimates were used that are representative of typical values for the kind of rocks and sediments encountered. The bulk density estimates increase the uncertainty in the pore water concentrations. However, they are not expected to introduce significant error.

5.1.3.2 Stable Isotope Results

Both $\delta^{18}\text{O}$ and δD analyses were performed on core samples collected from the upper 420 ft of R-15 and from the upper 127 ft of MCO-7.2. Geologic units sampled included alluvium, Qbt 1g of the Bandelier Tuff, the Tsankawi Pumice Bed, the Cerro Toledo interval, and the Otowi Member. Interpretation of the $\delta^{18}\text{O}$ and δD results are similar for both boreholes and only the $\delta^{18}\text{O}$ results are discussed here because of their better precision. The $\delta^{18}\text{O}$ results for R-15 indicate an evaporative zone (heavy isotope value) at the top of the alluvium that is typical of the near-surface (Figure 5.1-2). This evaporative zone, however, was not sampled in MCO-7.2 (Figure 5.1-3). Below the Tsankawi pumice bed, oxygen isotope values appear to be in quasi-steady state. These values become slightly lighter down to 740 ft (saturated zone) in R-15. Core samples were not collected between 420 and 740 ft and consequently, stable isotope analyses were not performed for this depth interval. There, however, may be some isotopic variation between those depths. Results of stable isotope analyses for a groundwater sample collected from 740 ft are shown in Figure 5.1-2. The 740 ft stable isotope data were supplied by the New Mexico Environment Department's (NMED's) Department of Energy Oversight Bureau. Below the evaporative zone, the R-15 isotope profile shows little variation with depth as compared to borehole R-9 (Broxton et al. 2000, 66599). This suggests that the flow system in this part of Mortandad Canyon may be more homogeneous or better mixed than in the vicinity of R-9 in Los Alamos Canyon. Finally, the isotope profiles of R-15 and MCO-7.2 are similar, which like the anion profiles, suggests that both boreholes have seen a similar hydrologic and geochemical history.

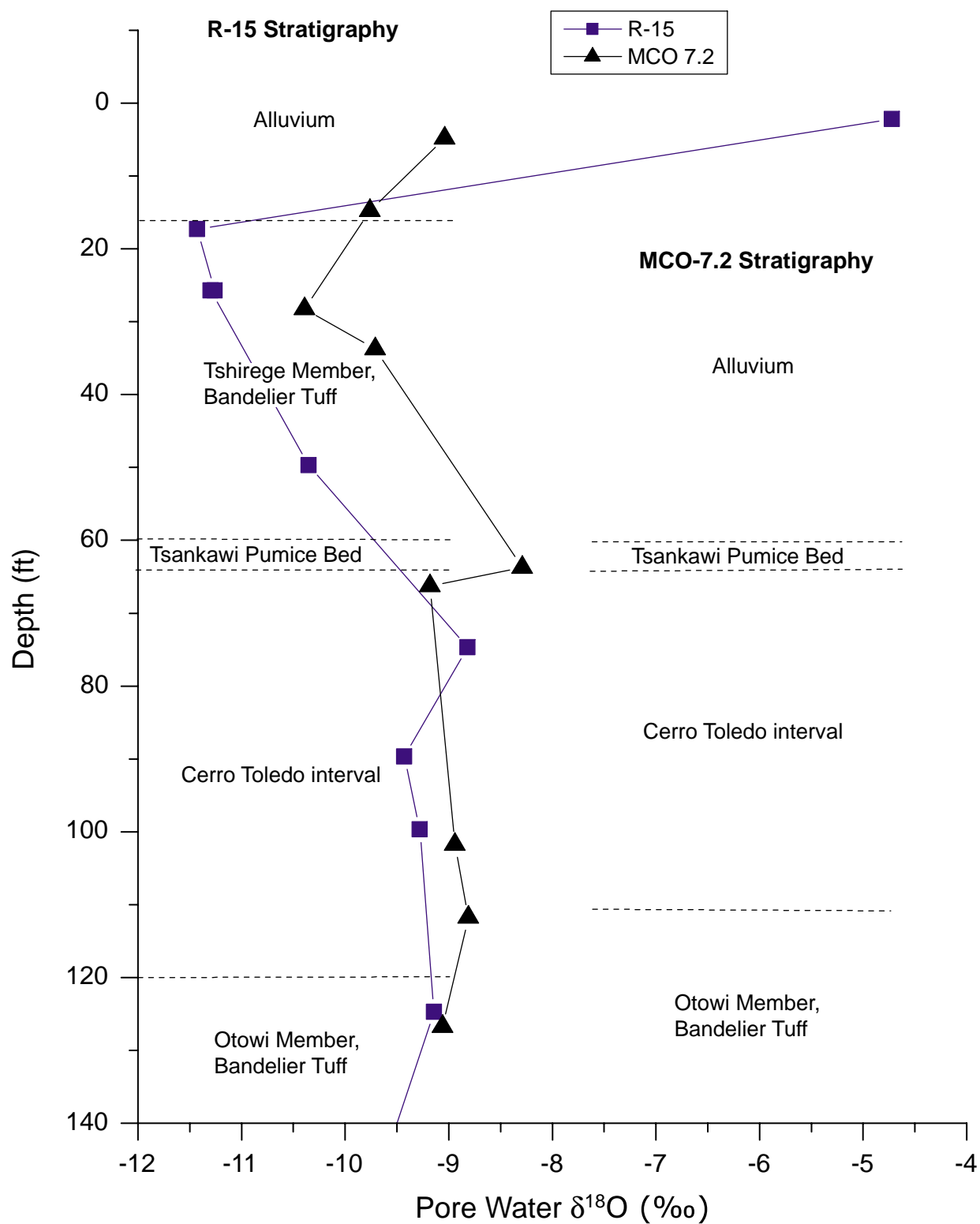
5.1.3.3 Anion Results

Core and cutting samples obtained from the R-15 and MCO-7.2 borehole were analyzed to obtain the vertical distributions of bromide, chloride, fluoride, nitrate, nitrite, oxalate, perchlorate, phosphate, and sulfate (Figures 5.1-4, 5.1-5, 5.1-6, and 5.1-7, Tables 5.1-3 and 5.1-4). The MCO-7.2 data are included because of its close proximity to R-15. MCO-7.2 is an alluvial borehole that is closer to the Mortandad Canyon channel than R-15. The R-15 anion samples are co-located with the moisture and matric potential samples described in this report. The sampling and analytical methods used were previously described in the R-9 well completion report (Broxton et al. 2000, 66599).



F5.1-2 / R-15 WELL COMPLETION RPT / 072500 / PTM

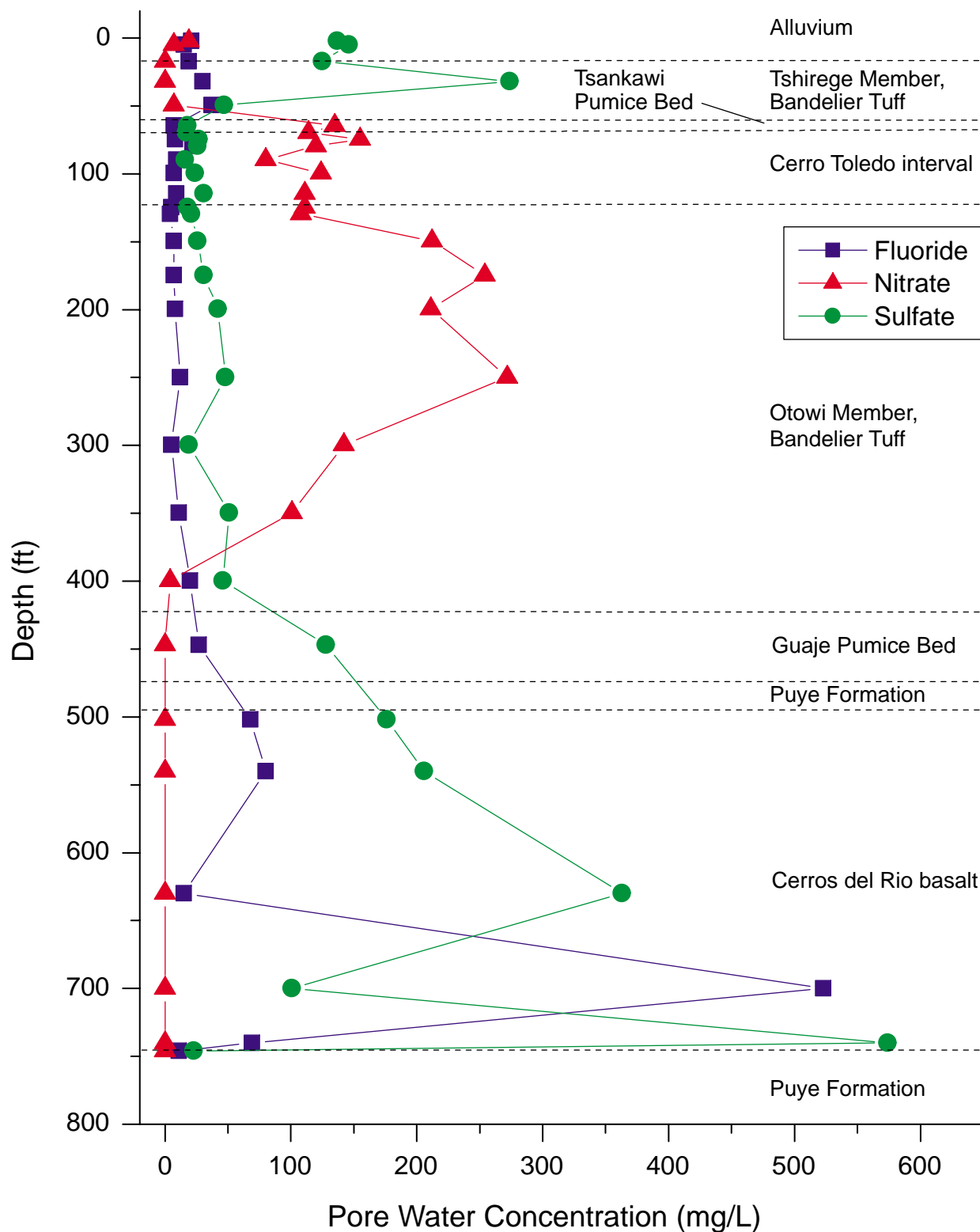
Figure 5.1-2. Pore water $\delta^{18}\text{O}$ profile for borehole R-15



Note: R-15 stratigraphy on left and MCO 7.2 on right.

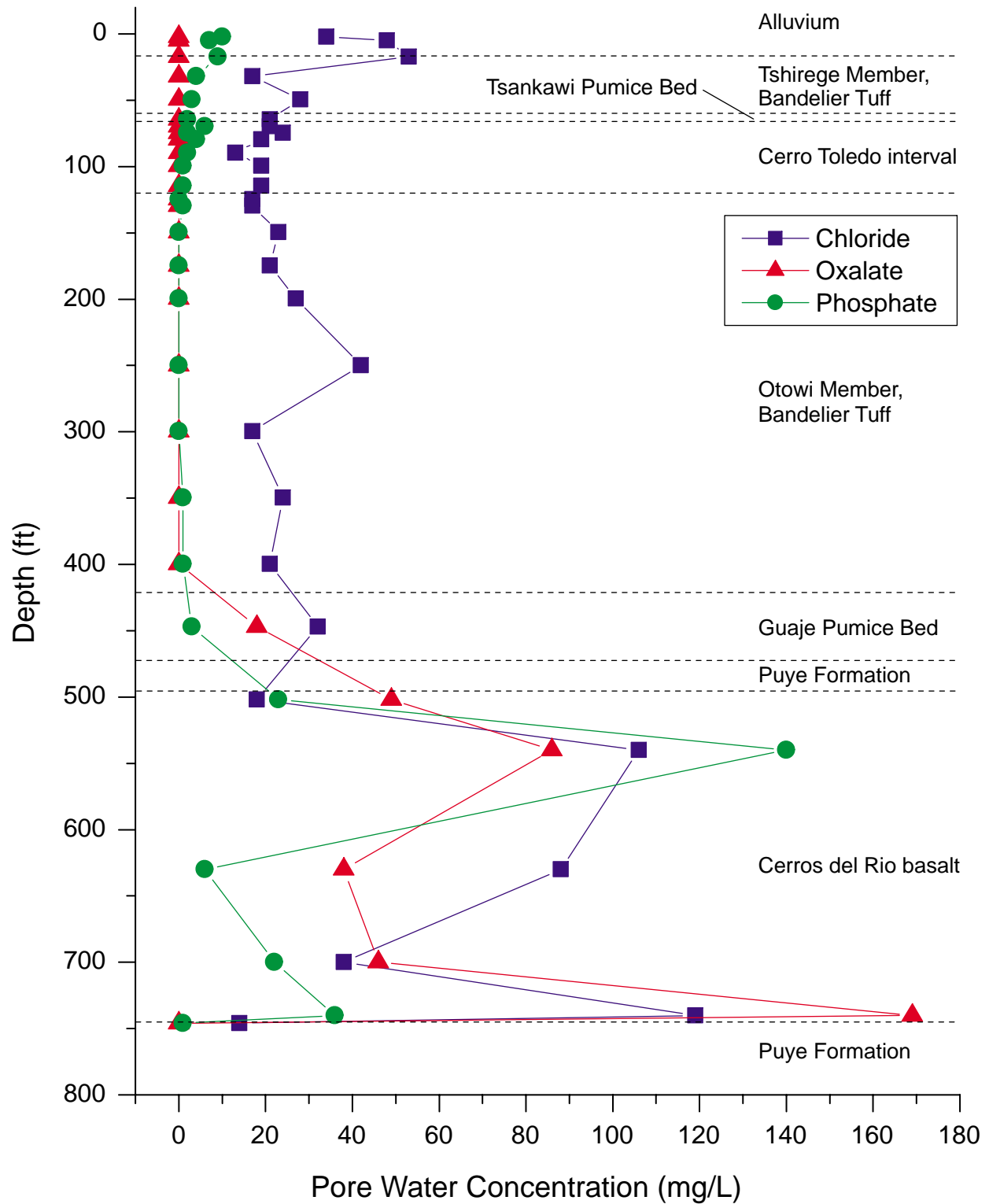
F5.1-3 / R-15 WELL COMPLETION RPT / 081700 / PTM

Figure 5.1-3. Pore water $\delta^{18}\text{O}$ profile for borehole R-15 and MCO-7.2



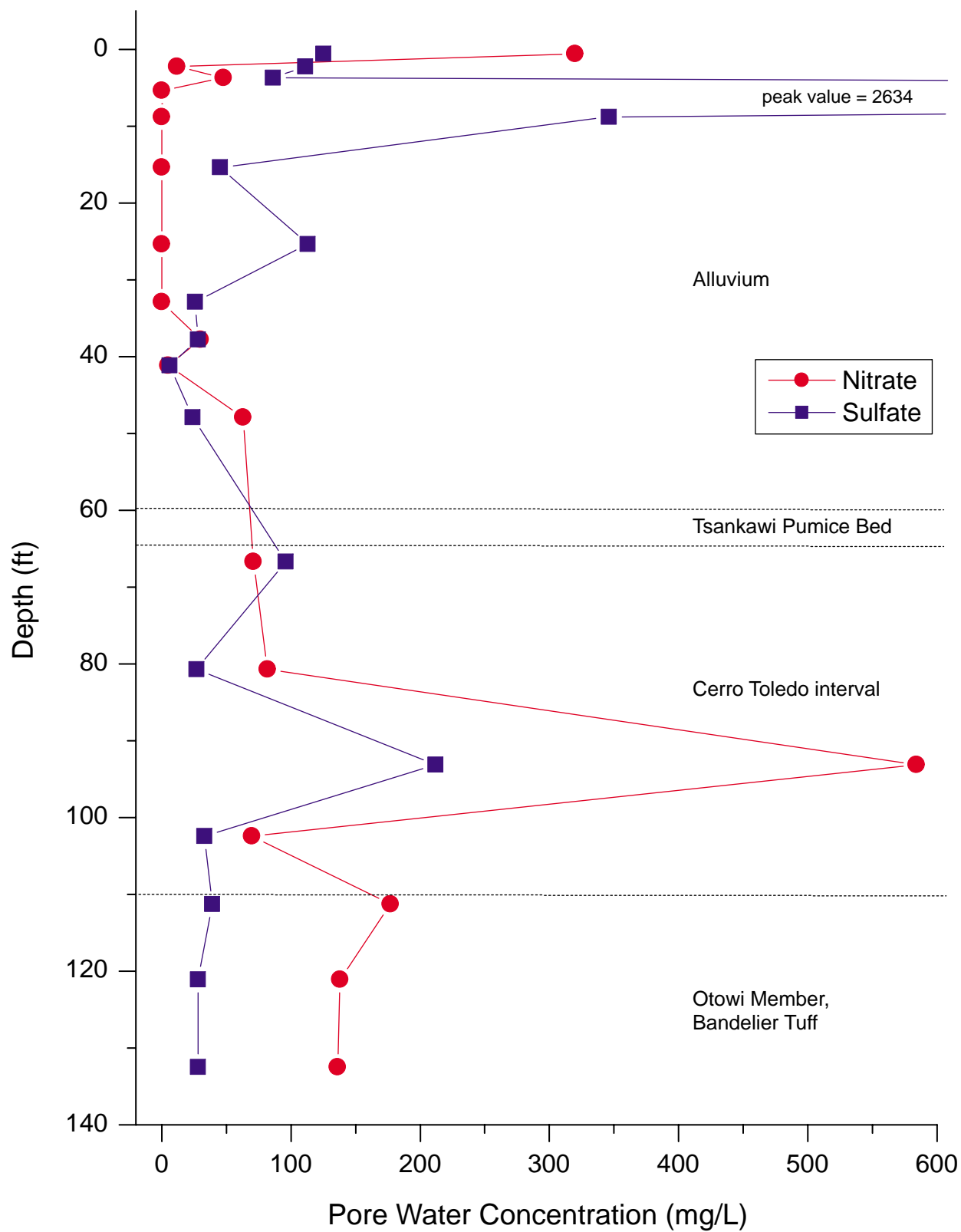
F5.1-4 / R-15 WELL COMPLETION RPT / 072400 / PTM

Figure 5.1-4. Pore water fluoride, nitrate, and sulfate concentrations for borehole R-15



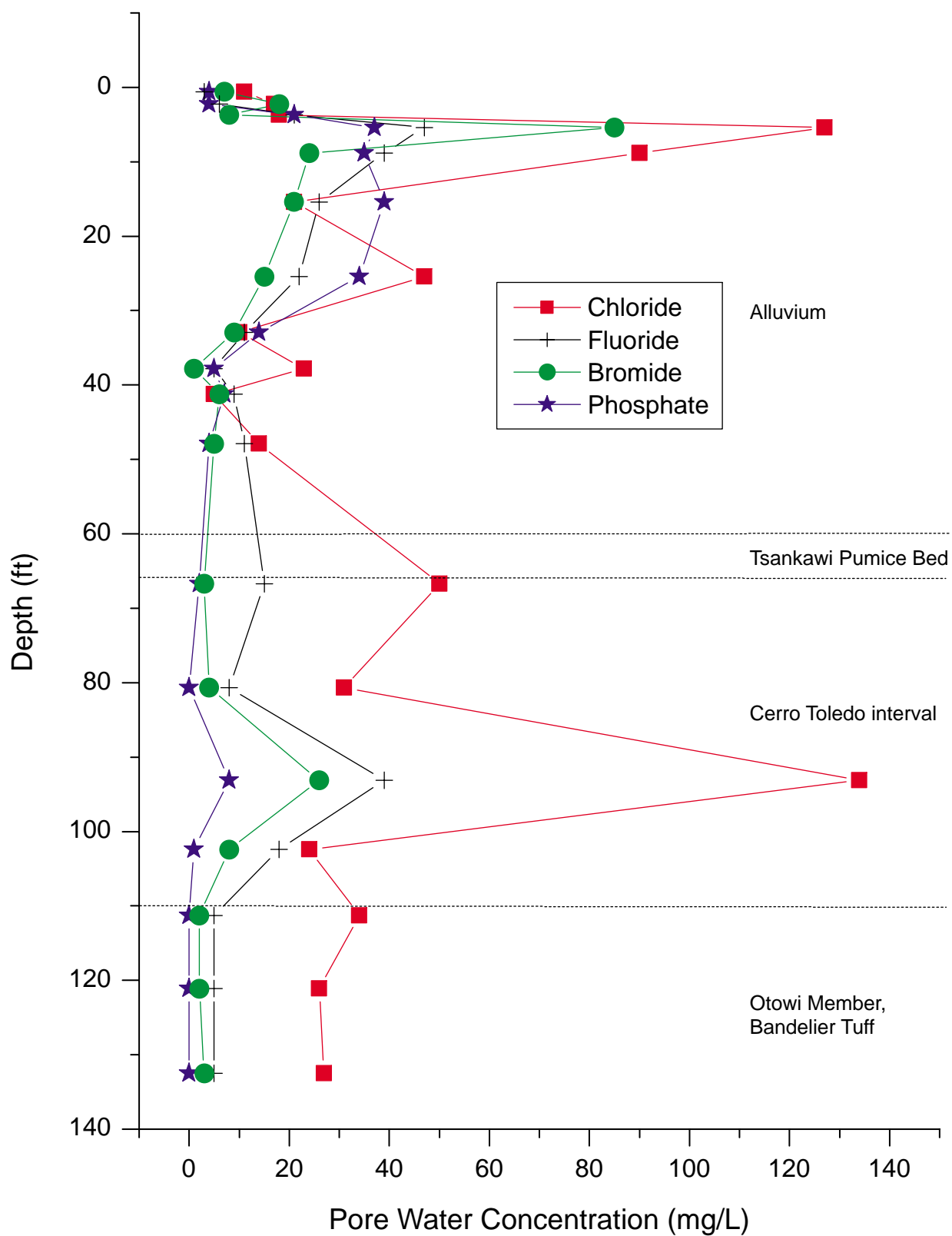
F5.1-5 / R-15 WELL COMPLETION RPT / 072400 / PTM

Figure 5.1-5. Pore water chloride, oxalate, and phosphate concentrations for borehole R-15



F5.1-6 / R-15 WELL COMPLETION RPT / 072400 / PTM

Figure 5.1-6. Pore water nitrate and sulfate concentrations for borehole MCO-7.2



F5.1-7 / R-15 WELL COMPLETION RPT / 072400 / PTM

Figure 5.1-7. Pore water chloride, fluoride, bromide, and phosphate concentrations for borehole MCO-7.2

Table 5.1-3
R-15 Anion Pore Water Concentrations

Depth (ft)	Bromide ^a	Chloride ^a	Fluoride ^a	Nitrate ^a	Nitrite ^a	Oxalate ^a	Perchlorate ^b	Phosphate ^a	Sulfate ^a
2	1	34	21	19	13	BD ^c	BD	10	137
5	1	48	15	7	66	BD	BD	7	146
17	BD	53	19	BD	BD	BD	BD	9	125
32	BD	17	30	BD	BD	BD	BD	4	274
49.5	BD	28	37	7	BD	BD	653	3	47
64.5	BD	21	7	135	BD	BD	167	2	18
69.5	BD	21	15	114	BD	BD	136	6	17
74.5	BD	24	8	155	BD	BD	160	2	27
79.5	BD	19	22	120	BD	BD	144	4	26
89.5	BD	13	9	80	BD	BD	107	2	16
99.5	BD	19	7	124	BD	BD	189	1	24
114.5	BD	19	9	111	BD	BD	122	1	31
124.5	BD	17	5	111	BD	BD	140	BD	18
129.5	BD	17	4	108	BD	BD	181	1	21
149.5	BD	23	7	212	BD	BD	261	BD	26
174.5	BD	21	7	254	BD	BD	267	BD	31
199.5	BD	27	8	211	BD	BD	246	BD	42
249.8	BD	42	12	272	BD	BD	403	BD	48
299.5	BD	17	5	142	BD	BD	241	BD	19
349.5	BD	24	11	101	BD	BD	260	1	51
399.6	BD	21	20	4	BD	BD	359	1	46
447	BD	32	27	BD	BD	18	BD	3	128
502	BD	18	68	BD	BD	49	BD	23	176
540	BD	106	80	BD	BD	86	BD	140	206
630	BD	88	15	BD	BD	38	BD	6	363
700	BD	38	523	BD	BD	46	BD	22	101
740	BD	119	69	BD	BD	169	1662	36	574
746	1	14	11	BD	BD	BD	83	1	23

^a mg/L.^b µg/L.^c BD = below detection.

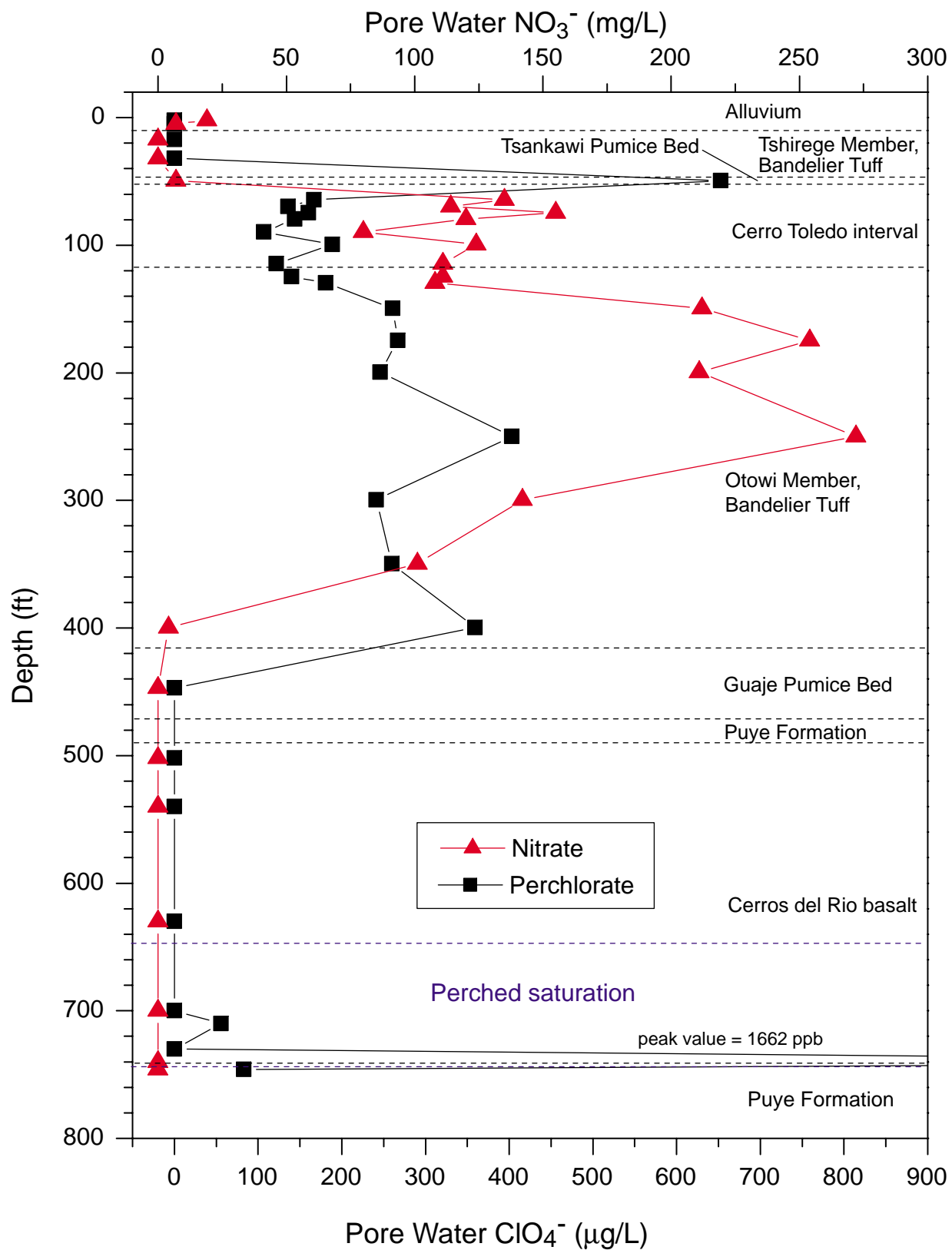
Table 5.1-4
MCO-7.2 Anion Pore Water Concentrations

Depth (ft)	Bromide ^a	Chloride ^a	Fluoride ^a	Nitrate ^a	Nitrite ^a	Oxalate ^a	Perchlorate ^b	Phosphate ^a	Sulfate ^a
0.6	7	11	3	320	648	BD ^c	BD	4	125
2.25	18	17	6	12	7	BD	279	4	111
3.7	8	18	21	48	2	BD	BD	21	86
5.4	85	127	47	BD	BD	BD	BD	37	2634
8.8	24	90	39	BD	BD	BD	2821	35	346
15.4	21	21	26	BD	BD	BD	BD	39	45
25.4	15	47	22	BD	BD	BD	BD	34	113
32.9	9	10	11	BD	BD	BD	26	14	26
37.8	1	23	5	30	BD	BD	202	5	28
41.2	6	5	9	5	BD	BD	30	7	6
47.9	5	14	11	63	BD	BD	179	4	24
66.7	3	50	15	71	BD	BD	130	2	96
80.7	4	31	8	82	BD	BD	251	0	27
93.1	26	134	39	584	BD	BD	689	8	212
102.4	8	24	18	70	BD	BD	138	1	33
111.3	2	34	5	177	BD	BD	211	BD	39
121.1	2	26	5	138	BD	BD	186	BD	28
132.5	3	27	5	136	BD	BD	170	BD	28

^a mg/L.^b µg/L.^c BD = below detection.

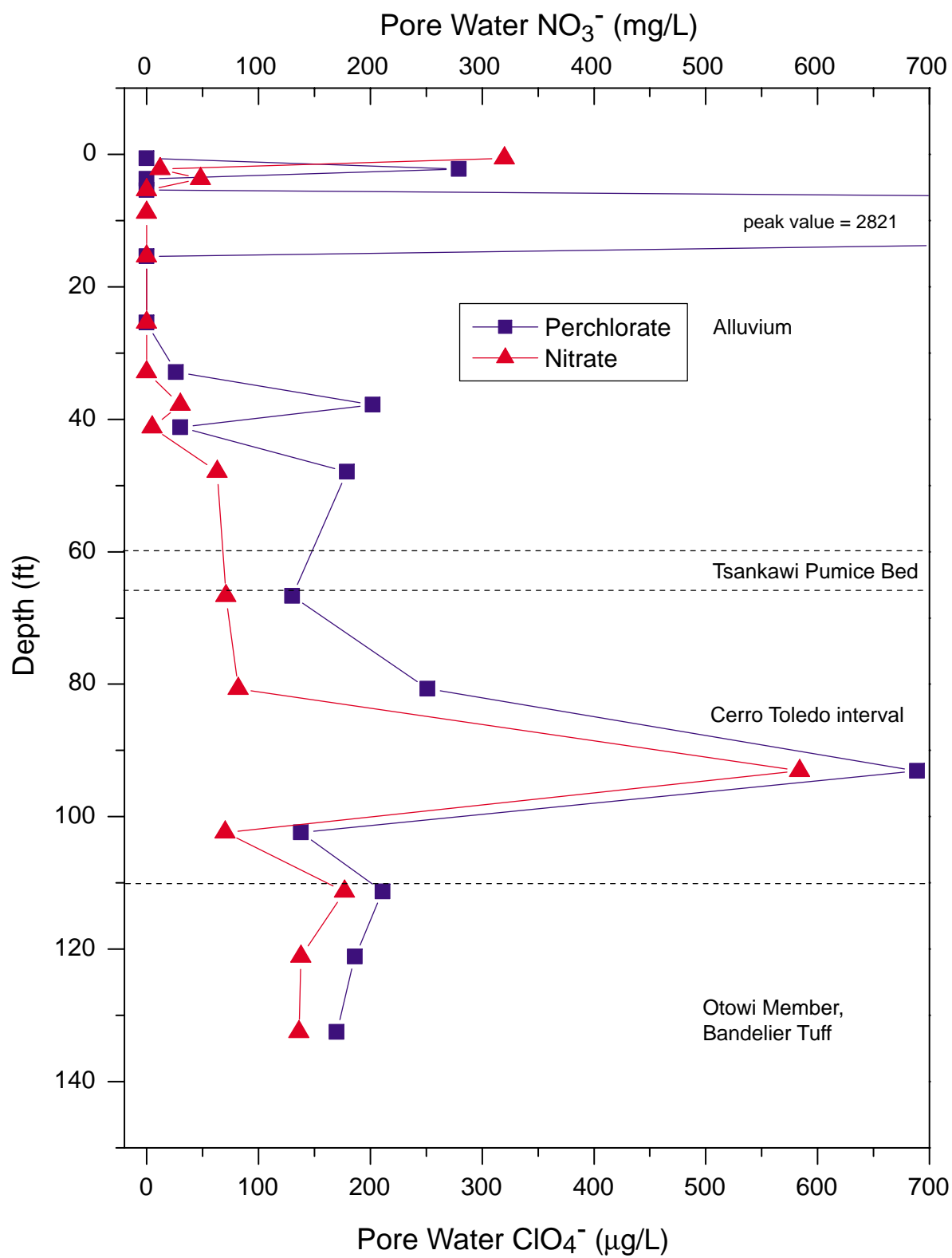
Because perchlorate concentrations are reported in µg/L, they are plotted separately from the other anions (Figures 5.1-8 and 5.1-9). Several samples collected from R-15 had bromide, nitrite, and oxalate below the detection limit (Table 5.1-3). Oxalate concentrations in MCO-7.2 samples were all less than detection, whereas nitrite was detected in three samples (Table 5.1-4). As a result, these anions are not shown in the figures. The lack of detection does not mean that these species are not present in the samples. Instead, the leaching process results in substantial dilution, and when an anion has a low concentration, the dilution can lower the concentration below the detection limit. In general, anion distributions in the two boreholes showed similar behavior with depth and have multi-peaked profiles. The increase in anion concentrations in R-15 between 700 and 740 ft are close to the Cerros del Rio basalt/Puye Formation contact and may be related to the perched saturated zone located at 646 to 740 ft.

In the case of both R-15 and MCO-7.2, there are some important observations regarding distributions of nitrate and perchlorate. In R-15, the highest nitrate concentrations occur within the Cerro Toledo interval and Otowi Member (65–400 ft) (Figure 5.1-8). Nitrate concentrations decline substantially below 400 ft and remain at relatively low values throughout the deeper part of the profile. In borehole MCO-7.2, high nitrate concentrations occur in the top 5 ft of the borehole and also within the Cerro Toledo interval and Otowi Member (80–130 ft) (Figure 5.1-9). The concentrations in both boreholes are well above those observed in the vadose zone elsewhere at the Laboratory (Table 5.1-5). These values indicate that the high concentrations are the result of contamination. The TA-50 outfall is a known source of nitrate that flows into Mortandad canyon, and previous studies have noted elevated nitrate in the Mortandad alluvium (Rogers and Gallaher 1995, 49824).



F5.1-8 / R-15 WELL COMPLETION RPT / 072500 / PTM

Figure 5.1-8. Pore water nitrate and perchlorate concentrations for borehole R-15



F5.1-9 / R-15 WELL COMPLETION RPT / 072500 / PTM

Figure 5.1-9. Pore water nitrate and perchlorate concentrations for borehole MCO-7.2

Table 5.1-5
Nitrate Pore Water and Cumulative Concentrations for Five Boreholes

Borehole	Average Conc.^a	Max Conc.^a	Cum. to 132 ft^b	Cum. to 667 ft^b
MCO-7.2	96	584	720	TS ^c
R-15	82	272	766	3398
R-9	6	18	1	57
R-12	1	16	13	41.1
R-25	0	0.6	0	1.2

^a mg/L.

^b g/m²; the depth of 132 ft was selected to represent the shallow vadose zone based on the maximum depth of MCO-7.2; the depth of 667 ft represents the deepest samples collected for R-25 and represents a deeper sampling of the vadose zone.

^c TS = too shallow; the max depth of the borehole is 132 ft.

In addition to nitrate, perchlorate is present in the vadose zone in both R-15 and MCO-7.2 (Figures 5.1-8 and 5.1-9). The perchlorate concentration profiles are similar between the two boreholes, indicating that the two locations have been subject to similar hydrogeochemical processes (movement of conservative or nonsorbing species). However, there are differences in perchlorate distributions between the boreholes. In MCO-7.2, the perchlorate profile shows a high concentration shallow peak at about 15 ft in the alluvium that is not present in R-15. In addition, MCO-7.2 has a second peak in the Cerro Toledo interval that is apparently displaced about 45 ft deeper than the R-15 peak. These concentration differences may be related to the proximity of MCO-7.2 to the Mortandad Canyon channel. The perchlorate concentration profiles are also similar in shape to the nitrate profiles (Figures 5.1-8 and 5.1-9), which reflect the fact that the two contaminants have the same source and because of their generally similar anion mobility in vadose and saturated zones. In the Tshirege unit Qbt 1g and deeper strata, both boreholes show perchlorate concentrations above 100 µg/L. In R-15, perchlorate concentrations drop off dramatically around 400 ft along with nitrate (Figure 5.1-8). Perchlorate concentrations remain below detection until the perched saturated zone within the Cerros del Rio basalt is encountered. The samples analyzed from this zone, however, were not saturated and some samples had large perchlorate concentrations (although no nitrate). Water collected directly from the borehole in the saturated interval contained perchlorate (see Section 5.2.2.1). Thus, perchlorate distributions observed in core samples collected from the vadose zone may be related to those observed in the saturated interval. A core sample collected at 740 ft contained 1662 µg/L perchlorate. This sample consisted of basalt and a clay-rich material (see Section 3.1.7.3 of this report). Basalt and clay-rich material separates were leached with deionized water for 72 hr and no perchlorate was found in the basalt sample. However, substantial concentrations of perchlorate were associated with the clay-rich separate. Increased concentrations of perchlorate within the perching layer are probably a result of a longer residence time, which allows for less dilution of solutes. Recharge to this perched saturated zone probably occurs west of R-15, which also influences solute distributions in the perching layer. This example illustrates how the different stratigraphic units are controlling not only groundwater flow in the canyon subsurface but contaminant distributions as well.

5.2 Hydrogeochemistry of Groundwater Samples

Groundwater samples were collected at depths of 482, 646, 1007, and 1100 ft and analyzed for screening constituents and parameters. Additional groundwater samples shall be collected after the R-15 well has been properly developed and all residual drilling mud has been extracted. Borehole water samples were analyzed for inorganic and organic chemicals and radionuclides to determine natural solute and contaminant distributions within the different saturated zones.

5.2.1 Methods

Groundwater samples for inorganic and organic chemicals and radionuclides were collected using a stainless-steel bailer. Temperature, turbidity, pH, and specific conductance were determined onsite from an aliquot collected during field sampling. Both filtered and nonfiltered samples were collected for chemical and radiochemical analyses. Groundwater samples were collected for analyses of dissolved organic carbon (DOC); stable isotopes of hydrogen, oxygen, and nitrogen; major cations and anions; metals; organic compounds; and radionuclides. Aliquots of the samples were pressure-filtered (nitrogen gas) through a 0.45- μm Gelman filter and acidified with analytical-grade HNO_3 to a pH of 2.0 or less for metal and radionuclide analyses. DOC samples were filtered with a special 0.45- μm silver filter to eliminate biodegradation of organic solutes, which may bias analytical results. All groundwater samples collected in the field were stored at 4°C until they were analyzed. Alkalinity was determined in the laboratory using standard titration techniques.

Groundwater samples were analyzed using techniques specified in EPA method SW-846 including IC for bromide, chloride, fluoride, oxalate, nitrate, nitrite, perchlorate, phosphate, and sulfate; graphite furnace atomic absorption (GFAA) for trace elements (aluminum, antimony, arsenic, barium, beryllium, boron, cadmium, calcium, cesium, chromium, cobalt, copper, iron, lead, lithium, magnesium, manganese, molybdenum, nickel, potassium, rubidium, selenium, silicon, silver, sodium, strontium, thallium, tin, titanium, vanadium, and zinc); colorimetry for total cyanide; CVAA for mercury; and ICPES for aluminum, antimony, arsenic, barium, beryllium, boron, cadmium, calcium, chromium, cobalt, copper, iron, lead, magnesium, manganese, molybdenum, nickel, potassium, selenium, sodium, thallium, vanadium, and zinc. This work was performed by a contract laboratory, Paragon Analytics, Inc. (IC, CVAA, and ICPES methods), and EES-1 (screening samples using IC and AA methods).

Tritium activity in groundwater was determined by liquid scintillation counting (LSC), direct counting for tritium (obtained by NMED's Department of Energy Oversight Bureau from the University of Miami), and electrolytic enrichment for low-level tritium; laser-induced kinetic phosphorimetric analysis (LIKPA) and inductively coupled plasma mass spectrometry (ICPMS) for antimony, beryllium, cadmium, lead, thallium, and uranium for groundwater samples collected after R-15 is developed; alpha spectrometry for americium, plutonium, and uranium isotopes; gamma spectrometry for cesium-137 and other isotopes; and gas proportional counting for strontium-90. This work was performed by contract laboratories including Paragon Analytics, Inc., GEL, Teledyne, CST-9, and the University of Miami.

Stable isotopes of oxygen (oxygen-18 and oxygen-16, $\delta^{18}\text{O}$) and hydrogen (hydrogen and deuterium, δD) were analyzed by Geochron Laboratories (Cambridge, Massachusetts) using isotope ratio mass spectroscopy (IRMS). Nitrogen isotopes (nitrogen-15 and nitrogen-14, $\delta^{15}\text{N}$) were analyzed by Coastal Science Laboratories, Inc. (Austin, Texas) using IRMS.

Laboratory blanks and field blanks were collected and analyzed in accordance with EPA and Laboratory procedures. The precision limits for major ions and trace elements were generally $\pm 10\%$.

A sample of drilling mud was collected from a potential zone of saturation (see Section 4.2.1.3) at 482 ft in the upper section of the Puye Formation and analyzed for tritium. Groundwater samples were collected at 646 ft within the perched zone in the Cerros del Rio basalt, and at 1007 and 1100 ft within the regional aquifer (Puye Formation). The groundwater sample collected from 646 ft was analyzed for semivolatile organic compounds (high explosive [HE] compounds, polychlorinated biphenyls [PCBs] and pesticides) using gas chromatography-mass spectrometry and high pressure liquid chromatography by Paragon Analytics, Inc.

5.2.2 Major Ion and Trace Element Chemistry

5.2.2.1 Quality of Groundwater Within Cerros del Rio Basalt

Field-measured parameters for the borehole groundwater samples, including pH, temperature, specific conductance, and turbidity, are provided in Table 5.2-1. These parameters were measured at the time of sample collection when groundwater was in contact with the atmosphere. Turbidity was also measured; however, turbidity values are qualitative due to the presence of bentonite colloids produced from the drilling mud and disaggregated aquifer material produced by drilling.

Table 5.2-1
Field-Measured Parameters for Groundwater Samples Collected at R-15

Geologic Unit	Cerros del Rio basalt	Puye Formation	Puye Formation
Depth (ft)	646	1007	1100
Date sampled	7/22/99	8/23/99	8/27/99
pH (standard units)	7.71	8.13	8.04
Temperature (°C)	16.8	19.8	22.1
Specific conductance (µSi/cm)	334	210	166
Turbidity (NTU) ^a	os ^b	os ^b	os ^b

Note: Perched zone occurs at 646 ft.

^a NTU = nephelometric turbidity unit.

^b os = off the scale because of very high turbidity values for open-borehole groundwater samples.

Groundwater from the perched zone in R-15 is dominantly a sodium-calcium-bicarbonate type as represented by the samples collected at a depth of 646 ft. Screening analytical results for the 646-ft perched zone are provided in Table 5.2-2. Only analytical results from filtered groundwater samples are reported due to the high bentonite (drilling mud) content present in the nonfiltered samples. Sodium concentrations in R-15 are mainly due to the presence of colloidal (sodium-rich) bentonite used during drilling. Based on analytical results from screening data, this perched groundwater was found to contain 3770 ± 850 pCi/L tritium, 11.5 parts per million (ppm) dissolved chloride, 63.9 ppm dissolved sodium, 1.15 ppm dissolved fluoride, 35.4 ppm dissolved sulfate, <0.02 ppm dissolved ammonium, <0.01 ppm nitrate (as nitrate), and 1.2 parts per billion (ppb) dissolved uranium. Under oxidizing conditions, uranium is predicted to predominately occur as $\text{UO}_2(\text{CO}_3)_2^{2-}$ (55.3%) and $\text{UO}_2(\text{CO}_3)_3^{4-}$ (41.8%) within the perched zone, based on model simulations using the computer code MINTEQA2 (Allison et al. 1991, 49930). These uranyl carbonate complexes are semisorbing onto hydrous ferric oxide and are not completely removed from aqueous solution (Langmuir 1997, 56037). The major ion chemistry of this perched zone is similar to that of the TA-50 treated discharge water (LANL 1997, 56835) and alluvial groundwater (Environmental Surveillance and Compliance Programs 1997, 56684) in Mortandad Canyon. Sulfate, fluoride, and tritium are solutes associated with the TA-50 discharge (LANL 1997, 56835), which are not significantly adsorbed at near-neutral pH conditions.

Perchloric acid (HClO_4) is used in actinide research conducted at the Laboratory and is a constituent of the treated effluent discharged from TA-50. Perchloric acid is a strong oxidizing agent. Perchloric acid dissociates to perchlorate at negative pH values ranging from -4.8 to -2.12, depending on the hydration state of the acid. Perchlorate (ClO_4^-) was detected at 12 ppb in a groundwater screening sample collected from the 646 ft perched zone. A groundwater sample collected from 1100 ft within the regional aquifer did not contain perchlorate (<0.002 ppb). Perchlorate has been detected in alluvial groundwater in 1999.

within Mortandad Canyon, ranging from 80 to 200 ppb. Perchlorate is mobile in groundwater and this anion does not adsorb onto aquifer material under near-neutral pH conditions. Perchlorate is not easily reduced to chloride (Cl⁻) under aerobic conditions typical of the canyon.

Table 5.2-2
Hydrochemistry of Borehole R-15, Mortandad Canyon

Depth (ft)	646	1007	1100
Geologic Unit	CR basalt	Puye Formation	Puye Formation
Sample Treatment	Filtered	Filtered	Filtered
Date Sampled	07/22/99	08/23/99	08/27/99
Temp °C	16.8	19.8	22.1
Ag (ppm)	<0.001	— ^a	<0.001
Std. Dev. (+/-)	—	—	—
Al (ppm)	<0.02	<0.02	<0.02
Std. Dev. (+/-)	—	—	—
Alk (Lab) (ppm CaCO ₃)	124	79.7	84.4
As (ppm)	0.0004	0.0002	0.0006
B (ppm)	0.029	0.046	0.041
Std. Dev. (+/-)	0.003	0.002	0.002
Ba (ppm)	0.030	0.015	0.031
Std. Dev. (+/-)	0.001	0.001	0.001
Be (ppm)	<0.002	<0.002	<0.002
Std. Dev. (+/-)	—	—	—
Br (ppm)	0.12	0.02	0.04
Ca (ppm)	18.4	6.93	12.3
Std. Dev. (+/-)	0.1	0.04	0.1
Cd (ppm)	<0.001	—	<0.001
Std. Dev. (+/-)	—	—	—
Cl (ppm)	11.5	4.47	3.20
ClO ₄ (ppm)	0.012	<0.002	<0.002
ClO ₃ (ppm)	<0.02	<0.02	<0.02
Co (ppm)	0.002	<0.002	<0.002
Std. Dev. (+/-)	0.002	—	—
CO ₃ (ppm)	0	0	0
Cond. (Lab) (µS/cm)	396	221	216
Cr (ppm)	<0.002	<0.002	<0.002
Std. Dev. (+/-)	—	—	—
Cs (ppm)	<0.002	<0.002	<0.002
Std. Dev. (+/-)	—	—	—
Cu (ppm)	0.003	<0.002	0.002
Std. Dev. (+/-)	0.002	—	0.002

Note: The data in this table should be used only for screening purposes.

Table 5.2-2 (continued)

Depth (ft)	646	1007	1100
Geologic Unit	CR basalt	Puye Formation	Puye Formation
Sample Treatment	Filtered	Filtered	Filtered
Date Sampled	07/22/99	08/23/99	08/27/99
F (ppm)	1.15	0.22	0.29
Fe (ppm)	0.01	0.17	<0.01
Std. Dev. (+/-)	0.01	0.01	—
Hardness (CaCO ₃ ppm)	62.6	25.1	46
HCO ₃ (ppm)	151	97.2	103
Hg (ppm)	0.00040	<0.00005	<0.00005
I (ppm)	<0.01	<0.01	<0.01
K (ppm)	3.34	4.3	3.33
Std. Dev. (+/-)	0.01	0.02	0.02
Li (ppm)	0.04	0.03	0.04
Std. Dev. (+/-)	0.01	0.01	0.01
Mg (ppm)	4.05	1.90	3.83
Std. Dev. (+/-)	0.01	0.02	0.01
Mn (ppm)	0.28	0.059	0.11
Std. Dev. (+/-)	0.01	0.02	0.01
Mo (ppm)	0.07	0.02	0.014
Std. Dev. (+/-)	0.01	0.01	0.002
Na (ppm)	60.9	36.6	27.0
Std. Dev. (+/-)	0.9	0.02	0.1
NH ₄ (ppm)	0.07	0.05	0.04
Ni (ppm)	0.014	<0.002	0.003
Std. Dev. (+/-)	0.002	—	0.002
NO ₂ (ppm)	<0.01	0.81	<0.01
NO ₃ (ppm)	<0.01	6.71	<0.01
Oxalate (ppm)	<0.02	0.47	<0.02
Pb (ppm)	<0.002	<0.002	<0.002
Std. Dev. (+/-)	—	—	—
pH (Lab)	8.01	8.08	7.47
PO ₄ (ppm)	<0.02	<0.02	<0.02
Rb (ppm)	0.006	0.006	0.006
Std. Dev. (+/-)	0.002	0.002	0.002
Sb (ppm)	0.0006	0.0004	0.0017
Se (ppm)	<0.0001	<0.0001	<0.0001
Si (ppm)	13.9	19.9	25.6
Std. Dev. (+/-)	0.1	0.1	0.2

Table 5.2-2 (continued)

Depth (ft)	646	1007	1100
Geologic Unit	CR basalt	Puye Formation	Puye Formation
Sample Treatment	Filtered	Filtered	Filtered
Date Sampled	07/22/99	08/23/99	08/27/99
SiO ₂ (ppm calc)	29.7	42.6	54.8
SO ₄ (ppm)	35.4	15.4	15.1
S ₂ O ₃ (ppm)	<0.01	<0.01	<0.01
Sn (ppm)	<0.005	<0.005	<0.005
Sr (ppm)	0.11	0.035	0.059
Std. Dev. (+/-)	0.01	0.001	0.001
Ti (ppm)	<0.002	0.002	<0.002
Std. Dev. (+/-)	—	0.001	—
Tl (ppm)	<0.002	<0.002	<0.002
V (ppm)	0.008	<0.002	<0.002
Std. Dev. (+/-)	0.002	—	—
Zn (ppm)	0.01	<0.01	<0.01
Std. Dev. (+/-)	0.01	—	—
TDS (ppm)	378.9	243.2	269.7
Cation Sum (meq/L) ^b	4.0048	2.229	2.209
Anion Sum (meq/L)	3.599	2.180	2.111
Balance (%)	+10.76	+2.22	+4.24

^a A dash in the table means "not analyzed" or sample concentration was below detection limit and no standard deviation was determined.

^b meq/L = milliequivalents per liter.

Oxidation of chloride ion to perchlorate in aqueous solution is given by the following half reaction:



This oxidation reaction is represented by

$$\text{Eh (volts)} = 1.39(\text{volts}) - 0.0592\text{pH},$$

where Eh is the oxidation-reduction potential for the half reaction and activity of Cl⁻ is equal to the activity of ClO₄⁻.

At a pH value of zero, chloride ion is stable relative to perchlorate ion at Eh values less than 1.39 volts; perchlorate and chloride are at equilibrium at an Eh value of 1.39 volts; and perchlorate is stable above an Eh value of 1.39 volts. This oxidation is also dependent on pH and at pH7, chloride is stable below an Eh value of 0.98 volt. Due to four strong covalent bonds between the oxygen and chlorine atoms within the tetrahedral perchlorate molecule, this species does not become easily reduced to chloride.

Subsequently, perchlorate may persist in aerobic surface water and groundwater environments for an unknown amount of time. Strong reducing agents, such as reactive organic matter and hydrogen sulfide, however, are capable of reducing perchlorate to chloride under anaerobic conditions.

Elevated concentrations of nitrate have been observed within alluvial groundwater in Mortandad Canyon since the early 1960s (LANL 1997, 56835). Sources of nitrate include discharges of nitric acid, treated sewage effluent (Ten Site Canyon), and urine produced from bioassay analyses. Organic forms of nitrogen (total Kjeldahl nitrogen) are also observed in alluvial groundwater within Mortandad Canyon (EPA, 1999). Nitrate is mobile in groundwater under oxidizing conditions. In the presence of organic matter and nitrate-reducing bacteria, nitrate becomes reduced to nitrite, nitrogen gas, and ammonium. Ammonium is less mobile in groundwater relative to nitrate and nitrite due to cation exchange. Groundwater samples collected from 646 ft (perched zone within Cerros del Rio basalt) and 1007 ft (Puye Formation) were analyzed for $\delta^{15}\text{N}$. Reported $\delta^{15}\text{N}$ values are -6.2‰ for the perched zone (average of -5.6‰ and -6.7‰) and +5.4‰ for the regional aquifer. From 1980 through 1989, isotopically-light nitric acid, which is enriched in nitrogen-14, was discharged from TA-50; that may account for the negative $\delta^{15}\text{N}$ values measured in the perched zone. Delta (δ) nitrogen-15 values as low as -37.9‰ have been observed in alluvial groundwater within Mortandad Canyon (Kendrick 1999, 66141). Nitrate within the regional aquifer is isotopically heavier than the nitrate observed in the perched zone. This implies that the sources of nitrate discharged into Mortandad Canyon vary in nitrogen chemistry based on the observed isotopic fractionation. Alluvial groundwater acts as a line-source of recharge for the perched zone within the Cerros del Rio basalt. Evidence for this type of recharge includes elevated activities of tritium and concentrations of nitrate and perchlorate observed at R-15.

5.2.2.2 Quality of Groundwater Within the Puye Formation

The top of the regional saturated zone at R-15 occurs in the Puye Formation at a depth of 964 ft. Groundwater samples were air-lifted from depths of 1007 and 1100 ft and analyzed for screening parameters only in the 1007-ft sample. Groundwater at these depths is characterized by a sodium-calcium-bicarbonate ionic composition with total dissolved solids (TDS) contents of 243 and 270 ppm, respectively (Table 5.2-2). The major cation and anion chemistry of these two groundwater samples has been impacted by the bentonite drilling mud resulting in biased concentrations of sodium and other major ions. Concentrations of dissolved chloride, nitrate (as nitrogen), and sulfate are 4.47 ppm, 1.53 ppm (6.71 ppm nitrate as nitrate), and 15.4 ppm, respectively, for the groundwater sample collected from 1007 ft. Concentrations of dissolved chloride, nitrate (as nitrogen), and sulfate are 3.20 ppm, <0.002 ppm (<0.01 ppm nitrate as nitrate), and 15.1 ppm (Table 5.2-2), respectively, for the groundwater sample collected from 1100 ft. Concentrations of perchlorate are less than 0.002 ppm in a groundwater sample collected at 1100 ft.

Both $\delta^{18}\text{O}$ and δD analyses were performed on a nonfiltered groundwater sample collected from the 1100-ft depth. Delta (δ) ^{18}O and δD ratios are -10.9‰ and -76‰, respectively, suggesting that the regional aquifer groundwater was ultimately derived from a meteoric source.

5.2.2.3 Radionuclide Chemistry

Activities of tritium were measured in groundwater samples collected from the regional aquifer at R-15, using three different analytical-counting methods. Activities of tritium, using LSC, in the regional aquifer are 220 ± 620 pCi/L, with a minimum detectable activity of 440 pCi/L for this groundwater sample (Table 5.2-3). The activity of tritium is 3.19 ± 9.58 pCi/L using direct counting, a more sensitive method (analytical results provided by the NMED's Department of Energy Oversight Bureau and performed by the

University of Miami [Wingo 1999, 64065]). Activities of tritium, measured by direct counting (University of Miami) and LSC (CST-9) in the perched zones, including the upper section of the Puye Formation and the Cerros del Rio basalt, and regional aquifer are provided in Table 5.2-3. Low activities of tritium (1.12 pCi/L) were detected in the regional aquifer at R-15 (1100 ft) using the electrolytic enrichment method at the University of Miami.

Table 5.2-3
Tritium Activity in Groundwater Zones at R-15

Depth (ft)	Sample Date	Activity (pCi/L)	Analytical Laboratory	Geologic Formation
Perched Zones				
482 (drilling mud)	06/25/99	57.5 ± 9.6	Univ. Miami ^a	Puye Fm.
646	07/22/99	3770 ± 850	CST-9	basalt
646	07/22/99	4151	Univ. Miami ^b	basalt
Regional Aquifer				
1007	08/23/99	220 ± 620	CST-9	Puye Fm.
1007	08/23/99	<3.19 ± 9.58	Univ. Miami ^b	Puye Fm.
1100	08/28/99	1.12 ± 0.32	Univ. Miami	Puye Fm.

Note: Analytical error is ±1 standard deviation. LANL and University of Miami perform LSC and direct counting methods, respectively, for measuring tritium activity in these groundwater samples.

^a Data provided by LANL.

^b Data provided by NMED's Department of Energy Oversight Bureau.

Activities of selected radionuclides measured in the 646-ft perched zone and the regional aquifer at R-15 are provided in Table 5.2-4. Both filtered and nonfiltered groundwater samples were analyzed for strontium-90, cesium-137, americium-241, plutonium isotopes, uranium isotopes, total uranium, neptunium-237, gross alpha, gross beta, and gross gamma. Strontium-90, cesium-137, plutonium-238, plutonium-239,240, and neptunium-237 were not detected in the groundwater samples collected from R-15. Americium-241, however, was detected in nonfiltered groundwater samples collected from the perched zone. Americium strongly adsorbs onto hydrous ferric oxide and other adsorbents such as bentonite (Langmuir 1997, 56037), which may account for the elevated activities of this radionuclide observed in the perched zone. Additional groundwater sampling and analyses are required to verify the preliminary activities of this radionuclide observed at R-15. Activities of uranium-234, uranium-235, and uranium-238 were detected in the groundwater samples. Higher activities of the uranium isotopes are associated with the nonfiltered samples because naturally occurring uranium occurs within the bentonite drilling mud and aquifer materials. Concentrations of total (nonisotopic) dissolved uranium are 1.10 and 1.29 µg/L within the perched zone for the two replicate groundwater samples. Concentrations of dissolved uranium in the regional aquifer (1100 ft) are 2.44 µg/L (Table 5.2-4). Uranium concentrations in nonfiltered groundwater samples collected from both the perched zone and regional aquifer are much higher than those measured in the filtered samples because natural uranium is associated with bentonite drilling mud. Activities of gross alpha, gross beta, and gross gamma in nonfiltered groundwater samples exceed those activities measured in filtered samples. Gross alpha and gross gamma activities are associated with isotopes within the uranium-238, uranium-235, and thorium-232 decay chains, whereas gross beta activities are probably associated with potassium-40 present in the bentonite drilling mud. Activities of tritium (Table 5.2-3) are much less than the gross beta activities measured in the R-15 groundwater samples.

Table 5.2-4
Radionuclide Activities in Filtered and Nonfiltered Groundwater Samples from Borehole R-15

Depth (ft)	646	646	1100	646	646	1100
Geologic Unit	Basalt	Basalt	Puye Formation	Basalt	Basalt	Puye Formation
Geologic Unit	Filtered	Filtered	Filtered	Nonfiltered	Nonfiltered	Nonfiltered
Strontium-90^a	-0.13 ± 0.46	0.12 ± 0.49	-0.17 ± 0.34	0.3 ± 1.1	0.31 ± 0.66	-0.04 ± 0.40
MDA^b	0.82	0.84	0.62	1.9	1.10	0.70
Cesium-137	-0.7 ± 2.2	0.1 ± 2.2	-1.1 ± 2.0	-0.4 ± 2.2	0.0 ± 2.1	0.8 ± 2.1
Plutonium-238	-0.0029 ± 0.0154	0.0121 ± 0.0162	0.0167 ± 0.0164	0.021 ± 0.030	0.057 ± 0.038	0.0111 ± 0.0150
MDA	0.043	0.029	0.013	0.062	0.041	0.026
Plutonium-239,240	0.0123 ± 0.0166	0.0093 ± 0.0150	0.0083 ± 0.0134	-0.0071 ± 0.0192	0.0090 ± 0.0192	-0.0017 ± 0.0138
MDA	0.029	0.015	0.013	0.049	0.0035	0.026
Americium-241	0.0046 ± 0.0148	0.0025 ± 0.0022	0.044 ± 0.028	0.123 ± 0.052	0.207 ± 0.078	0.0072 ± 0.0142
MDA	0.015	0.027	0.026	0.041	0.058	0.028
Uranium-234	0.488 ± 0.112	0.495 ± 0.112	1.44 ± 0.24	11.85 ± 1.48	20.0 ± 3.2	18.7 ± 2.2
MDA	0.041	0.052	0.070	0.074	1.42	0.041
Uranium-235	0.027 ± 0.028	0.045 ± 0.032	0.043 ± 0.032	0.577 ± 0.130	0.97 ± 0.50	0.698 ± 0.140
MDA	0.051	0.043	0.047	0.034	0.47	0.030
Uranium-238	0.304 ± 0.084	0.301 ± 0.082	0.683 ± 0.138	8.60 ± 1.08	16.6 ± 2.8	13.25 ± 1.62
MDA	0.036	0.035	0.047	0.054	0.63	0.045
Uranium (µg/L)^c	1.10 ± 0.15	1.29 ± 0.17	2.44 ± 0.33	30.9 ± 4.2	34.9 ± 4.7	43.5 ± 5.9
MDC^d	0.10	0.10	0.10	10.00	10.00	1.00
Neptunium-237	0.00 ± 0.01	0.00 ± 0.01	0.01 ± 0.03	0.03 ± 0.05	-0.01 ± 0.04	0.02 ± 0.02
MDA	0.02	0.02	0.05	0.09	0.08	0.03
Gross Alpha	1.53 ± 0.81	0.7 ± 1.3	2.5 ± 1.1	183 ± 26	140 ± 18	66.2 ± 7.8
Gross Beta	3.35 ± 0.78	2.7 ± 1.1	2.5 ± 1.4	125 ± 18	98 ± 14	50.5 ± 5.6
Gross Gamma	280 ± 45	317 ± 46	223 ± 18	260 ± 20	299 ± 22	253 ± 20
MDA	66	66	19	18	19	18

Notes: 1. Activities are reported in picocuries per liter.

2. Error of two standard deviations is reported.

^a Radionuclides and parameters analyzed by Paragon Analytics, Inc.

^b MDA = minimum detectable activity.

^c KPA = kinetic phosphorimetric analysis.

^d MDC = minimum detectable concentration.

5.2.3 Summary of Groundwater Geochemistry

Solute chemical data show the presence of possible elevated concentrations of anions (chloride, fluoride, nitrate, and sulfate) within groundwater samples collected from the perched zone at 646 ft and from the regional aquifer at 1007 ft during the drilling of R-15. Because of the combined effects of the dissolution of bentonite drilling mud and desorption of inorganic species from the mud during sample preservation, elevated dissolved concentrations of sodium, chloride, nitrate, sulfate, and other species may have biased the borehole groundwater chemistry. Dissolved concentrations of fluoride (1.15 ppm) and perchlorate (0.012 ppm) observed in the perched groundwater at a depth of 646 ft are above background values for

these two solutes. Background concentrations of fluoride are typically less than 0.5 ppm, whereas background concentrations of perchlorate are less than 0.002 ppm. Fluoride, produced from dissociation of hydrofluoric acid, and perchlorate are constituents of the TA-50 treated water discharged into Mortandad Canyon and these two anions are observed in alluvial groundwater (LANL 1997, 56835).

Elevated activities of tritium (3770 ± 850 pCi/L) observed within the perched zone at R-15 strongly suggest that a component of groundwater in these zones is less than 50 yr old, which is derived from Laboratory discharges and/or atmospheric fallout (Adams et al. 1995, 47192; Blake et al. 1995, 49931). Activities of tritium were measured in groundwater samples collected in the regional aquifer at R-15 (1100 ft), using three different analytical-counting methods. Activities of tritium, using LCS, in the regional aquifer are 220 ± 620 pCi/L, with a minimum detectable activity of 440 pCi/L for this groundwater sample. The activity of tritium is 3.19 ± 9.58 pCi/L using direct counting, a more sensitive method (data provided by the NMED's Department of Energy Oversight Bureau [Dale 1999, 64058]). Activities of tritium are less than detection in the R-15 groundwater samples using LSC and direct counting methods. Low activities of tritium (1.12 pCi/L) were detected in the regional aquifer at R-15 (1100 ft) using the electrolytic enrichment method at the University of Miami. The concentration of nitrate (as nitrogen) is 1.53 ppm, which is elevated above background for the regional groundwater in the Pajarito Plateau area.

Strontium-90, cesium-137, plutonium-238, plutonium-239,240, and neptunium-237 were not detected in the groundwater samples collected from R-15. Americium-241, however, was detected in replicate nonfiltered groundwater samples collected from the perched zone within the Cerros del Rio basalt. Additional groundwater sampling and analyses are required to verify the preliminary activities of this radionuclide observed at R-15. Activities of uranium-234, uranium-235, and uranium-238 were detected in the groundwater samples. Higher activities of the uranium isotopes are associated with the nonfiltered samples because natural uranium occurs within the bentonite drilling mud and aquifer materials.

Dissolved uranium concentrations of 1.10 and 1.29 $\mu\text{g/L}$ have been measured by Paragon Analytics, Inc., using LIKPA method, within the perched zone (646 ft) at R-15. These values are within Laboratory background with respect to uranium concentrations for 54 groundwater and spring samples (mean value of 0.92 ± 1.42 $\mu\text{g/L}$) collected on the Pajarito Plateau and surrounding areas. A dissolved uranium concentration of 2.44 $\mu\text{g/L}$ was measured in the regional aquifer (1100 ft) (borehole water sample).

6.0 WASTE MANAGEMENT

Management of waste streams generated during R-15 drilling, sampling, and well installation activities was conducted in accordance with the site-specific waste characterization strategy form (WCSF). Core collected during the Phase I investigation was archived at the FSF. Wastes consisted of disposable sampling equipment, personal protective equipment (PPE), plastic sheeting, sorbent pads, and decontamination water. Pursuant to the WCSF, if any borehole materials demonstrated field screening results above background values, the materials were managed as waste. However, no borehole materials exhibited elevated field screening hits; therefore borehole materials were managed onsite during Phase II drilling as follows:

- Dry drill cuttings were contained in 55-gal. drums, directly from the dust-suppression system discharge, and were transferred and staged within a bermed waste-management storage area onsite. The material was reused by spreading it at the base of the uphill site berm and covering with topsoil during site restoration.
- Wet drill cuttings generated during injection of TORKease or EZ-MUD slurries mixed with municipal hydrant water (during drilling in unsaturated zones) were transferred and contained

within a bermed waste-management storage area onsite. This material was reused by evaporating the liquid and spreading the remaining material at the base of the uphill site berm, and covering with topsoil during site restoration.

- Groundwater generated as a result of drilling through saturated zones, purging, and well development operations was contained and transferred directly to 3000-gal. storage tanks staged within the bermed waste management storage area onsite. Water from different saturated zones was segregated into separate tanks. A total of 25,000 gal. of groundwater was generated from all saturated intervals during drilling and development. The water is stored onsite and will be discharged for site restoration in accordance with an approved notice of intent.
- Disposable sampling equipment and PPE were placed in drum liners, sealed, labeled, and stored onsite in accordance with the WCSF. A total of two bags were generated. A waste profile form was prepared and approved for disposal of the bags at the Los Alamos County landfill.
- Plastic sheeting and sorbent pads placed beneath the drill rig and heavy equipment to contain leaking hydraulic fluid, lubricants, and antifreeze were contained in two 55-gal. drums and were managed and disposed of as New Mexico special waste.

7.0 SURVEY ACTIVITIES

7.1 Geodetic Survey

The location of R-15 was determined by geodetic survey on September 21, 2000, using a Wild/Leica TC1600 total station. Control was second-order, class II monuments placed by Johnson Controls Northern New Mexico; these second order monuments were derived from the 1992/1993 Laboratory-wide control network. The survey located the brass monument in the southwest corner of the well (Table 7.1-1). Horizontal well coordinates are based on New Mexico State Plane Grid Coordinates, Central Zone (North American Datum 83), and are expressed in feet. Elevation is expressed in feet above mean sea level using the National Geodetic Vertical Datum of 1929. The Facility for Information Management, Analysis, and Display (FIMAD) location identification number for R-15 is MO-00051.

Table 7.1-1
Geodetic Data for Well R-15

	Northing (ft)	Easting (ft)	Elevation (ft)
Brass Monument	1768272.5	1635308.6	6820.0

7.2 Surface Radiological Survey

A surface radiological survey was conducted by a radiological control technician (RCT) before site construction or drilling activities began at R-15. The site-construction radiation survey was conducted on September 7, 1999, and consisted of collecting alpha, beta, and gamma background measurements and conducting statistical analysis to calculate action levels. Established action levels are used as a basis to determine if borehole materials screened during drilling exhibit radioactivity above surface background values. The survey consisted of 19 points on a grid projected over the work area. Each point was surveyed using direct reading alpha, beta/gamma, and dose rate meters. Alpha was measured using a Ludlum Model 139 with air proportional probe; beta/gamma was measured using a Ludlum Model 12 with 44-9 probe; dose rate was measured using a Ludlum Model 19 R/hr meter. Calculated background values for the drill site were 0 counts per minute (cpm) for alpha, 191 cpm for beta/gamma, and 14.2 R/hr for dose rate.

8.0 WELL DESIGN, CONSTRUCTION, AND DEVELOPMENT

8.1 Well Design

R-15 was designed as a single-completion well with a stainless-steel screen. The screen, with a nominal length of 60 ft, is located at the top of the regional zone of saturation. The screen extends from 5 ft above the top of the water table to approximately 51 ft into the saturation. This screen length ensures that the well can continue to function even if the water table declines, due to pumpage of water from nearby water-supply wells.

A decision was made to install R-15 as a single-completion well rather than a multiple-screen well because it was considered risky to place a screen in the perched horizon that could allow transfer of contaminated perched water into the regional zone of saturation. Placement of annular fill materials ensures that the perched zone is isolated from the regional aquifer in R-15. Separate intermediate-depth wells will be installed in Mortandad Canyon to sample the perched zone found in R-15.

8.2 Well Construction

Characterization well R-15 was constructed in September 1999. Figure 8.2-1 shows final construction information.

8.3 Well Development

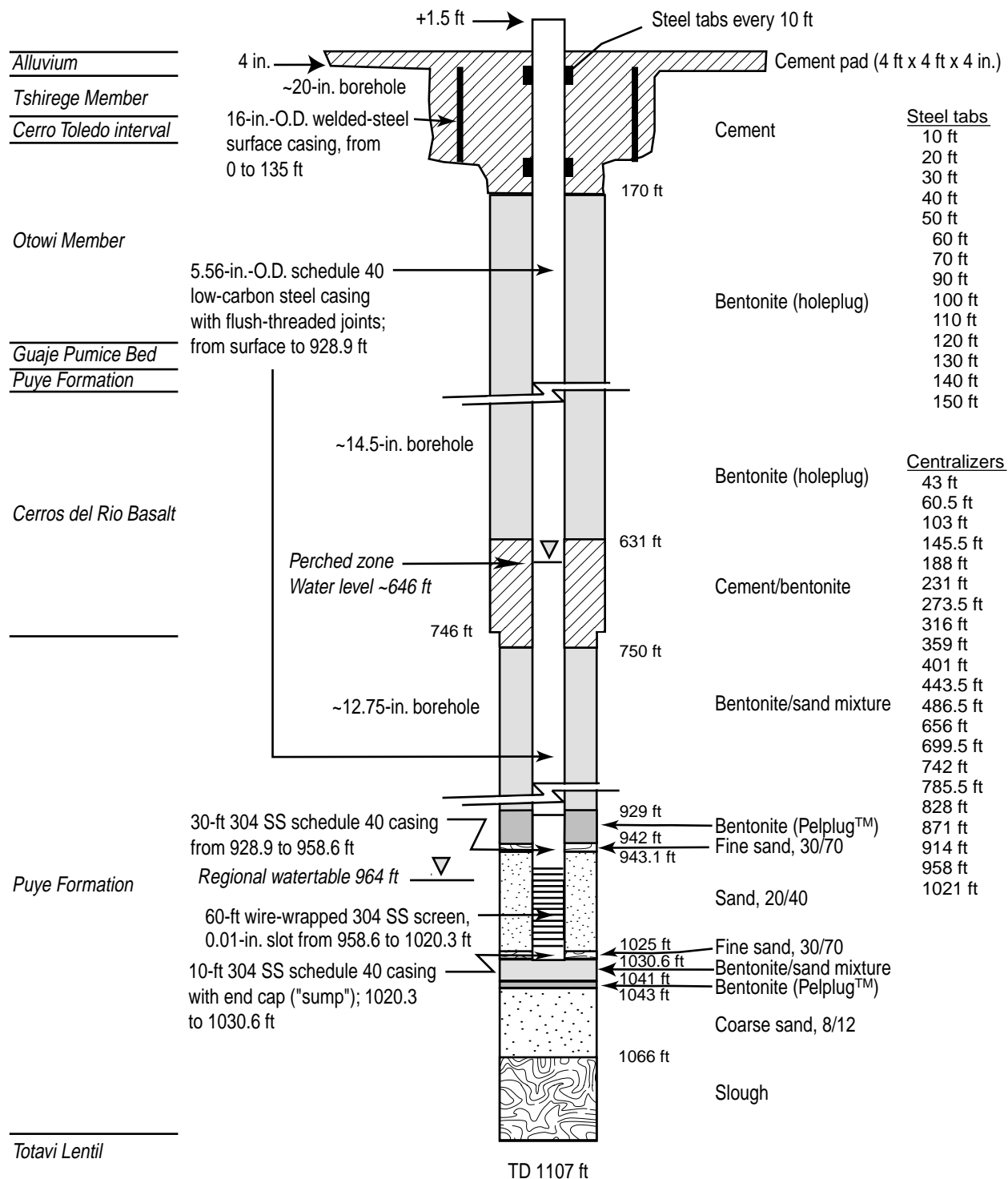
Development of R-15 involved two phases. First, the well screen was washed with regional aquifer water and surged with a jetting tool for 9 hr. Next, the well was pumped for 73.0 hr at an average rate of 9 gpm over a period of 5 days:

2/16/00 – 6.0 hr,
2/17/00 – 9.5 hr,
2/18/00 – 11.5 hr,
2/19/00 – 22.0 hr, and
2/20/00 – 24.0 hr.

The initial well development of R-15 was immediately followed by a pumping test of the regional aquifer. Because this pumping test continued to remove water from the well, it was part of the development process. Groundwater samples were collected at various times during pumping and the turbidity was determined to be less than 5 nephelometric turbidity units (NTUs). Based on flow-meter readings before and after pumping, 41,130 gal. of groundwater were removed from R-15 during the pumping test. Figure 8.3-1 shows the decrease in turbidity during the pumping test.

8.4 Pump Installation

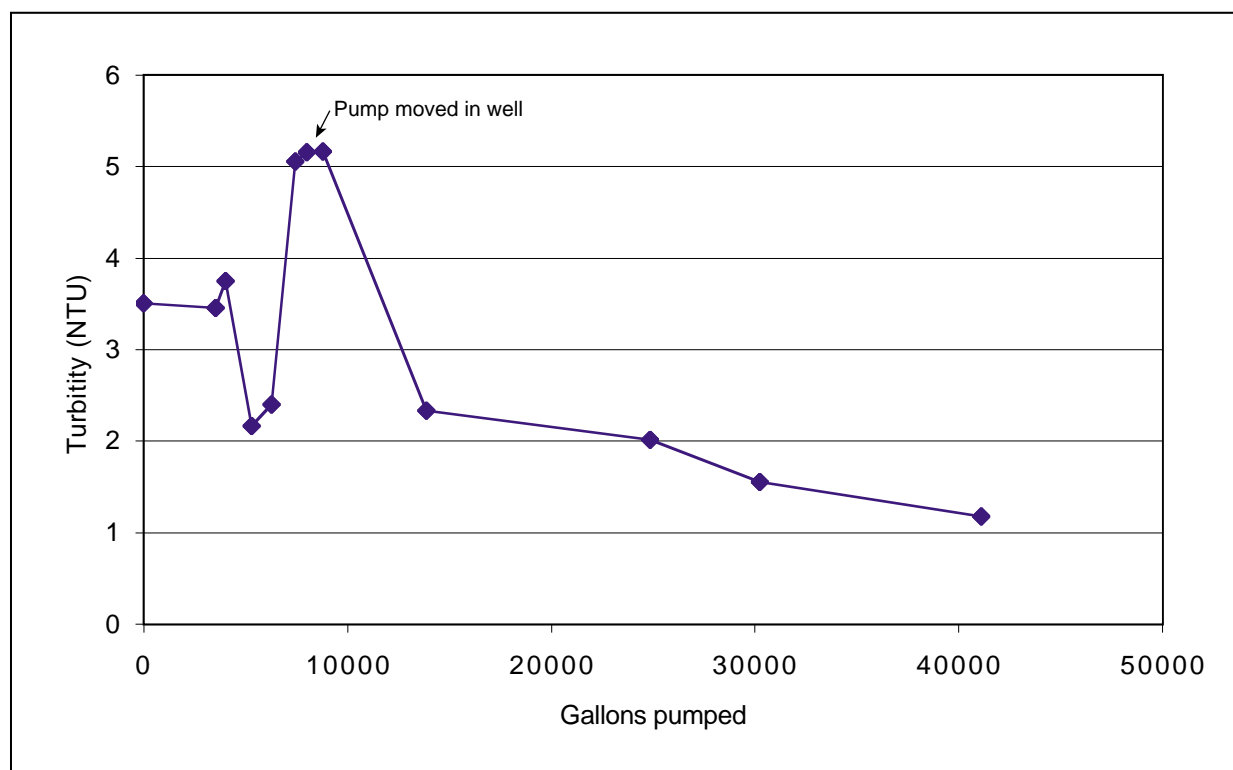
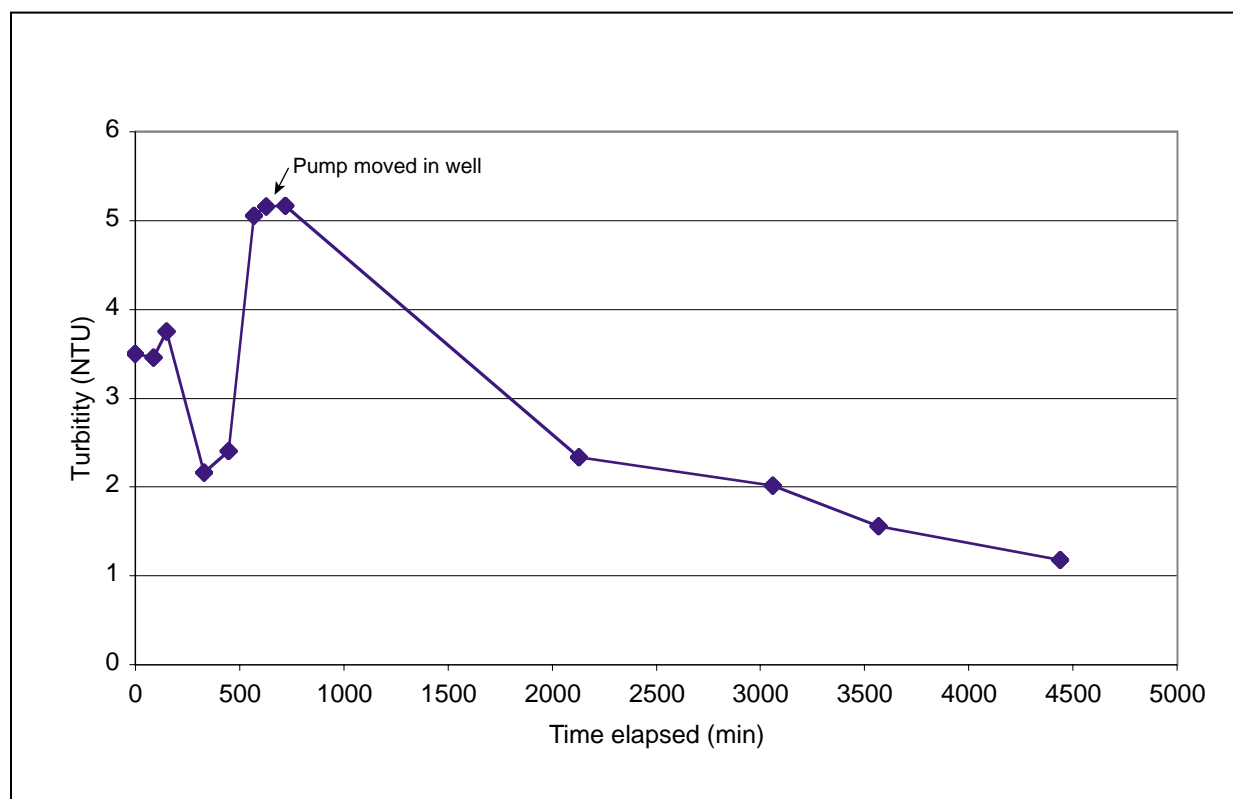
A submersible pump was installed in well R-15 by Rio Grande Well Supply of Santa Fe, New Mexico. The pump is a 3-horsepower Grundfos™ Model 10S30-34, 4-in.-outside diameter (O.D.), submersible pump that operates on a 460-volt, 3-phase power supply provided by a portable diesel generator. The power cable is No. 12, 3CWG jacketed submersible wire, secured to the pump riser pipe with cable ties. The pump was installed on 1.25-in., 304 stainless-steel NPT riser pipe with 3000-lb couplings. The pump intake was set 1018.6 ft below the top of the 5-in. well casing; this places the intake approximately 50 ft below the static water level in the well. The pump was installed with a check valve and a weep hole drilled in the riser pipe at point near the static water level in the well to allow water to drain from the piping. The pump capacity is approximately 10 gal./min at 700-ft depth.



Not To Scale

F8.2-1 / R-15 WELL COMPLETION RPT / 083000 / PTM

Figure 8.2-1. As-built well completion diagram of well R-15



F8.3-1 / R-15 WELL COMPLETION RPT / 083000 / PTM

Figure 8.3-1. Changes in turbidity as a function of time and water removed during pumping

A 1-in.-I.D., flush-threaded, schedule 40, polyvinyl chloride (PVC) pipe with a bottom cap was installed to a depth just above the submersible pump body to serve as a conduit for a pressure transducer. The bottom 20 ft of the PVC pipe was perforated to provide a hydraulic connection with the well. The PVC pipe was secured to the pump riser pipe with cable ties.

The pump riser and PVC pipe are securely hung and sealed at the top of the well casing by a 3000-lb-capacity landing plate. The pump discharge was completed with a ball valve and threaded nipple to allow connection of appropriate tubing for well purging and sample collection. The pump, power cable, and all piping was washed with Alconox™ detergent and steam-cleaned prior to installation.

8.5 Wellhead Protection

A reinforced concrete vault was installed to provide wellhead protection. Figure 8.5-1 shows plan and profile views of the wellhead configuration.

9.0 SITE RESTORATION

The R-15 drill site area was recontoured to match the surrounding topography using a backhoe. The surface of the drill pad was roughened and native dryland seed was applied to the denuded areas. Straw mulch was then spread over the seeded areas and wheel-rolled to crimp in the straw and cover the seed.

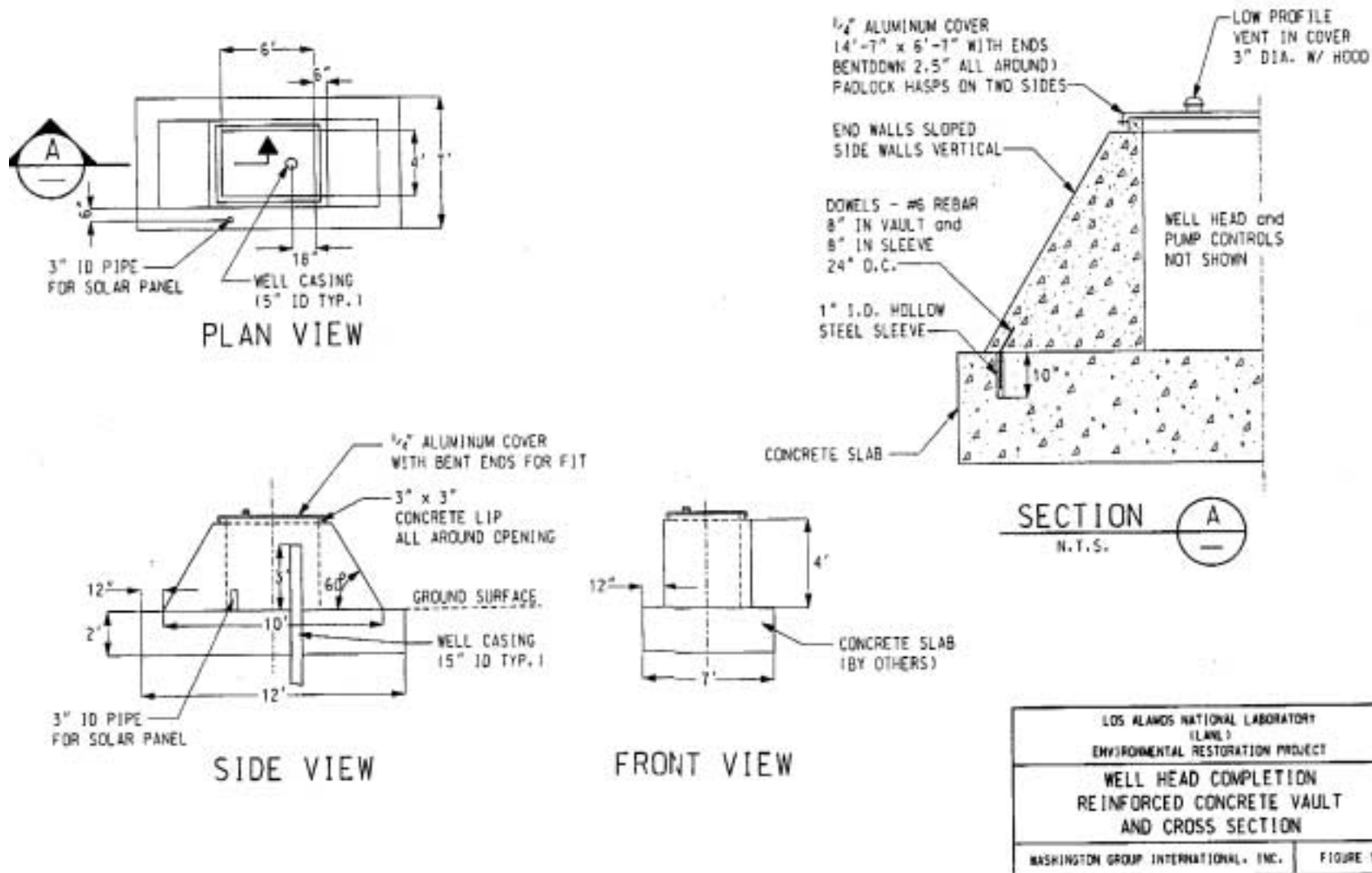
10.0 MODIFICATIONS TO WORK PLANS

Table 10.0-1 compares the planned characterization activities in the “Task/Site Work Plan for Operable Unit 1049: Mortandad Canyon” (LANL 1997, 56835), the hydrogeologic work plan (LANL 1998, 59599), the core document (LANL 1997, 55622), and the “Field Implementation Plan for the Drilling and Testing of LANL Regional Characterization Well R-15” (LANL 1999, 64062) with characterization activities performed in R-15. The characterization activities in the hydrogeologic work plan and the core document are the same; therefore, planned characterization activities for these two documents are shown together in Table 10.0-1.

The final depth and completion design of R-15 was based on ongoing evaluations of hydrogeologic data collected at R-15 and discussions with the groundwater integration team and NMED.

The amount of core collected in R-15 during Phase II drilling was a significant deviation from the amount specified in the hydrogeologic work plan and the core document. In both documents R-15 is designated as a type 2 well (100% coring). During actual drilling operations, 100% core was collected from the upper 420 ft of R-15 using an HSA method. In R-15, good performance of the HSA system was achieved, particularly in the Bandelier Tuff, and continuous core could be collected without penalizing the drilling rate. Little core was collected during Phase II drilling because of an agreement between the groundwater integration team and NMED that collection of continuous core was too costly for the value of the information derived from the core.

The sand filter pack was originally designed to extend 2 ft above and below the well screen according to the hydrologic work plan and the R-15 field implementation plan. However, placement of annular materials during well construction resulted in a longer sand pack (10 ft above and below the well screen). Because of the porous nature of the geologic unit in the vicinity of the screen, it was believed that significant settling and loss of annular materials to the formation could result in bentonite migrating next to the screen. Bentonite next to the screen would adversely impact the measurement of water-quality parameters and affect the hydraulic properties of the well screen.



F8.5-1 / R-15 WELL COMPLETION RPT / 082300 / PTM

Figure 8.5-1. Well R-15 wellhead diagram

Table 10.0-1
Activities Planned for R-15 Compared with Work Performed

	Work Plan for Mortandad Canyon^a	Hydrogeologic Work Plan^b and Core Document for Canyons Investigations^c	R-15 Field Implementation Plan^d	R-15 Actual Work
Planned Depth (ft)	1240 ft	100 to 500 into the regional aquifer	Nominally 1000	Total depth = 1107 ft; into regional saturation
Drilling Method	Auger or rotary drilling	Methods may include, but are not limited to, HSA, air-rotary/Odex/Stratex, air-rotary/Barber rig, mud-rotary drilling	Phase I drilling consists of HSA to a depth of 420 ft. Air-rotary methods including downhole percussion hammers on 4.5-in.- and 7-in.-O.D. dual-wall casings to drill open hole; air-rotary 101-mm Geobarrel system to collect continuous core; air-rotary Holte and Stratex casing-advance systems and downhole percussion hammers to simultaneously drill and advance casing in the borehole	Same as field implementation plan, HSA Phase I: HSA Phase II: with casing advance and rotary assisted by mud behind the casing/air rotary
Amount of Core	100% core	100% core	Approximately 10% of the borehole	39% of R-15; most of the core collected from 0 to 420 ft
Lithologic Log	Log to be prepared from core, cuttings, drilling performance	Log to be prepared from core, cuttings, drilling performance	Log to be prepared from core, cuttings, drilling performance	Log was prepared from core, cuttings, and drilling performance
Number of Water Samples Collected for Contaminant Analysis	A water sample will be collected from each saturated zone. Well to be sampled at completion and at six months.	A water sample will be collected from each saturated zone. The number of sampling events after well completion are not specified.	A water sample will be collected from each saturated zone. The geochemistry project leader and technical team will determine the number and locations of samples based on conditions encountered. The number of sampling events after well completion are not specified. Up to six water samples are planned.	To date, water samples were collected from two saturated zones encountered during Phase II drilling.

Table 10.0-1 (continued)

	Work Plan for Mortandad Canyon ^a	Hydrogeologic Work Plan ^b and Core Document for Canyons Investigations ^c	R-15 Field Implementation Plan ^d	R-15 Actual Work
Water Sample Analytes	<p>Trace Elements/Metals: Al, Sb, As, Ba, Be, B, Cd, Ca, Cr, Co, Cu, Fe, Pb, Mg, Mn, Hg, Ni, K, Se, Ag, Na, Ti, U, V, Zn</p> <p>Anions: Br, ClO₃, Cl, F, NO₃, NO₂, PO₄, HCO₃, SO₄</p> <p>Other Chemicals: Si, cyanide</p> <p>Radionuclides: ³H, ⁹⁰Sr, ¹³⁷Cs, ²³⁴U, ²³⁵U, ²³⁸U, ²³⁸Pu, ^{239,240}Pu, ²⁴¹Am</p> <p>Organic Compounds: pesticides, PCBs, VOCs, semivolatile organic compounds (SVOCs)</p> <p>Other Analyses: ¹⁴C, ¹³C, ¹⁸O/¹⁶O, D/H, DOC</p>	Radiochemistry I, II, and III analytes; ³ H, gamma spectroscopy scan; general inorganic chemicals; metals; stable isotopes	<p>Trace Elements/Metals: Al, Sb, As, Ba, Be, B, Cd, Ca, Cr, Co, Cu, Fe, Pb, Mg, Mn, Hg, Ni, K, Se, Ag, Na, Ti, U, V, Zn, NH₄</p> <p>Anions: Br, ClO₃, Cl, F, NO₃, NO₂, PO₄, HCO₃, SO₄</p> <p>Other Chemicals: Si, cyanide, total organic carbon, dissolved organic carbon fractionation</p> <p>Radionuclides: ³H, ⁹⁰Sr, ¹³⁷Cs, ²⁴¹Am, ²³⁴U, ²³⁵U, ²³⁸U, ²³⁸Pu, ^{239,240}Pu, gamma spectroscopy, gross-alpha, gross-beta, gross gamma</p> <p>Organic Compounds: VOCs, SVOCs, high explosive compounds</p> <p>Other Analyses: ¹⁴C, ¹³C, ¹⁸O/¹⁶O, D/H, ¹⁵N/¹⁴N</p>	Same as field implementation plan except for the addition of perchlorate. PCBs and pesticides will be analyzed for during quarterly sampling of the well.
Water Sample Field Measurements	Alkalinity, dissolved oxygen, pH, specific conductance, temperature, turbidity	Alkalinity, pH, specific conductance, temperature, turbidity	Alkalinity, dissolved oxygen (completed well only), pH, specific conductance, temperature, turbidity	pH, specific conductance, temperature, turbidity. Alkalinity was measured in the laboratory.
Number of Core/Cuttings Samples Collected for Contaminant Analysis	Collect and preserve seven cores to represent major hydrogeologic units and zones above and below major hydrogeologic contacts	Twenty samples of core or cuttings to be analyzed for contaminants in each borehole	Up to 23 core/cuttings samples planned; number of samples dependant on number of saturated zones encountered	During Phase I drilling, 24 core samples were collected for contaminant chemistry/ geochemistry analyses. During Phase II drilling, one core sample was collected for contaminant chemistry/geochemical/ mineralogical analyses.

Table 10.0-1 (continued)

	Work Plan for Mortandad Canyon ^a	Hydrogeologic Work Plan ^b and Core Document for Canyons Investigations ^c	R-15 Field Implementation Plan ^d	R-15 Actual Work
Core/Cuttings Sample Analytes	<p>Trace Elements/Metals: Al, Sb, As, Ba, Be, Br, Cd, Ca, Cr, Co, Cu, Fe, Pb, Mg, Mn, Hg, Ni, K, Se, Ag, Na, Ti, Tl, U, V, Zn</p> <p>Anions: B, Cl, F, SO₄, PO₄</p> <p>Other Inorganic Chemicals: Si, cyanide</p> <p>Radionuclides: ³H, ⁹⁰Sr, ¹³⁷Cs, ²³⁰Th, ²³²Th, ²³⁴U, ²³⁵U, ²³⁸U, ²³⁸Pu, ^{239,240}Pu, gamma spectroscopy, gross-alpha, gross-beta, gross gamma</p>	Uppermost sample to be analyzed for a full range of compounds; deeper samples to be analyzed for Radiochemistry I, II, and III analytes; ³ H; and metals; four samples to be analyzed for VOCs	<p>Trace Elements/Metals: Sb, As, Ba, Be, Cd, Cr, Co, Cu, Fe, Pb, Mn, Hg, Mo, Ni, Nb, Rb, Se, Ag, Sr, Tl, U, V, Y, Zn, Zr</p> <p>Major Elements: Al, Ca, Fe, Mg, Mn, P, K, Si, Na, Ti</p> <p>Anions: Br, Cl, F, SO₄, NO₃</p> <p>Other Inorganic Chemicals: cyanide</p> <p>Radionuclides: ³H, ⁹⁰Sr, ¹³⁷Cs, ²⁴¹Am, ²³⁴U, ²³⁵U, ²³⁸U, ²³⁸Pu, ^{239,240}Pu, gamma spectroscopy, gross alpha, gross beta, gross gamma</p> <p>VOCs and SVOCs to be determined in four samples and where PID detects occur</p>	Same as field implementation plan except that uranium (nonisotopic) was not analyzed. Perchlorate was added to anion leach tests. Mineralogic analyses were conducted on core and cuttings.
Hydraulic Property Analyses	Bulk density, dry density, Kd, porosity, mineralogy, moisture content, moisture potential, saturated hydraulic conductivity	Physical properties to be determined on 5 samples and will typically include moisture content, porosity, particle density, bulk density, saturated hydraulic conductivity, and water retention characteristics. Approximately 10 samples of core or cuttings will be collected for mineralogy, petrography, and rock chemistry.	The following physical properties will be determined in each of the major stratigraphic units: particle size (sedimentary units) moisture content, matric potential, porosity, particle density, bulk density, saturated hydraulic conductivity, and water retention characteristics. In addition, approximately 15 samples of core or cuttings will be selected by the geology project leader for mineralogy, petrography, and rock chemistry.	Core samples were collected and preserved for potential use as samples for hydrological property testing. Selection of samples for testing will be based on characterization requirements identified during development of groundwater flow and transport models. During Phase I drilling, total of 86 samples were collected for moisture content and 111 samples were collected for matric potential. A total of 25 samples were collected for geologic characterization including mineralogy, petrography, and rock chemistry. Aquifer performance testing was conducted at R-15 after well development.

Table 10.0-1 (continued)

	Work Plan for Mortandad Canyon^a	Hydrogeologic Work Plan^b and Core Document for Canyons Investigations^c	R-15 Field Implementation Plan^d	R-15 Actual Work
Geophysics	Natural gamma, neutron moisture, and density logs may be collected.	In general, open-hole geophysics includes caliper, electromagnetic induction, natural gamma, magnetic susceptibility, borehole color videotape, fluid temperature (saturated), fluid resistivity (saturated), single-point resistivity (saturated), and spontaneous potential (saturated). In general, cased-hole geophysics includes gamma-gamma density, natural gamma, and thermal neutron.	In stable open borehole environments, geophysics measurements will include caliper, electromagnetic induction, natural gamma, magnetic susceptibility, color camera, borehole digital camera, gamma-gamma, and thermal/epithermal neutron logs. In the cased borehole, geophysics measurements will include gamma-gamma density, natural gamma, and thermal neutron logs. The need for specific logs to be determined by the technical team.	Performed gamma and induction log in open borehole and gamma in cased hole.
Water-Level Measurements			Waters levels will be determined for each saturated zone by water-level meter or by pressure transducer.	Waters levels were determined for each saturated zone by water-level meter or by pressure transducer.
Slug Tests			Slug tests planned for all zones of saturation encountered.	Slug tests were conducted in the perched system. A slug test was attempted in the regional aquifer, but the water level recovered before the pressure transducer could be installed.
Air Permeability/ Borehole Anemometry		Conducted in Bandelier Tuff at 10-ft intervals after removing the HSA and/or Odex/Stratex casing	In unsaturated environments, borehole anemometry and straddle packer air permeability measurements will be made in stable open-borehole environments at locations determined in the field.	Air permeability was measured in part of the borehole.
Surface Casing		Approximately 20-in. O.D., extends from land surface to 10-ft depth in underlying competent layer and grouted in place	10-in.-diameter low-carbon steel casing set to a minimum depth of 20 ft with a 3-ft stickup	16-in.-O.D. welded-steel casing set from land surface to 135 ft
Minimum Well Casing Size	4 in.	6 5/8-in. O.D.	5-in. I.D.	5-in. I.D.

Table 10.0-1 (continued)

	Work Plan for Mortandad Canyon ^a	Hydrogeologic Work Plan ^b and Core Document for Canyons Investigations ^c	R-15 Field Implementation Plan ^d	R-15 Actual Work
Well Screen	10-ft stainless steel with top at top of static water level	Machine-slotted (0.01-in.) stainless-steel screen(s) with flush-jointed threads; number and length of screens to be determined on a site-specific basis and proposed to NMED	60 ft of prepacked, 6.68-in.-diameter, machine-slotted (0.01-in.) stainless-steel screen with flush-jointed threads 5 ft of the screen to extend above the static water level; screen specifications based on well life expectancy of 50 yr and on discussions with NMED	60 ft wire-wrapped 304 stainless-steel screen, 0.01-in. slot size; 5 ft of the screen extends above static water level.
Filter Material		>90% silica sand, properly sized for the 0.010-in. slot size of the well screen; extends 2 feet above and below the well screen	>98% silica sand, properly- sized for the 0.010-in. slot size of the well screen; extends 2 ft above and below the well screen	Sand filter pack, 20/40, 10 ft above and below screen.
Conductor Casing		Carbon-steel casing from land surface to top of stainless-steel casing	Carbon-steel casing 5.56 in. in diameter extending from land surface to dielectric coupling at top of stainless-steel casing; 10 ft of 5.56-in.-diameter stainless-steel casing below dielectric coupling	Same as hydrogeologic work plan.
Backfill materials (exclusive of filter materials)		Uncontaminated drill cuttings below sump and bentonite above sump	Bentonite in borehole below well; fine sand in transition zone 10 ft above and 3 ft below filter pack; bentonite above transition zone to bottom of surface casing; cement grout between surface casing and borehole wall and between surface casing and well casing	Sand capped by bentonite below sump; bentonite and/or cement from land surface to top of screen (see Figure 8.2-1)
Sump		Stainless-steel casing	5.56-in.-diameter stainless-steel casing 10 ft long	Same as field implementation plan
Bottom Seal		Bentonite	Bentonite	Bentonite

^a LANL 1997, 56835.

^b LANL 1998, 59599.

^c LANL 1997, 55622.

^d LANL 1998, 64062.

Other modifications to R-15 planned activities were relatively minor for the two saturated zones encountered during Phase II drilling. In both cases, perchlorate and nitrogen-15/nitrogen-14 were added to the analytical suite for water samples based on nitrogen-15/nitrogen-14 ratios measured at R-12, TA-50, and alluvial groundwater within Mortandad Canyon. Perchlorate has been observed in alluvial groundwater within Mortandad Canyon.

11.0 IMPLICATIONS FOR CONCEPTUAL GEOLOGIC, HYDROGEOLOGIC, AND GEOCHEMICAL MODELS

In descending order, geologic units penetrated in R-15 included alluvium, the Tshirege Member of the Bandelier Tuff, tephra and volcanoclastic sediments of the Cerro Toledo interval, the Otowi Member of the Bandelier Tuff, the Guaje Pumice Bed, the fanglomerate facies of the Puye Formation, basaltic rocks of the Cerros del Rio volcanic field, more Puye fanglomerate, and the axial Rio Grande facies of the Puye Formation (Totavi Lentil).

With the exception of Cerros del Rio basalt and the absence of deeper lavas, stratigraphic units encountered in R-15 and depths of their contacts were predicted with good accuracy by the current three-dimensional stratigraphic model for the Pajarito Plateau (Figure 3.1-2). Most contacts were within 40 ft of their predicted value; this accuracy reflects the relatively high density of water supply wells, test wells, and R-wells that were used to constrain the three-dimensional model in this part of the Laboratory. The interfingering relations between the Cerros del Rio basalt and Puye Formation also were accurately portrayed in the three-dimensional stratigraphic model.

The predicted depths to contacts and thicknesses for the basaltic rocks of the Cerros del Rio volcanic field were notably less accurate than for the other stratigraphic units. Modeled contacts for the Cerros del Rio basalt probably will always be less predictable than other stratigraphic units because of the unique factors controlling its distribution. These basalts were erupted from vents that are now buried beneath the eastern part of the Pajarito Plateau by the Bandelier Tuff and in places by the Puye Formation. The number and locations of these vents are not known. Additionally, the thickness and distribution of basaltic lava flows vary as a function of vent type (e.g., cinder cones versus fissure flows), volume of basaltic magma erupted, distance from the vent area, fluidity of the lavas, and topography onto which the lavas were erupted.

In particular, the landscape onto which these basalts were erupted had a major effect on their distribution. Basalts behave like other fluids, flowing through existing drainages and ponding in low-lying basins. If the topographic relief is subdued or if the eruptions are voluminous enough, the basaltic lava flows may fill in low-lying areas before spreading out as more predictable sheet-like bodies. Currently, the three-dimensional stratigraphic model for the Cerros del Rio basalt lumps together all flow units regardless of their source vents. The Cerros del Rio basalt appears to be an important hydrogeologic unit for hosting perched groundwater on the Pajarito Plateau. The distribution of individual flow units and the orientation of their contacts may be the primary controls on groundwater flow directions for these perched systems. The ability to more accurately predict groundwater flow through these rocks will improve as the identity of individual flow units and the locations of their source vents become better known through information gained from additional drilling activities and through ongoing investigations to identify flow units by their chemistry, petrography, and age.

The axial Rio Grande facies of the Puye Formation (Totavi Lentil) was partially penetrated during the drilling of R-15. Although only partially penetrated, it is likely this rock unit forms the basal deposits of the Puye Formation at this location based on the thickness of the Puye Formation in other nearby wells. In contrast, axial Rio Grande deposits were found to overlie the upper fanglomerate of the Puye Formation

in well R-12 and were absent in well R-9. The axial Rio Grande facies evidently does not form a continuous sheet-like deposit at the base of the Puye Formation, as suggested by earlier investigations. Rather, this facies appears to be comprised of isolated deposits of limited areal extent that represent the course of the ancestral Rio Grande at different points in time during development of the Puye alluvial fan. The term "axial facies" is useful to retain because of the unique provenance and lithologic character of the clasts comprising these deposits, but the depiction of these deposits as a time-stratigraphic unit at the base of the Puye Formation should be examined critically in future drilling.

Although many contacts were reliably predicted, other aspects of the geology at R-15 were unanticipated. In particular, the general absence of clay alteration and the abundance of glass preserved in the central and lower Puye Formation were not expected. Lack of alteration is particularly surprising because this section in R-15 is saturated, whereas the same intervals in R-9 and R-12 are unsaturated but fully altered to clay. Because of the importance of clay in hydrologic and geochemical processes, the distribution of alteration patterns in the Puye Formation will require further clarification to produce more accurate predictions of groundwater flowpaths beneath the Laboratory.

Saturation in the alluvium immediately east of the sediment traps in Mortandad Canyon appears to be limited to the center axis of the canyon (e.g., MCO-7.2) and does not extend to the south side of the canyon at R-15.

Two saturated groundwater zones were clearly identified during Phase II drilling operations at R-15. The tops of the saturated zones occurred at depths of 646 and 964 ft. The upper zone contains perched groundwater and the lower is believed to be associated with the regional aquifer.

The saturated zone at a depth of 646 ft occurs in the lower part of basaltic rocks of the Cerros del Rio volcanic field. Saturated porosity is provided by fractures in basalt. The perching layer consists of clay-rich material at the base of the Cerros del Rio basalt.

During Phase I drilling, tritium was detected in core samples collected from 22.3 to 414.8 ft, with activities ranging from 5.3 pCi/L (0.077 pCi/g) to 5405 pCi/L (22.2 pCi/g). The highest activities of tritium were measured at 319.8 ft within the Otowi Member of the Bandelier Tuff. Tritium was the only radionuclide detected in R-15 during Phase I drilling, which may have resulted from vapor-phase and/or aqueous-phase transport. Activities of strontium-90, cesium-137, plutonium-238, plutonium-239/240, and americium-241 were below detection in the core samples.

Perched groundwater has been found in all four of the wells (R-9, R-12, R-15, and R-25) installed to date during implementation of the hydrogeologic work plan. These results suggest that perched groundwater is more common than previously recognized, particularly in or near the major canyon systems. Preliminary water-quality data from these perched zones suggest that none of the perched groundwaters identified to date are connected between canyons. Alluvial groundwater acts as a source of line recharge to underlying perched zones found in Mortandad Canyon, Sandia Canyon, Los Alamos Canyon, Pueblo Canyon, and Cañon de Valle. Nonetheless, these perched systems share some common features. For example, the largest perched groundwater systems in R-9, R-12, and R-15 are associated with the Cerros del Rio basalt. Perched water occurs in the lower basalt flow units of all three boreholes. In R-9 and R-15, clay-rich rocks associated with the brecciated base of lava flows appear to be important perching horizons. Also, tritium activities are elevated above background values for these perched systems, though none exceeds state and federal drinking water standards (20,000 pCi/L). These above-background tritium values indicate that at least part of the groundwater in these perched zones was recharged from the surface during the past 50 yr.

Elevated activities of tritium (3770 ± 850 pCi/L) observed within the perched zone at R-15 strongly suggest that a component of groundwater in this zone is less than 50 yr old. A portion of the water within the perched zone is derived from Laboratory discharges and/or atmospheric fallout (Adams et al. 1995, 47192; Blake et al. 1995, 49931).

Strontium-90, cesium-137, plutonium-238, plutonium-239,240, and neptunium-237 were not detected in the groundwater samples collected from R-15. Americium-241, however, was detected in replicate nonfiltered groundwater samples collected from the perched zone within the Cerros del Rio basalt. Additional groundwater sampling and analyses are required to verify the preliminary activities of this radionuclide observed at R-15. Activities of uranium-234, uranium-235, and uranium-238 were detected slightly above background in the groundwater samples. Higher activities of the uranium isotopes are associated with the nonfiltered samples because naturally occurring uranium occurs within the bentonite drilling mud and aquifer materials.

Groundwater from the perched zone in R-15 is dominantly a sodium-calcium-bicarbonate type solution as represented by the screening samples collected at depth of 646 ft. This perched groundwater was found to contain 3770 ± 850 pCi/L tritium, 0.012 ppm dissolved perchlorate, 11.5 ppm dissolved chloride, 63.9 ppm dissolved sodium, 1.5 ppm dissolved fluoride, 35.4 ppm dissolved sulfate, <0.02 ppm dissolved ammonium, <0.01 ppm nitrate (as nitrate), and 1.2 ppb dissolved uranium. Bentonite drilling mud has biased the borehole water chemistry by dissolving/desorbing sodium, sulfate, nitrate, and other species from the mud. The chemistry of this perched zone, however, is similar to that of the TA-50 treated discharge water and alluvial groundwater in Mortandad Canyon. Sulfate, fluoride, chloride, perchlorate, and tritium are solutes associated with the TA-50 discharge, which are not significantly adsorbed at near-neutral pH conditions.

The regional water table was encountered at a depth of 964 ft at an elevation of 5856 ft in the Puye Formation at R-15. The groundwater occurs at a higher elevation than at R-9 (5694.8 ft) and R-12 (5699.5 ft), located approximately 1.3 mi to the northeast and 1.1 mi to the east of R-15, respectively. The elevation of the water table in R-15 is approximately 26 ft lower than the static water level in nearby TW-8 (depth to groundwater is 996 ft at an elevation of 5882 ft). This saturated zone is believed to represent the regional aquifer because its elevation is consistent with that found in nearby supply wells PM-1 and PM-3, and in two test wells (TW-3 and TW-8). The regional aquifer at well R-15 behaves like a leaky confined aquifer.

The groundwater composition at the top of the regional saturated zone is dominantly a sodium-bicarbonate type as represented by the screening samples collected at a depth of 1007 ft. The major ion chemistry of the groundwater sample, however, has been impacted by bentonite drilling mud. Low activities of tritium (1.12 pCi/L) were detected in the regional aquifer at R-15 (1100 ft) using the electrolytic enrichment method at the University of Miami. The concentration of nitrate (as nitrogen) is 1.53 ppm, which is elevated above background for the regional groundwater in the Pajarito Plateau area.

Anions (including perchlorate, chloride, nitrate, fluoride, and sulfate) are mobile species (nonsorbing) under near-neutral pH conditions and breakthrough of these species is observed at R-9, R-12, and R-15. Perchlorate has only been observed in the perched zone and not in the regional aquifer at R-15. Strontium-90, plutonium, and americium isotopes that adsorb onto geologic material are much less frequently observed at R-9, R-12, and R-15. Colloidal transport of americium-241 is a viable (untested) hypothesis for explaining spurious detection of this radionuclide in some core and groundwater samples collected from R-15. The contaminant hydrochemistry, however, is a dynamic process and is expected to change over time within alluvial and perched groundwater zones.

12.0 RESPONSIBILITIES

The authors of this report had the following responsibilities. P. Longmire was the geochemistry principal investigator who coordinated the collection, analysis, and interpretation of chemical data collected for core, cuttings, and groundwater. He was the principal compiler of this report. D. Broxton was the technical team leader for the drilling program and coordinated the drilling and testing programs. W. Stone and D. Rogers supervised the hydrology investigations for the saturated and unsaturated zones, respectively. R. Gilkeson and R. Hull were responsible for the design, planning, and technical oversight of drilling operations and for coordinating borehole testing activities. J. Marin was the field team leader who provided oversight of the site geologist, site safety officer, sampling, waste-management activities, and health safety; he provided the description of survey activities in this report. Marin was the well-site geologist who prepared preliminary lithologic logs; collected and preserved samples for geologic, moisture, and hydrologic characterization; and compiled drilling statistics. S. McLin conducted aquifer performance tests, and installed pressure transducers at R-15 to record water levels. B. Newman coordinated the analyses of stable isotopes and anion chemistry of the core samples. R. Warren and D. Vaniman were the geology principal investigators who collected petrographic, chemical, and mineralogic data to determine the geologic characteristics of rock units. R. Warren coordinated moisture and matric potential analyses.

In addition to the authors of this report, numerous individuals contributed to this investigation.

Stewart Brothers Drilling Company provided drilling services under the direction of P. Garcia, the drilling supervisor. The drilling crew consisted of S. White, L. Chaves, and M. Brown.

Dynatec Drilling, Inc. (formerly Tonto Environmental Drilling Company) provided drilling services under the direction of L. Thoren, the drilling supervisor. The drilling crew consisted of C. Howe, G. Woodward, J. Van Horn, and J. Rivera.

R. Baran and D. Barney were the site safety officers and the radiological control technicians for drilling activities. R. Bjarke provided Laboratory oversight for radiological controls.

S. Bolivar and J. Skalski provided contract oversight for drilling activities and field support. S. Hagelberg, J. Valdez, M. Clevenger, and A. Garcia provided sample and data management support. J. Marin, D. Harris, J. Santo, and J. Sena supported water sampling activities.

D. Counce was the analyst for water chemistry analyses used for screening of groundwaters collected from saturated zones. E. Kluk and M. Snow were analysts for moisture and matric potential determinations.

The groundwater integration team, led by C. Nylander, participated in the planning and evaluation of data collected during this investigation. S. McLin provided equipment and field support for water-level measurements.

G. Turner provided Department of Energy (DOE) oversight during the investigation.

J. Young of NMED provided regulatory oversight during drilling operations. M. Dale and C. Hanlon-Meyer from the NMED's DOE Oversight Bureau collected sample splits from groundwater zones and acted as liaisons with the regulators. M. Dale provided results of tritium analyses for the perched zone and regional aquifer.

K. Bitner, D. Hickmott, L. Soholt, and H. Wheeler-Benson were reviewers for the document.

The geodetic survey was performed by Bill Kopp of ESH-19.

J. Torline was editor for this document; P. Maestas was the compositor.

A. Pratt supported all phases of this investigation as leader of the Canyons Focus Area. D. Daymon supported this investigation as leader of the Groundwater Investigations Focus Area.

13.0 REFERENCES

Adams, A. I., F. Goff, and D. Counce, February 1995. "Chemical and Isotopic Variations of Precipitation in the Los Alamos Region, New Mexico," Los Alamos National Laboratory Report LA-12895-MS, Los Alamos, New Mexico. (Adams et al. 1995, 47192)

Allison, J. D., D. S. Brown, and K. J. Novo-Gradac, March 1991. "MINTEQA2/PRODEFA2, A Geochemical Assessment Model for Environmental Systems: Version 3.0 User's Manual," EPA/600/3-91/021, Office of Research and Development, Athens, Georgia. (Allison et al. 1991, 49930)

Blake, W. D., F. Goff, A. I. Adams, and D. Counce, May 1995. "Environmental Geochemistry for Surface and Subsurface Waters in the Pajarito Plateau and Outlying Areas, New Mexico," Los Alamos National Laboratory Report LA-12912-MS, Los Alamos, New Mexico. (Blake et al. 1995, 49931)

Bouwer, H., and R. C. Rice, 1976. "A Slug Test for Determining Hydraulic Conductivity of Unconfined Aquifers with Completely or Partially Penetrating Wells," in *Water Resources Research*, Vol. 12, pp. 423–428. (Bouwer and Rice 1976, 64056)

Brookins, D. G., 1984. *Geochemical Aspects of Radioactive Waste Disposal*, Springer-Verlag, New York, New York. (Brookins 1984, 12453)

Broxton, D. E., and S. L. Reneau, 1996. "Buried Early Pleistocene Landscapes Beneath the Pajarito Plateau, Northern New Mexico," in *New Mexico Geological Society Guidebook*, 47th Field Conference, Jemez Mountains Region, New Mexico, pp. 325–334. (Broxton and Reneau 1996, 55429)

Broxton, D. E., G. H. Heiken, S. J. Chipera, and F. M. Byers, Jr., June 1995. "Stratigraphy, Petrography, and Mineralogy of Bandelier Tuff and Cerro Toledo Deposits," in "Earth Science Investigations for Environmental Restoration, Los Alamos National Laboratory Technical Area 21," Los Alamos National Laboratory Report LA-12934-MS, Los Alamos, New Mexico. (Broxton et al. 1995, 50121)

Broxton, D. E., P. A. Longmire, P. G. Eller, and D. Flores, June 1995. "Preliminary Drilling Results for Boreholes LADP-3 and LADP-4" (excerpt), Los Alamos National Laboratory Report LA-12934-MS, Los Alamos, New Mexico. (Broxton et al. 1995, 50119)

Broxton, D. E., R. Gilkeson, P. Longmire, J. Marin, R. Warren, D. Vaniman, A. Crowder, B. Newman, B. Lowry, D. Rogers, W. Stone, S. McLin, G. WoldeGabriel, D. Daymon, and D. Wycoff, September 2000. "Characterization Well R-9 Completion Report," Los Alamos National Laboratory Report LA-UR-00-4120, Los Alamos, New Mexico. (Broxton et al. 2000, 66599)

Broxton, D. E., R. Warren, D. Vaniman, B. Newman, A. Crowder, M. Everett, R. Gilkeson, P. Longmire, J. Marin, W. Stone, S. McLin, and D. Rogers, September 2000. "Characterization Well R-12 Completion Report," Los Alamos National Laboratory Report LA-UR-00-3785, Los Alamos, New Mexico. (Broxton et al. 2000, 66601)

Dale, M., July 29, 1999. "R-15(740) Preliminary Data and OB's Analyte Suite," e-mail message to G. Turner (DOE-LAAO), D. Broxton (LANL EES-1), S. Yanicak (DOE-LAAO), K. Mullen (LANL ESH-18), C. Hanlon-Meyer (NMED) from M. Dale (DOE-AL), Albuquerque, New Mexico. (Dale 1999, 64058)

Environmental Surveillance and Compliance Programs, September 1997. "Environmental Surveillance and Compliance at Los Alamos during 1996," Los Alamos National Laboratory Report LA-13343-ENV, Los Alamos, New Mexico. (Environmental Surveillance and Compliance Programs 1997, 56684)

Freeze, R. A., and J. A. Cherry, 1979. *Groundwater*, ISBN 0-13-365312, Prentice Hall, Englewood Cliffs, New Jersey. (Freeze and Cherry 1979, 64057)

Gee, G. W., M. D. Campbell, G. S. Campbell, and J. H. Campbell, 1992. "Rapid Measurement of Low Soil Water Potentials Using a Water Activity Meter," *Soil Science Society of America Journal*, Vol. 56, pp. 1068–1070. (Gee et al. 1992, 58717)

Griggs, R. L., 1964. "Geology and Ground-Water Resources of the Los Alamos Area New Mexico," with a section on Quality of Water by John D. Hem, US Geological Survey Water-Supply Paper 1753, Washington, DC. (Griggs 1964, 8795)

Kendall, C., and T. B. Coplen, 1985. "Multisample Conversion of Water to Hydrogen by Zinc for Stable Isotope Determination," *Analytical Chemistry*, Vol. 57, pp. 1437–1446. (Kendall and Coplen 1985, 64061)

Kendrick, B., January 1999. "Revised Summary Table," memorandum from B. Kendrick, TechLaw Inc., to P. Longmire, Los Alamos National Laboratory, Los Alamos, New Mexico. (Kendrick 1999, 66141)

Langmuir, D., 1997. *Aqueous Environmental Geochemistry*, Prentice-Hall, Inc., Upper Saddle River, New Jersey. (Langmuir 1997, 56037)

LANL (Los Alamos National Laboratory), October 25, 1995. "Groundwater Protection Management Program Plan" (draft), Revision 2.0, Los Alamos, New Mexico. (LANL 1995, 50124)

LANL (Los Alamos National Laboratory), November 1995. "Task/Site Work Plan for Operable Unit 1049: Los Alamos Canyon and Pueblo Canyon," Los Alamos National Laboratory Report LA-UR-95-2053, Los Alamos, New Mexico. (LANL 1995, 50290)

LANL (Los Alamos National Laboratory), April 1997. "Core Document for Canyons Investigations," Los Alamos National Laboratory Report LA-UR-96-2083, Los Alamos, New Mexico. (LANL 1997, 55622)

LANL (Los Alamos National Laboratory), September 1997. "Work Plan for Mortandad Canyon," Los Alamos National Laboratory Report LA-UR-97-3291, Los Alamos, New Mexico. (LANL 1997, 56835)

LANL (Los Alamos National Laboratory), March 1998. "Field Implementation Plan for the Drilling and Testing of LANL Regional Characterization Well R-12," Los Alamos, New Mexico. (LANL 1998, 59162)

LANL (Los Alamos National Laboratory), May 22, 1998. "Hydrogeologic Workplan," Los Alamos, New Mexico. (LANL 1998, 59599)

LANL (Los Alamos National Laboratory), June 1999. "Field Implementation Plan for Drilling and Testing of Regional Characterization Well R-15," Los Alamos National Laboratory Report, Los Alamos, New Mexico. (LANL 1999, 64062)

Purtymun, W. D., January 1984. "Hydrologic Characteristics of the Main Aquifer in the Los Alamos Area: Development of Ground Water Supplies," Los Alamos National Laboratory Report LA-9957-MS, Los Alamos, New Mexico. (Purtymun 1984, 6513)

Purtymun, W. D., January 1995. "Geologic and Hydrologic Records of Observation Wells, Test Holes, Test Wells, Supply Wells, Springs, and Surface Water Stations in the Los Alamos Area," Los Alamos National Laboratory Report LA-12883-MS, Los Alamos, New Mexico. (Purtymun 1995, 45344)

Rogers, D. B., July 1998. "Impact of Tritium Disposal on Surface Water and Groundwater at Los Alamos National Laboratory Through 1997," Los Alamos National Laboratory Report LA-13465-SR, Los Alamos, New Mexico. (Rogers 1998, 59169)

Rogers, D. B., and B. M. Gallaher, September 1995. "The Unsaturated Hydraulic Characteristics of the Bandelier Tuff," Los Alamos National Laboratory Report LA-12968-MS, Los Alamos, New Mexico. (Rogers and Gallaher 1995, 49824)

Ryti, R. T., P. A. Longmire, D. E. Broxton, S. L. Reneau, and E. V. McDonald, May 7, 1998. "Inorganic and Radionuclide Background Data for Soils, Canyon Sediments, and Bandelier Tuff at Los Alamos National Laboratory" (draft), Los Alamos National Laboratory Report, Los Alamos, New Mexico. (Ryti et al. 1998, 58093)

Shurbaji, A. R., and A. R. Campbell, 1997. "Study of Evaporation and Recharge in Desert Soil Using Environmental Tracers, New Mexico, USA," *Environmental Geology*, Vol. 29, pp. 147–151. (Shurbaji and Campbell 1997, 64063)

Socki, R. A., H. R. Karlsson, and E. K. Gibson, 1992. "Extraction Technique for Determination of Oxygen-18 in Water Using Preevacuated Glass Vials," *Analytical Chemistry*, Vol. 64, pp. 829–831. (Socki et al. 1992, 64064)

Vaniman, D., G. Cole, J. Gardner, J. Conaway, D. Broxton, S. Reneau, M. Rice, G. WoldeGabriel, J. Blossom, and F. Goff, 1996. "Development of a Site-Wide Geologic Model for Los Alamos National Laboratory," progress report to the Earth Sciences Council of the Environmental Restoration Project, Los Alamos National Laboratory, Los Alamos National Laboratory Report LA-UR-00-2059. Los Alamos, New Mexico. (Vaniman et al. 1996, 63991)

Waresback, D. B., August 1986. "The Puye Formation, New Mexico: Analysis of a Continental, Rift-Filling, Volcaniclastic Alluvial-Fan Sequence," Master of Science in Geology thesis, University of Texas, Arlington, Texas. (Waresback 1986, 58715)

Wingo, R. M., September 13, 1999. "R-15, Tritium Values," New Mexico Environment Department memorandum to S. Yanicak, DOE-LAAO, Los Alamos, New Mexico. (Wingo 1999, 64065)

Appendix A

Lithologic Log

LOS ALAMOS NATIONAL LABORATORY
REGIONAL HYDROGEOLOGIC CHARACTERIZATION PROJECT
ENVIRONMENTAL RESTORATION, CANYONS FOCUS AREA
BOREHOLE LOG

BOREHOLE ID: R-15				TA/OU: 05/1049		Page 1 of 12			
DRILLING COMPANY: Stewart Bros./Dynatec		START DATE: September 10, 1998		END DATE: September 17, 1999					
DRILLING EQ/METHOD: Failing F-10/Foremost DR24				SAMPLING EQ/METHOD: Wireline core barrel sampling					
GROUND ELEVATION: 6820'				TOTAL DEPTH = 1107' bgs					
DRILLER: White/Thoren		GEOLOGY P.I.: Rick Warren		SITE GEOLOGIST: Jon Marin					
Depth (ft)	Elevation (ft)	Core Run # (amt.-recov./amt. attemp.)	Core Run	Cuttings Collected	Hydrologic Property (Physprop) and Geochemical (Geochem) Samples (CAMO-9x-xxxx)	Moisture/Matric Pot. R15-depth (ft)	Lithology	Graphic Log	Lithologic Symbol
0	6815				GEOCHEM 98-241 (2.0-2.5)	R-15-2	ALLUVIUM: very dry, light to dark brown, silt and sand, soft, rounded sanidine and quartz grains.		Qal
5	6810					R-15-5			
10	6805				GEOCHEM 98-211 (2.6-17.0)		UNIT 1G TSHIREGE MEMBER, BANDELIER TUFF: dry, grayish orange pink (5 YR 7/2), 10-20% light grayish white obloid vitric pumice lapilli to 1 cm in non-indurated ash matrix, 20% quartz phenocrysts in matrix and 15% in lapilli to 1 mm, 5-10% oxidized lithics.		Qbt
15	6800				GEOCHEM 98-242 (17.0-17.5)				
20	6795				GEOCHEM 98-212 (17.5-20.0)	R-15-17			
25	6790				GEOCHEM 98-253 (22.0-22.5)				
30	6785				GEOCHEM 98-213 (25.0-25.3)	R-15-22			
35	6780				GEOCHEM 98-243 (25.3-26.0)	R-15-25.5			
40	6775				PHYSPROP (32.0-32.5)				
45	6770				GEOCHEM 98-254 (39.5-40.0)	R-15-32			
50	6765								
55	6760				GEOCHEM 98-214 (40.0-41.5)	R-15-39.5			
60	6755				PHYSPROP (44.5-45.0)	R-15-44.5			
65	6750				GEOCHEM 98-244 (49.5-50.0)	R-15-49.5			
70	6745				PHYSPROP (54.5-55.0)	R-15-54.5			
75	6740				GEOCHEM 98-255 (59.5-60.0)				
80	6735				GEOCHEM 98-215 (63.3-64.3)	R-15-59.5			
85	6730				PHYSPROP (64.5-65.0)				
90	6725				GEOCHEM 98-215 (65.0-65.8)	R-15-64.5	TSANKAWI PUMICE BED: moist, 70% chalky pumice lapilli up to 1 cm in ash matrix.		Qct
95	6720				GEOCHEM 98-217 (68.3-69.3)	R-15-67			
100	6715				GEOCHEM 98-256 (69.5-70.0)	R-15-69.5	CERRO TOLEDO INTERVAL: moist, pumiceous non-stratified red-brown ash matrix supporting chalky, 30% pumice lapilli up to 1 cm.		Qct
					GEOCHEM 98-245 (74.5-75.0)	R-15-74.5			
					GEOCHEM 98-218 (75.8-76.6)		CERRO TOLEDO INTERVAL: moist, stratified, reddish brown clayey silt matrix; 50% chalky pumice lapilli up to 1 cm; dark gray Tchicoma lithics to 5%.		Qct
					PHYSPROP (79.5-80.0)	R-15-79.5			
					GEOCHEM 98-257 (84.5-85.0)	R-15-84.5	CERRO TOLEDO INTERVAL: pumice fall; moist, up to 60% white chalky pumice lapilli in red-brown ash matrix.		Qct
					GEOCHEM 98-219 (87.0-87.4)	R-15-86.1			
					GEOCHEM 98-246 (89.5-90.0)	R-15-87.5	CERRO TOLEDO INTERVAL: dry sand and gravel, up to 30% quartzite in light gray mafic-rich sandy matrix.		Qct
					GEOCHEM 98-220 (90.8-91.6)	R-15-89.5			
					PHYSPROP (94.5-95.0)	R-15-94.5	CERRO TOLEDO INTERVAL: dry sand, medium-grained, very clean, well sorted.		Qct
					GEOCHEM 98-247 (99.5-100.0)				
					GEOCHEM 98-221 (100.0-104.5)	R-15-99.5	CERRO TOLEDO INTERVAL: moist sand and gravel.		Qct
					GEOCHEM 98-258 (104.5-110.0)		CERRO TOLEDO INTERVAL: moist clayey silt, reddish brown.		Qct

LOS ALAMOS NATIONAL LABORATORY
REGIONAL HYDROGEOLOGIC CHARACTERIZATION PROJECT
ENVIRONMENTAL RESTORATION, CANYONS FOCUS AREA
BOREHOLE LOG

BOREHOLE ID: R-15			TA/OU: 05/1049			Page 2 of 12			
DRILLING COMPANY: Stewart Bros./Dynatec			START DATE: September 10, 1998			END DATE: September 17, 1999			
DRILLING EQ/METHOD: Failing F-10/Foremost DR24			SAMPLING EQ/METHOD: Wireline core barrel sampling						
GROUND ELEVATION: 6820'			TOTAL DEPTH = 1107' bgs						
DRILLER: White/Thoren			GEOLOGY P.I.: Rick Warren			SITE GEOLOGIST: Jon Marin			
Depth (ft)	Elevation (ft)	Core Run # (amt.-recov./amt. attemp.)	Core Run	Cuttings Collected	Hydrologic Property (Physprop) and Geochemical (Geochem) Samples (CAMO-9x-xxxx)	Moisture/Matric Pot. R15-depth (ft)	Lithology	Graphic Log	Lithologic Symbol
105	6710				GEOCHEM 98-258 (104.5-105.0)	R-15-104.5	CERRO TOLEDO INTERVAL: moist clayey silt, reddish brown.		
110	6705				GEOCHEM 98-222 (105.0-105.8)	R-15-109.5	CERRO TOLEDO INTERVAL: moist sand, oxidized, grayish brown, fine-grained, well sorted.		Qct
115	6700				PHYSPROP (109.5-110.0)	R-15-114.5	CERRO TOLEDO INTERVAL: moist sand, clean, light brown (5 YR 6/4) to light brown (5 YR 5/6) fine-grained, well sorted.		
120	6695				GEOCHEM 98-223 (112.5-114.5)	R-15-119.5			
125	6690				GEOCHEM 98-259 (114.5-115.0)	R-15-124.5			
130	6685				GEOCHEM 98-224 (115.0-115.8)	R-15-129.5			
135	6680				PHYSPROP (119.5-120.0)	R-15-134.5			
140	6675				GEOCHEM 98-225 (120.0-120.8)	R-15-139.5			
145	6670				GEOCHEM 98-252 (124.5-125.0)	R-15-144.5			
150	6665				PHYSPROP (129.5-130.0)	R-15-149.5			
155	6660				PHYSPROP (134.5-135.0)	R-15-154.5			
160	6655				PHYSPROP (139.5-140.0)	R-15-159.5			
165	6650				GEOCHEM 98-260 (144.5-145.0)	R-15-164.5			
170	6645				GEOCHEM 98-226 (148.3-149.3)	R-15-169.5			
175	6640				PHYSPROP (149.5-150.0)	R-15-174.5			
180	6635				GEOCHEM 98-227 (150.0-150.8)	R-15-179.5			
185	6630				PHYSPROP (154.5-155.0)	R-15-184.5			
190	6625				PHYSPROP (159.5-160.0)	R-15-189.5			
195	6620				PHYSPROP (164.5-165.0)	R-15-194.5			
200	6615				GEOCHEM 98-261 (169.5-170.0)	R-15-199.5			
					GEOCHEM 98-228 (170.0-170.8)				
					PHYSPROP (174.5-175.0)				
					GEOCHEM 98-248 (179.5-180.0)				
					GEOCHEM 98-249 (184.5-185.0)				
					PHYSPROP (189.5-190.0)				
					PHYSPROP (194.5-195.0)				
					PHYSPROP (199.5-200.0)				
					PHYSPROP (204.5-205.0)				
					PHYSPROP (209.5-210.0)				
							OTOWI MEMBER, BANDELIER TUFF: moist to dry ash flow tuff, non-indurated, grayish orange pink (5 YR 7/2), 2% vitric equant pumice lapilli with excellent tube structures to 5 cm and containing up to 30% quartz phenocrysts, 1% Tschicoma lithics to 4 cm).		Qbo
							OTOWI MEMBER, BANDELIER TUFF: same as above (SAA), pale yellowish brown (10 YR 6/2).		

LOS ALAMOS NATIONAL LABORATORY
REGIONAL HYDROGEOLOGIC CHARACTERIZATION PROJECT
ENVIRONMENTAL RESTORATION, CANYONS FOCUS AREA
BOREHOLE LOG

BOREHOLE ID: R-15				TA/OU: 05/1049		Page 3 of 12			
DRILLING COMPANY: Stewart Bros./Dynatec				START DATE: September 10, 1998		END DATE: September 17, 1999			
DRILLING EQ/METHOD: Failing F-10/Foremost DR24				SAMPLING EQ/METHOD: Wireline core barrel sampling					
GROUND ELEVATION: 6820'				TOTAL DEPTH = 1107' bgs					
DRILLER: White/Thoren		GEOLOGY P.I.: Rick Warren		SITE GEOLOGIST: Jon Marin					
Depth (ft)	Elevation (ft)	Core Run # (amt.-recov./amt. attemp.)	Core Run	Cuttings Collected	Hydrologic Property (Physprop) and Geochemical (Geochem) Samples (CAMO-9x-xxxx)	Moisture/Matric Pot. R15-depth (ft)	Lithology	Graphic Log	Lithologic Symbol
205	6610				PHYSPROP (214.5-215.0')	R-15-204.5	OTOWI MEMBER, BANDELIER TUFF: same as above (SAA), pale yellowish brown (10 YR 6/2).		
210	6605				PHYSPROP (219.5-220.0')	R-15-209.5			
215	6600				PHYSPROP (224.5-225.0')	R-15-214.5			
220	6595				GEOCHEM 98-262 (229.5-230.0')	R-15-219.5			
225	6590				GEOCHEM 98-229 (230.0-231.3')	R-15-224.5			
230	6585				PHYSPROP (234.5-235.0')	R-15-229.5			
235	6580				PHYSPROP (239.5-240.0')	R-15-234.5			
240	6575				PHYSPROP (244.5-245.0')	R-15-239.5			
245	6570				PHYSPROP (249.0-249.5')	R-15-244.5	OTOWI MEMBER, BANDELIER TUFF: SAA, indurated enough to place unwrapped in core box.		Qbo
250	6565				PHYSPROP (254.5-255.0')	R-15-249.8			
255	6560				PHYSPROP (259.5-260.0')	R-15-254.5			
260	6555				PHYSPROP (264.0-264.5')	R-15-259.5			
265	6550				GEOCHEM 98-263 (269.5-270.0')	R-15-264.8			
270	6545				GEOCHEM 98-230 (270.0-272.5')	R-15-269.5	OTOWI MEMBER, BANDELIER TUFF: SAA, non-indurated with rare pumice lapilli.		
275	6540				PHYSPROP (274.5-275.0')	R-15-274.5			
280	6535				PHYSPROP (279.5-280.0')	R-15-279.5			
285	6530				PHYSPROP (284.5-285.0')	R-15-284.5			
290	6525				PHYSPROP (289.5-290.0')	R-15-289.5			
295	6520				PHYSPROP (294.5-295.0')	R-15-294.5			

LOS ALAMOS NATIONAL LABORATORY
REGIONAL HYDROGEOLOGIC CHARACTERIZATION PROJECT
ENVIRONMENTAL RESTORATION, CANYONS FOCUS AREA
BOREHOLE LOG

BOREHOLE ID: R-15			TA/OU: 05/1049			Page 4 of 12			
DRILLING COMPANY: Stewart Bros./Dynatec			START DATE: September 10, 1998			END DATE: September 17, 1999			
DRILLING EQ/METHOD: Failing F-10/Foremost DR24			SAMPLING EQ/METHOD: Wireline core barrel sampling						
GROUND ELEVATION: 6820'			TOTAL DEPTH = 1107' bgs						
DRILLER: White/Thoren			GEOLOGY P.I.: Rick Warren			SITE GEOLOGIST: Jon Marin			
Depth (ft)	Elevation (ft)	Core Run # (amt.-recov./amt. attemp.)	Core Run	Cuttings Collected	Hydrologic Property (Physprop) and Geochemical (Geochem) Samples (CAMO-9x-xxxx)	Moisture/Matric Pot. R15-depth (ft)	Lithology	Graphic Log	Lithologic Symbol
300	6515				GEOCHEM 98-250 (299.5-300.0')	R-15-299.5	OTOWI MEMBER, BANDELIER TUFF: SAA, non-indurated with rare pumice lapilli.		
305	6510				PHYSPROP (304.5-305.0')	R-15-304.5	OTOWI MEMBER, BANDELIER TUFF: SAA, non-indurated with rare pumice lapilli, 5% fine- to medium-grained Tschicoma lithics to 2 mm.		
310	6505				PHYSPROP (309.5-310.0')	R-15-309.5			
315	6500				PHYSPROP (314.5-315.0')	R-15-314.5			
320	6495				PHYSPROP (319.5-320.0')	R-15-319.5			
325	6490				GEOCHEM 98-264 (324.5-325')	R-15-324.5	OTOWI MEMBER, BANDELIER TUFF: SAA, indurated enough to place unwrapped in core box.		
330	6485				GEOCHEM 98-231 (325.0-327.5')	R-15-329.5	OTOWI MEMBER, BANDELIER TUFF: moist ash flow tuff, SAA.		
335	6480				PHYSPROP (329.5-330.0')	R-15-334.5	OTOWI MEMBER, BANDELIER TUFF: dry, ash flow tuff, SAA.		
340	6475				PHYSPROP (334.5-335.0')	R-15-339.5			
345	6470				PHYSPROP (339.5-340.0')	R-15-344.5	OTOWI MEMBER, BANDELIER TUFF: moist ash flow tuff, non-indurated, pale yellowish brown (10 YR 6/2).		Qbo
350	6465				PHYSPROP (344.5-345.0')	R-15-349.5			
355	6460					R-15-354.5			
360	6455				PHYSPROP (349.5-350.0')	R-15-359.5			
365	6450				PHYSPROP (354.5-355.0')	R-15-364.5			
370	6445				PHYSPROP (359.5-360.0')	R-15-369.5			
375	6440				PHYSPROP (364.5-365.0')	R-15-374.5			
380	6435				PHYSPROP (369.5-370.0')	R-15-379.5	OTOWI MEMBER, BANDELIER TUFF: pumice swarm, 20% vitric equant lapilli up to 3 cm, partially oxidized with up to 20% quartz phenocrysts to 1 mm.		
385	6430				GEOCHEM 98-265 (379.5-380')	R-15-384.5			
390	6425				GEOCHEM 98-232,233 (380.0-384.0')	R-15-389.5	OTOWI MEMBER, BANDELIER TUFF: moist ash flow tuff, non-indurated, pale yellowish brown (10 YR 6/2).		
395	6420				PHYSPROP (384.5-385.0')	R-15-389.5			
					PHYSPROP (389.5-390.0')	R-15-394.2			
					PHYSPROP (394.2-394.6')				
					PHYSPROP (394.6-				

Qbo

LOS ALAMOS NATIONAL LABORATORY
REGIONAL HYDROGEOLOGIC CHARACTERIZATION PROJECT
ENVIRONMENTAL RESTORATION, CANYONS FOCUS AREA
BOREHOLE LOG

BOREHOLE ID: R-15			TA/OU: 05/1049			Page 5 of 12			
DRILLING COMPANY: Stewart Bros./Dynatec			START DATE: September 10, 1998			END DATE: September 17, 1999			
DRILLING EQ/METHOD: Failing F-10/Foremost DR24			SAMPLING EQ/METHOD: Wireline core barrel sampling						
GROUND ELEVATION: 6820'			TOTAL DEPTH = 1107' bgs						
DRILLER: White/Thoren			GEOLOGY P.I.: Rick Warren			SITE GEOLOGIST: Jon Marin			
Depth (ft)	Elevation (ft)	Core Run # (amt.-recov./amt. attemp.)	Core Run	Cuttings Collected	Hydrologic Property (Physprop) and Geochemical (Geochem) Samples (CAMO-9x-xxxx)	Moisture/Matric Pot. R15-depth (ft)	Lithology	Graphic Log	Lithologic Symbol
400	6415				PHYSPROP (399.6-400.0')	R-15-399.6	OTOWI MEMBER, BANDELIER TUFF: moist ash flow tuff, non-indurated, pale yellowish brown (10 YR 6/2).		Qbo
405	6410				PHYSPROP (404.2-404.6')	R-15-404.2			
410	6405				PHYSPROP (404.6-405')	R-15-409.6			
415	6400				PHYSPROP (409.6-410.0')	R-15-414.2			
420	6395				PHYSPROP (414.2-414.6')	R-15-419.2			
425	6390				GEOCHEM 98-266 (414.6-415.0')		GUAJE PUMICE BED: dry, light tannish white to very pale orange (10 YR 8/2) vitric pumice lapilli aggregate; lapilli have minute mafic accessory minerals and show poorly defined tube structures in honey combed texture.		Qbog
430	6385				GEOCHEM 98-234 (415.0-419.0')				
435	6380				PHYSPROP (419.2-419.6')				
440	6375				GEOCHEM 98-251 (419.6-420.0')		GUAJE PUMICE BED: dry, lithic-rich, 15% pumice lapilli.		Qbog
445	6370					R-15-447	GUAJE PUMICE BED: dry, lithic-rich, pumice lapilli (40%), Tschicoma lithics (20%) subrounded quartz and sanidine grains (10%).		
450	6365					R-15-452	GUAJE PUMICE BED: dry, light tannish white to very pale orange (10 YR 8/2) to very light gray N8 vitric pumice aggregate (90%); dark gray to black dacite Tschicoma formation lithics to 10%.		
455	6360						GUAJE PUMICE BED: dry, lithic-rich, pumiceous aggregate.		Tpf
460	6355								
465	6350								
470	6345						PUYE FORMATION: dry, Tschicoma formation volcanic clasts, 70% grayish red (5 YR 4/2), 30% medium light gray N6.		Tpf
475	6340								
480	6335								
485	6330								
490									

LOS ALAMOS NATIONAL LABORATORY
REGIONAL HYDROGEOLOGIC CHARACTERIZATION PROJECT
ENVIRONMENTAL RESTORATION, CANYONS FOCUS AREA
BOREHOLE LOG

BOREHOLE ID: R-15				TA/OU: 05/1049		Page 6 of 12			
DRILLING COMPANY: Stewart Bros./Dynatec				START DATE: September 10, 1998		END DATE: September 17, 1999			
DRILLING EQ/METHOD: Failing F-10/Foremost DR24				SAMPLING EQ/METHOD: Wireline core barrel sampling					
GROUND ELEVATION: 6820'				TOTAL DEPTH = 1107' bgs					
DRILLER: White/Thoren		GEOLOGY P.I.: Rick Warren		SITE GEOLOGIST: Jon Marin					
Depth (ft)	Elevation (ft)	Core Run # (amt. - recov./amt. attempt.)	Core Run	Cuttings Collected	Hydrologic Property (Physprop) and Geochemical (Geochem) Samples (CAMO-9x-xxxx)	Moisture/Matric Pot. R15-depth (ft)	Lithology	Graphic Log	Lithologic Symbol
490	6325						PUYE FORMATION: dry, Tschicoma formation volcanic clasts, 70% grayish red (5 YR 4/2), 30% medium light gray N6.		Tpf
495	6320				PHYSPROP (494.0-495.0')	R-15-497			
500	6315				PHYSPROP (501.0-501.5')	R-15-502	PALEOSOL: moist, dark brown, clayey silt with 20% oxidized weathered basalt fragments.		
505	6310					R-15-507	BASALT OF THE CERROS DEL RIO VOLCANIC FIELD, UNDIVIDED: weathered oxidized vesicular basalt (60%), moist dark brown clayey silt 40%.		
510	6305					R-15-512			
515	6300					R-15-517	BASALT OF THE CERROS DEL RIO VOLCANIC FIELD, UNDIVIDED: dry, medium light gray N6 to locally moderate yellowish brown (10YR 5/4), aphanitic groundmass, vesicular, clay in fractures.		
520	6295				PHYSPROP (520.5-521.0')	R-15-522			
525	6290					R-15-527			
530	6285					R-15-532	BASALT OF THE CERROS DEL RIO VOLCANIC FIELD, UNDIVIDED: dry, medium dark gray N4, massive, aphanitic groundmass, non-vesicular.		
535	6280					R-15-537			
540	6275					R-15-540	BASALT OF THE CERROS DEL RIO VOLCANIC FIELD, UNDIVIDED: dry, brownish gray (5 YR 4/1), coarse-grained ophitic texture, 75% plagioclase laths and larger anhedral masses, 20% anhedral to subhedral pyroxene phenocrysts up to 2.0 mm; 5% equant light green olivine crystals to 1.0 mm.		Tb2
545	6270								
550	6265								
555	6260								
560	6255								
565	6250								
570	6245								
575	6240						BASALT OF THE CERROS DEL RIO VOLCANIC FIELD, UNDIVIDED: dry, medium dark gray N4, massive, aphanitic groundmass, non-vesicular, plagioclase laths to 0.1 mm.		
580									

LOS ALAMOS NATIONAL LABORATORY
REGIONAL HYDROGEOLOGIC CHARACTERIZATION PROJECT
ENVIRONMENTAL RESTORATION, CANYONS FOCUS AREA
BOREHOLE LOG

BOREHOLE ID: R-15			TA/OU: 05/1049			Page 7 of 12					
DRILLING COMPANY: Stewart Bros./Dynatec			START DATE: September 10, 1998			END DATE: September 17, 1999					
DRILLING EQ/METHOD: Failing F-10/Foremost DR24			SAMPLING EQ/METHOD: Wireline core barrel sampling								
GROUND ELEVATION: 6820'			TOTAL DEPTH = 1107' bgs								
DRILLER: White/Thoren			GEOLOGY P.I.: Rick Warren			SITE GEOLOGIST: Jon Marin					
Depth (ft)	Elevation (ft)	Core Run # (amt.-recov./amt. attemp.)	Core Run	Cuttings Collected	Hydrologic Property (Physprop) and Geochemical (Geochem) Samples (CAMO-9x-xxxx)	Moisture/Matric Pot. R15-depth (ft)	Lithology	Graphic Log	Lithologic Symbol		
580	6235						BASALT OF THE CERROS DEL RIO VOLCANIC FIELD, UNDIVIDED: dry, dark gray to brownish gray (5 YR 4/1), coarse-grained ophitic texture, 75% plagioclase laths and larger anhedral masses, 20% anhedral to subhedral pyroxene phenocrysts up to 2.0 mm; 5% equant light green olivine crystals to 1.0 mm.		Tb2		
585	6230										
590	6225										
595	6220										
600	6215										
605	6210										
610	6205										
615	6200										
620	6195										
625	6190										
630	6185					R-15-630					
635	6180										
640	6175					R-15-640					
645	6170				PHYSPROP (643.0-646.0')	R-15-648	BASALT OF THE CERROS DEL RIO VOLCANIC FIELD, UNDIVIDED: moist, reddish gray, oxidized, clay armor, some subrounded chips suggest possible old alluvium.		Tb2		
650	6165										
655	6160										
660	6155					R-15-660					
665	6150										
670	6145					R-15-670					

LOS ALAMOS NATIONAL LABORATORY
REGIONAL HYDROGEOLOGIC CHARACTERIZATION PROJECT
ENVIRONMENTAL RESTORATION, CANYONS FOCUS AREA
BOREHOLE LOG

BOREHOLE ID: R-15			TA/OU: 05/1049			Page 8 of 12			
DRILLING COMPANY: Steward Bros./Dynatec			START DATE: September 10, 1998			END DATE: September 17, 1999			
DRILLING EQ/METHOD: Failing F-10/Foremost DR24			SAMPLING EQ/METHOD: Wireline core barrel sampling						
GROUND ELEVATION: 6820'			TOTAL DEPTH = 1107' bgs						
DRILLER: White/Thoren			GEOLOGY P.I.: Rick Warren			SITE GEOLOGIST: Jon Marin			
Depth (ft)	Elevation (ft)	Core Run # (amt. - recov./amt. attempt.)	Core Run	Cuttings Collected	Hydrologic Property (Physprop) and Geochemical (Geochem) Samples (CAMO-9x-xxxx)	Moisture/Matric Pot. R15-depth (ft)	Lithology	Graphic Log	Lithologic Symbol
675	6140				PHYSPROP (675.0-678.0')	R-15-675	BASALT OF THE CERROS DEL RIO VOLCANIC FIELD, UNDIVIDED: moist, reddish gray, oxidized, clay armor, some subrounded chips suggest possible old alluvium.		
680	6135					R-15-680			
685	6130					R-15-685	BASALT OF THE CERROS DEL RIO VOLCANIC FIELD, UNDIVIDED: dry, massive, ophitic texture, few vesicles, no clay.		
690	6125					R-15-690			
695	6120				PHYSPROP (695.0-698.0')	R-15-695			
700	6115					R-15-700	BASALT OF THE CERROS DEL RIO VOLCANIC FIELD, UNDIVIDED: dry, greenish gray aphanitic glassy groundmass, moderately vesicular, orange clay in vesicles.		
705	6110					R-15-705			
710	6105					R-15-710			Tb2
715	6100					R-15-715			
720	6095					R-15-720			
725	6090				PHYSPROP (725.0-728.0')	R-15-725			
730	6085					R-15-730	BASALT OF THE CERROS DEL RIO VOLCANIC FIELD, UNDIVIDED: dry, massive, non-vesicular, no clay.		
735	6080					R-15-735			
740	6075	R-1(1.5/3.5)			GEOCHEM 99-121 (742.0-742.4)	R-15-740	PALEOSOL: moist, orange brown, clayey silt, basalt fragments up to 2 inches.		
745	6070	R-2(0/0.5) R-3(0.7/1.0) R-4(1.7/5.0)			GEOCHEM 99-122 (744.0-744.5)	R-15-746	BASALT OF THE CERROS DEL RIO VOLCANIC FIELD, UNDIVIDED: moist, reddish gray, oxidized, heavy clay (up to 1 cm thick) in fractures and vesicles; possible old alluvium.		
750	6065	R-5(0/1.5)			PHYSPROP (746.0-746.5')		PUYE FORMATION: silty sand with abundant clay; rare basalt fragments of 2-3 mm.		
755	6060						unrecovered		
760	6055						PUYE FORMATION: fine gravel, mostly 2-5 mm with clasts to 2 cm. Coarser clasts all Tschicoma lavas; finer clasts include Tschicoma and fine-grained white siltstone		Tpf
765	6050						PUYE FORMATION: clasts of Tschicoma up to 4 cm; buff sandstone fragments among finer gravels to 4 mm; sand-size quartz.		
770	6045						PUYE FORMATION: clasts of mottled and gray Tschicoma lavas up to 3 cm; quartz sand and sandstone clasts absent.		

Tb2

Tpf

LOS ALAMOS NATIONAL LABORATORY
REGIONAL HYDROGEOLOGIC CHARACTERIZATION PROJECT
ENVIRONMENTAL RESTORATION, CANYONS FOCUS AREA
BOREHOLE LOG

BOREHOLE ID: R-15				TA/OU: 05/1049				Page 9 of 12			
DRILLING COMPANY: Stewart Bros./Dynatec				START DATE: September 10, 1998				END DATE: September 17, 1999			
DRILLING EQ/METHOD: Failing F-10/Foremost DR24				SAMPLING EQ/METHOD: Wireline core barrel sampling							
GROUND ELEVATION: 6820'				TOTAL DEPTH = 1107' bgs							
DRILLER: White/Thoren				GEOLOGY P.I.: Rick Warren				SITE GEOLOGIST: Jon Marin			
Depth (ft)	Elevation (ft)	Core Run # (amt.-recov./amt. attemp.)	Core Run	Cuttings Collected	Hydrologic Property (Physprop) and Geo-chemical (Geochem) Samples (CAMO-9x-xxxx)	Moisture/Matric Pot. R15-depth (ft)	Lithology	Graphic Log	Lithologic Symbol		
775	6040						PUYE FORMATION: clasts of mottled and gray Tschicoma lavas up to 3 cm; quartz sand and sandstone clasts absent.		TpF		
780	6035						PUYE FORMATION: finer clasts (<2 cm, mostly 1 cm or smaller); Tschicoma lithologies include paler brown and possibly silicified lavas; distinctive red/black vitrophyre with flame of ~10x flattening ratio.				
785	6030						PUYE FORMATION: Tschicoma gravels of ~1 cm with sands of variable quartz abundance.				
790	6025										
795	6020										
800	6015										
805	6010										
810	6005										
815	6000						PUYE FORMATION: Tschicoma gravels of 1-2 cm in sands with common quartz.				
820	5995										
825	5990										
830	5985						PUYE FORMATION: rare Tschicoma gravels to 2 cm; sands with variable quartz abundance; some clay present.				
835	5980										
840	5975										
845	5970						PUYE FORMATION: Tschicoma gravels to 2 cm, rounded, mafic-poor with prominent sieved feldspar phenocrysts. Abundant quartz in sand fraction.				
850	5965						PUYE FORMATION: angular Tschicoma gravels with variable quartz abundance in sand fraction.				
855	5960						PUYE FORMATION: Tschicoma gravels to 2 cm, rounded, mafic-poor with prominent sieved feldspar phenocrysts. Abundant quartz in sand fraction.				
860	5955						PUYE FORMATION: fine gravels (<1 cm) of Tschicoma lithologies; quartz grains in sand component relatively rare.				
865	5950						PUYE FORMATION: Tschicoma gravels to 2 cm; distinctive red/black vitrophyre with fiamme of ~10x flattening ratio; white clay coating on some gravels; no quartz in sand component.				
870	5945						PUYE FORMATION: angular Tschicoma gravels to 4 cm; quartz in sand component rare; clay coats some gravels at 877-879.				

Tpf

LOS ALAMOS NATIONAL LABORATORY
REGIONAL HYDROGEOLOGIC CHARACTERIZATION PROJECT
ENVIRONMENTAL RESTORATION, CANYONS FOCUS AREA
BOREHOLE LOG

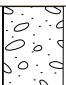
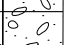
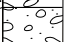
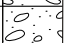
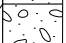

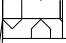

BOREHOLE ID: R-15				TA/OU: 05/1049				Page 10 of 12			
DRILLING COMPANY: Stewart Bros./Dynatec				START DATE: September 10, 1998				END DATE: September 17, 1999			
DRILLING EQ/METHOD: Failing F-10/Foremost DR24				SAMPLING EQ/METHOD: Wireline core barrel sampling							
GROUND ELEVATION: 6820'				TOTAL DEPTH = 1107' bgs							
DRILLER: White/Thoren				GEOLOGY P.I.: Rick Warren				SITE GEOLOGIST: Jon Marin			
Depth (ft)	Elevation (ft)	Core Run # (amt.- recov./amt. attemp.)	Core Run	Cuttings Collected	Hydrologic Property (Physprop) and Geo- chemical (Geochem) Samples (CAMO-9x-xxxx)	Moisture/Matric Pot. R15-depth (ft)	Lithology	Graphic Log	Lithologic Symbol		
875	5940						PUYE FORMATION: angular Tschicoma gravels to 4 cm; quartz in sand component rare; clay coats some gravels at 877-879.		Tpf		
880	5935						PUYE FORMATION: abundance of quartz-bearing 2-3 cm Tschicoma gravels; sand component includes common quartz; gravel component less abundant at 909-913.				
885	5930										
890	5925										
895	5920										
900	5915										
905	5910						PUYE FORMATION: gravels (2-3 cm) of diverse Tschicoma lavas with little sand.				
910	5905										
915	5900										
920	5895						PUYE FORMATION: abundance of quartz-bearing Tschicoma gravels to 1 cm size; sparse sand component.				
925	5890						PUYE FORMATION: gravels of mixed Tschicoma lava types, 1-2 cm; sparse sand component.				
930	5885						PUYE FORMATION: angular quartz-bearing Tschicoma lavas predominate as cobbles of ~1 cm to 949 ft, increasing to 2-3 cm to 973-ft depth. Sand component relatively sparse.				
935	5880										
940	5875										
945	5870										
950	5865										
955	5860						PUYE FORMATION: sand component predominates over fine (<1 cm) gravels; Tschicoma detritus of mixed lithologies, plus gray-glass rhyolites and basalts. Sands rounded and quartz component frosted.				
960	5855										
965	5850										
970	5845										

LOS ALAMOS NATIONAL LABORATORY
REGIONAL HYDROGEOLOGIC CHARACTERIZATION PROJECT
ENVIRONMENTAL RESTORATION, CANYONS FOCUS AREA
BOREHOLE LOG

BOREHOLE ID: R-15			TA/OU: 05/1049			Page 11 of 12			
DRILLING COMPANY: Stewart Bros./Dynatec			START DATE: September 10, 1998			END DATE: September 17, 1999			
DRILLING EQ/METHOD: Failing F-10/Foremost DR24			SAMPLING EQ/METHOD: Wireline core barrel sampling						
GROUND ELEVATION: 6820'			TOTAL DEPTH = 1107' bgs						
DRILLER: White/Thoren			GEOLOGY P.I.: Rick Warren			SITE GEOLOGIST: Jon Marin			
Depth (ft)	Elevation (ft)	Core Run # (amt.-recov./amt. attemp.)	Core Run	Cuttings Collected	Hydrologic Property (Physprop) and Geochemical (Geochem) Samples (CAMO-9x-xxxx)	Moisture/Matric Pot. R15-depth (ft)	Lithology	Graphic Log	Lithologic Symbol
975	5840						PUYE FORMATION: sand component predominates over fine (<1 cm) gravels; Tschicoma detritus of mixed lithologies, plus gray-glass rhyolites and basalts. Sands rounded and quartz component frosted.		
980	5835						PUYE FORMATION: rhyolitic and vitrophyric fine (<1 cm) gravels; rare Tschicoma detritus. Sand predominates with abundant volcanic glass.		
985	5830						PUYE FORMATION: fine gravels (~0.5 cm) dominated by white rhyolitic detritus; abundant sand with vitric sand-size detritus.		
990	5825						PUYE FORMATION: coarse gravels (to 2 cm) of white rhyolitic and darker dacitic lithologies in vitric sand.		
995	5820						PUYE FORMATION: monolithologic layer of reworked aphyric vitric pumice; pumice fragments small (<0.5 cm) and clay-coated.		
1000	5815						PUYE FORMATION: gravels to 1 cm of gray rhyolite lava, dense white rhyolitic pumice, and less common siliceous lithologies; rare cobbles to 3-cm size of biotite rhyolite.		
1005	5810						PUYE FORMATION: sand-rich interval with rare cobbles of siliceous volcanic rocks to 2-cm size; common sand size 1-2 mm.		
1010	5805						PUYE FORMATION: fine (1 mm) sand with little gravel.		
1015	5800						no recovery.		
1020	5795						PUYE FORMATION: gravels of rhyolitic and Tschicoma rhyodacitic lithologies; abundant sand.		
1025	5790						PUYE FORMATION: predominant rhyolitic gravels plus less common clasts of olivine-porphyrific basalt to 3-cm size.		
1030	5785						PUYE FORMATION: dominantly rhyolitic gravels to 1 cm; coarse sand (~2 mm).		
1035	5780						PUYE FORMATION: fine gravels (0.5 cm) with siliceous volcanic lithologies plus fused (contact-melted?) sandstone.		
1040	5775						PUYE FORMATION: fine gravels (0.5 cm) dominated by siliceous volcanic lithologies.		
1045	5770						PUYE FORMATION: fine gravels (0.5 cm) of rhyolitic lithologies and pyroxene-amphibole Tschicoma lavas.		
1050	5765						PUYE FORMATION: fine gravels (0.5 cm) of rhyolitic lithologies; 1-2 mm sand component.		
1055	5760						PUYE FORMATION: gravels of rhyolitic lithologies to 1-cm size; sand commonly 2-mm size.		
1060	5755						PUYE FORMATION: monolithologic layer of reworked aphyric vitric pumice; pumice fragments dense, poorly vesicular, mostly gravel size (~1-2 cm) and clay-coated.		
1065	5750						PUYE FORMATION: fine gravels (0.5 cm) of rhyolitic lithologies; 1-2 mm sand component.		
1070	5745								

Tpf

LOS ALAMOS NATIONAL LABORATORY
REGIONAL HYDROGEOLOGIC CHARACTERIZATION PROJECT
ENVIRONMENTAL RESTORATION, CANYONS FOCUS AREA
BOREHOLE LOG

BOREHOLE ID: R-15				TA/OU: 05/1049				Page 12 of 12			
DRILLING COMPANY: Stewart Bros./Dynatec				START DATE: September 10, 1998				END DATE: September 17, 1999			
DRILLING EQ/METHOD: Failing F-10/Foremost DR24				SAMPLING EQ/METHOD: Wireline core barrel sampling							
GROUND ELEVATION: 6820'				TOTAL DEPTH = 1107' bgs							
DRILLER: White/Thoren				GEOLOGY P.I.: Rick Warren				SITE GEOLOGIST: Jon Marin			
Depth (ft)	Elevation (ft)	Core Run # (amt. - recov./amt. attempt.)	Core Run	Cuttings Collected	Hydrologic Property (Physprop) and Geochemical (Geochem) Samples (CAMO-9x-xxxx)	Moisture/Matric Pot. R15-depth (ft)	Lithology	Graphic Log	Lithologic Symbol		
1075	5740						PUYE FORMATION: fine gravels (0.5 cm) of rhyolitic lithologies; 1-2 mm sand component.		Tpf		
1080	5735						PUYE FORMATION: gravels to 0.75 cm include rhyolitic flow-banded lavas and pyroxene-bearing Tschicoma lavas.				
1085	5730						PUYE FORMATION: sand unit with very rare gravel.				
1090	5725						PUYE FORMATION: fine gravels (0.5 cm) of rhyolitic and rarer intermediate Tschicoma lithologies; 1-2 mm sand component.				
1095	5720						PUYE FORMATION: unit of coarse sand (~2 mm) with very rare rhyolitic gravels.		Tpt		
1100	5715						PUYE FORMATION: sand with gravels (1-2 cm) of rhyolitic, rhyodacitic, and strongly cemented sandstone lithologies.				
1105							TOTAVI LENTIL: sand with rounded cobbles (1 to 3 cm) of varied Tschicoma lavas, quartzite (1% to 10%), silicified and chloritized lavas. Sand component includes distinctive grains of rose quartz.				
							TOTAVI LENTIL: sand with well-rounded cobbles (to 5 cm) of mixed volcanoclastics with sparse (1%) red quartzite.				

Appendix B

Descriptions of Geologic Samples

Sample No.	Description*	Discussion
R15-64.5	B	This sample of very friable core is pinkish gray vitric nonwelded tuff with common white pumice to 3.5 mm. Scarce to common felsic phenocrysts include very conspicuous quartz. Lithics to 2 mm are scarce to rare. No mafics were observed.
R15-64.5	T	Crystal-rich nonwelded vitric tuff; ~25% fragmented alkali-feldspar phenocrysts (to 1 mm in size) and 15% euhedral to fragmented quartz phenocrysts (to 1.5 mm in size) with <1% amphibole (to 1.5 mm, pale blue-green to olive-green pleochroism). Pumice mostly 0.5–1.0 mm but ranging in size to 3 mm.
R15-69.5	B	This sample of very friable core is very light brown vitric nonwelded tuff with common white pumice to 5 mm, with a single light gray banded, vitric hydroclastic shard recognized. Scarce dark brownish black, irregular patches to 1.5 mm represent manganese staining. Scarce to rare felsic phenocrysts include probable quartz to 2 mm. Lithics to 1.5 mm are scarce to rare. No mafics were observed.
R15-69.5	T	Fine-grained sandstone matrix with large (to 5 mm) aphyric vitric pumice. Clay alteration in pumice as well as sandstone matrix. Sand grains are mostly 0.1 to 0.2 mm in diameter, in abundant clay matrix. Sand abundance of quartz>glass>feldspar (sanidine and plagioclase) with rare mafic grains (pyroxene, biotite, amphibole, and olivine).
R15-74.5P7	B	This is a sample of ultrasonically cleaned, vitric pumice fragments from core between 74.3- and 74.5-ft depths in R15. These pinkish gray pumices contain rare dark brown orthopyroxene in prisms to 1.5 mm, magnetite, and a single 2-mm albite twinned plagioclase.
R15-74.5P7	T	Thin section contains four fragments of vitric aphyric pumice, each 1 to 2 cm in size. Pale yellow-brown clay lines of fills many vesicles in the pumice rims but not in the pumice interiors. Rare clusters (to 2 mm in size) of shattered feldspar with interpenetrate twinning.
R15-532D	B	This sample of ultrasonically cleaned cuttings retained on size 7 sieve (>2.8 mm) is grayish black, fine to medium-grained basalt with scattered, round vesicles to 3 mm diameter scarce to common phenocrysts of olive olivine to 3.5 mm and plagioclase laths to 1.5 mm.
R15-562D	B	This sample of ultrasonically cleaned cuttings retained on size 7 sieve (>2.8 mm) is dark gray, somewhat microvesicular, coarse-grained basalt, probably ophitic, with phenocrysts of common dark reddish brown olivine to 3 mm and scarce plagioclase laths to 2.5 mm. Very rare grayish pink clay thinly coats vesicles.
R15-577D	B	This sample of ultrasonically cleaned cuttings retained on size 7 sieve (>2.8 mm) is dark gray, fine-grained basalt with scarce to common phenocrysts of olive olivine and plagioclase, both to 3 mm. A few fragments of medium gray coarse-grained basalt have caved from the overlying interval.
R15-610D	B	This sample of ultrasonically cleaned cuttings retained on size 7 sieve (>2.8 mm) is light gray coarse-grained basalt with phenocrysts of common dark reddish brown unaltered olivine to 1.5 mm and scarce plagioclase to 1 mm. Grayish orange pink clay occurs as rare, thin fracture coatings.
R15-610D	T	Olivine basalt containing olivine phenocrysts to 2 mm (~5%) and plagioclase laths and blocks to 1 mm, grading into groundmass size range. Maximum symmetrical extinction angles on phenocryst albite twins are ~30° (~An-55). One of the five basalt fragments in the thin section contains olivine phenocrysts severely altered to iddingsite.
R15-660D	B	This sample of basalt cuttings consists of clasts ~2–4 cm in diameter with tenacious coatings of cemented silt. Coatings can not be removed by scraping and ultrasonic cleaning. Clasts were lightly crushed in a percussion mortar and hand picked to obtain clean interior pieces for XRF analysis. Crushed fragments with minor remnants of surface coatings were selected for thin-section preparation.

Sample No.	Description*	Discussion
R15-660D	T	Olivine basalt containing phenocrysts of olivine to 2 mm (~4–5%) and clusters of sieved clinopyroxene to 0.3 mm, with feldspar laths to 0.75 mm. Groundmass is intersertal. Clasts of basalt coated by adhesive layer of eolian mica, silt, and basalt detritus; coatings occur as two generations, finer-grained silt underlying coarser-grained silt.
R15-705D	B	This sample of ultrasonically cleaned cuttings retained on size 7 sieve (>2.8 mm) is dark gray to brownish black, medium- to very coarse-grained basalt with phenocrysts of abundant light green olivine to 2 mm and scarce to common plagioclase to 1 mm. Scattered grayish orange pink clay, with thin underlying hematitic layer, coats a few fragments, and occurs as massive vesicle fillings up to 5 mm thick.
R15-705D	T	Olivine basalt containing olivine phenocrysts to 2 mm (~3%), but most olivine is intergranular in the sample groundmass. Maximum symmetrical extinction angles on phenocryst albite twins are ~25° (~An-50). One of the 10 basalt fragments in the thin section is similar to the others but has a vitric matrix.
R15-772-D	B	Volcaniclastic sediment, dry-sieved into weighed splits of >4 mm (30.5 g), 4–2 mm (17.5 g), and <2 mm (5.3 g), then recombined for binocular-microscope examination. Clasts consist of dark black/gray and red mottled Tschicoma volcanic cobbles to ~3 cm in size, gray pyroxene-porphyrific Tschicoma lavas (black pyroxene phenocrysts to ~1 mm in size).
R15-772-D10	T	Sample of sediment R15-772-D was dry-sieved to >2 mm and ultrasonically cleaned to obtain split for thin-section preparation. Thin section of 11 fragments contains 9 volcanic clasts and 2 clasts of fine-grained silt with microcrystalline carbonate cement (probable soil material). The volcanic clasts include 6 fragments of plagioclase-clinopyroxene-orthopyroxene lava, 2 clasts of plagioclase-clinopyroxene-amphibole lava, and 1 clast of plagioclase-clinopyroxene-orthopyroxene-quartz lava, albeit with only rare (<<1%) rounded quartz.
R15-787-D	B	Volcaniclastic sediment, dry-sieved into weighed splits of >4 mm (26.5 g), 4–2 mm (19.4 g), and <2 mm (3.9 g), then recombined for binocular-microscope examination. Volcaniclastic sediment; dark black/gray and red mottled Tschicoma volcanic cobbles to ~2 cm in size, pale-brown amphibole-porphyrific Tschicoma volcanic cobbles, silicified lavas, and red/black flow-banded volcanic clasts up to 5 mm in size.
R15-787-D10	T	Sample of sediment R15-787-D was dry-sieved to >2 mm and ultrasonically cleaned to obtain split for thin-section preparation. Thin section contains 8 volcanic clasts including 4 clasts of plagioclase-clinopyroxene-orthopyroxene lava, 3 clasts of plagioclase-clinopyroxene-orthopyroxene-amphibole lava, and 1 clast of plagioclase-amphibole-biotite-quartz lava.
R15-787-VT	T	Four hand-picked fragments of a single volcanic lithology from R15-787-D. This is the red/black flow-banded lithology, which is a crystal-rich plagioclase-orthopyroxene-clinopyroxene lava with possible amphibole remnants rimmed by small equant clinopyroxenes. Sample contains many indicators of disequilibrium, including clusters of 0.05–0.2 mm clinopyroxene replacing other phases (probably amphibole); coarser clinopyroxene phenocrysts (0.3 mm) may represent a later generation of clinopyroxene associated with smaller orthopyroxene phenocrysts.
R15-879-D	B	Volcaniclastic sediment, dry-sieved into weighed splits of >4 mm (17.6 g), 4–2 mm (22.0 g), and <2 mm (13.7 g), then recombined for binocular-microscope examination. Volcanic clasts include very coarse angular fragments of Tschicoma lava to 4 cm in size with gray to brown matrix and sieved feldspar phenocrysts. Brown clay coats several fragments.

Sample No.	Description*	Discussion
R15-879-D10	T	Sample of sediment R15-879-D was dry-sieved to >2 mm and ultrasonically cleaned to obtain split for thin-section preparation. Thin section contains 9 volcanic clasts including 2 clasts of plagioclase-clinopyroxene-orthopyroxene lava with relic biotite, 1 clast of plagioclase-clinopyroxene-orthopyroxene lava without relic biotite, 1 clast of plagioclase-clinopyroxene-orthopyroxene-quartz lava, and 1 clast of quartz-amphibole-biotite lava, 1 clast of plagioclase-clinopyroxene-amphibole lava, 1 clast of plagioclase-biotite-amphibole lava with rare clinopyroxene, and 2 clasts too small for adequate description.
R15-965-D	B	Volcaniclastic sediment, dry-sieved into weighed splits of >4 mm (29.2 g), 4–2 mm (22.8 g), and <2 mm (7.2 g), then recombined for binocular-microscope examination. Volcanic clasts include an essentially monolithologic sample with gray to red/brown mottled quartz-biotite-pyroxene Tschicoma lavas, with clusters of sieved plagioclase, in clasts up to 2 cm in size.
R15-965-D10	T	Sample of sediment R15-965-D was dry-sieved to >2 mm and ultrasonically cleaned to obtain split for thin-section preparation. Thin section contains 9 volcanic clasts, one 2 mm grain of unstrained quartz, and one 4 mm grain of sieved feldspar. Volcanic clasts include 4 clasts of plagioclase-clinopyroxene-orthopyroxene lava, 1 clast of plagioclase-clinopyroxene-orthopyroxene-biotite-quartz lava, 1 clast of clinopyroxene-orthopyroxene-amphibole-quartz lava, 1 clast of amphibole-clinopyroxene lava, 1 clast of plagioclase-clinopyroxene-orthopyroxene-quartz lava with strongly sieved plagioclase phenocrysts, and 1 clast of plagioclase-clinopyroxene-orthopyroxene-quartz lava with acicular pyroxenes.
R15-979-D	B	Volcaniclastic sediment, dry-sieved into weighed splits of >4 mm (12.0 g), 4–2 mm (21.5 g), and <2 mm (16.2 g), then recombined for binocular-microscope examination. Volcanic clasts (up to 1 cm in size) are dispersed in sand to fine gravel; clasts include dark black non-vesicular olivine basalt and red amphibole-biotite intermediate-composition lavas.
R15-979-D10	T	Sample of sediment R15-979-D was dry-sieved to >2 mm and ultrasonically cleaned to obtain split for thin-section preparation. Thin section contains 14 volcanic clasts including 4 clasts of plagioclase-amphibole-clinopyroxene lava, 3 clasts of vitric tephra consisting of aphyric pumice of 1.5 mm in a fine ash matrix and angular grains of quartz-plagioclase-sanidine with altered mafics, 2 aphyric vitric pumices, 2 clasts of altered plagioclase-clinopyroxene lava with mottled clay, 1 clast of extensively altered plagioclase-clinopyroxene lava, 1 dense devitrified pumice with quartz-sanidine-plagioclase phenocrysts, and 1 clast of olivine-clinopyroxene intergranular basalt.
R15-1009	B	Tephra layer, monolithologic, of aphyric vitric white rhyolitic pumice up to 2–3 mm in size. Pumices have thin coatings of pale-brown clay and are somewhat rounded.
R15-1009-PU	T	Thin section contains 11 fragments of vitric aphyric pumice. Pumices are nonwelded with very sparse clay alteration. Minute trace minerals include quartz, clinopyroxene, and hematite.
R15-1037-D	B	Volcaniclastic sediment, dry-sieved into weighed splits of >4 mm (2.2 g), 4–2 mm (2.9 g), and <2 mm (19.3 g), then recombined for binocular-microscope examination. Volcanic clasts (up to 3 cm in size) are dispersed in abundant sand; clasts include dark black non-vesicular olivine basalt, gray/red mottled amphibole-plagioclase intermediate-composition lavas, and rhyolitic lavas.
R15-1037-D10	T	Sample of sediment R15-1037-D was dry-sieved to >2 mm and ultrasonically cleaned to obtain split for thin-section preparation. Thin section contains 9 volcanic clasts including 2 clasts of altered red plagioclase-clinopyroxene-orthopyroxene lava, 2 clasts of porous vesicular pumice with rare sanidine, 1 extensively altered porous (50% porosity) volcanic rock with sparse clinopyroxene and plagioclase microphenocrysts, 1 clast of plagioclase-clinopyroxene-orthopyroxene-quartz lava with rounded xenocrysts of strained quartzite and of microcline, 1 dense vitric aphyric pumice with very rare sanidine microphenocrysts, 1 clast of plagioclase-quartz lava with extensive clay-silica alteration, and 1 clast of trachytic lava with feldspars in a porous matrix.

Sample No.	Description*	Discussion
R15-1067	B	Tephra layer, monolithologic, of aphyric vitric white rhyolitic pumice up to 0.5 cm in size. Pumices have thin coatings of pale-brown clay and are somewhat rounded. Pumices are dense, with only modest vesicularity.
R15-1067-PU	T	Thin section contains 7 fragments of vitric sparsely-porphyritic pumice (~3% microphenocrysts). Pumices are nonwelded with microphenocrysts of quartz-plagioclase-sanidine-biotite-magnetite.
R15-1099-D	B	Volcaniclastic sediment, dry-sieved into weighed splits of >4 mm (1.5 g), 4–2 mm (3.2 g), and <2 mm (17.0 g), then recombined for binocular-microscope examination. Coarse sand with few clasts larger than 0.5 cm; rare clasts include gray/pink flow-banded rhyolite, gray rhyolites, and red pyroxene-dacite.
R15-1099-D10	T	<p>Sample of sediment R15-1099-D was dry-sieved to >2 mm and ultrasonically cleaned to obtain split for thin-section preparation. Thin section contains 20 fragments of volcanic lithologies and adhering or separate sandstones. Lithologies may be separated into unaltered volcanic clasts, altered volcanic clasts, and sandstones.</p> <p>Unaltered volcanic clasts (12 clasts): 2 clasts of quartz-sanidine-plagioclase vitric lava, 2 clasts of aphyric vesicular vitric pumice with trace plagioclase-pyroxene-biotite, 2 clasts of plagioclase-clinopyroxene-amphibole-biotite lava with sandstone coating, 2 clasts of plagioclase-rich lava with altered ferromagnesian remnants, 1 clast of plagioclase-clinopyroxene-orthopyroxene lava, 1 clast of plagioclase-clinopyroxene-amphibole-biotite lava, 1 vitric biotite-porphyritic vesicular pumice, and 1 clast of plagioclase-porphyritic yellow vitric lava.</p> <p>Altered volcanic clasts (6 clasts): 4 clasts of volcanic lithology with plumose argillic-feldspathic alteration and rare remnant plagioclase and quartz phenocrysts, 1 clast of brown silicified lava with radial-fabric chalcedony and remnant quartz phenocrysts, and 1 clast of extensively chloritized lava with possible pseudomorphs after pyroxene.</p> <p>Sandstones (2 clasts); 2 clasts of sandstone, one containing sand grains of quartz-plagioclase-olivine and glass shards in a pale-brown clay matrix and the other containing sand grains of quartz-plagioclase-amphibole-clinopyroxene-olivine and fine-grained intermediate volcanic lithologies in a dark clay matrix.</p>
R15-1103-D	B	Volcaniclastic sediment, dry-sieved into weighed splits of >4 mm (10.7 g), 4–2 mm (8.7 g), and <2 mm (27.6 g), then recombined for binocular-microscope examination. Highly rounded 1-cm clasts of dacite and quartzite (10%) in sands that include a component of rose quartz. Sample includes small light-brown clay bodies a few mm in diameter.
R15-1103-D10	T	Sample of sediment R15-1103-D was dry-sieved to >2 mm and ultrasonically cleaned to obtain split for thin-section preparation. Thin section contains 11 clasts, 2 of which are granitic and 9 of which are volcanic. The 2 granitic clasts are quartz-albite-microcline-muscovite granites with strained quartz and muscovite-laced plagioclase. The volcanic lithologies include 2 clasts of devitrified flow-banded lava with trace feldspar and biotite, 2 clasts of plagioclase-porphyritic lava with saccharoidal devitrified matrix, 2 clasts of crystal-rich plagioclase-clinopyroxene-amphibole-magnetite lava with prominent yellow to green/brown pleochroic amphiboles, 1 clast of plagioclase-clinopyroxene-biotite lava, 1 clast of plagioclase-clinopyroxene-amphibole-biotite-magnetite lava, and 1 clast of plagioclase-amphibole microporphyritic vitric lava with ~80% yellow perlitic glass matrix.

* B = description under binocular microscope and T = thin section narratives.

Appendix C

Moisture and Matric-Potential Results

Sample ID*	Upper Depth (ft)	Lower Depth (ft)	Geologic Unit	Gravimetric Moisture (%)	Activity (H ₂ O)	Temperature (°C)	Matric Potential (cm)
R15-2	1.7	2	Alluvium	7.11	1.001	25.90	7.03E+02
R15-5	4.7	5	Alluvium	6.62	0.997	26.11	-4.23E+03
R15-17	16.7	17	Tshirege Qbt 1g	4.76	0.982	26.12	-2.55E+04
R15-22	21.7	22	Tshirege Qbt 1g	9.42	0.989	26.22	-1.63E+04
R15-25.5	25.3	25.5	Tshirege Qbt 1g	15.77	0.988	26.35	-1.70E+04
R15-32	31.7	32	Tshirege Qbt 1g	9.31	0.991	26.43	-1.34E+04
R15-39.5	39.3	39.5	Tshirege Qbt 1g	6.49	0.994	26.49	-9.18E+03
R15-44.5	44.3	44.5	Tshirege Qbt 1g	7.83	0.998	26.53	-3.53E+03
R15-49.5	49.3	49.5	Tshirege Qbt 1g	9.64	0.998	26.48	-3.52E+03
R15-54.5	54.3	54.5	Tshirege Qbt 1g	11.59	1.000	26.62	-7.05E+02
R15-59.5	59.3	59.5	Tshirege Qbt 1g	16.94	1.000	26.12	0.00E+00
R15-64.5	64.3	64.5	Tshirege Qbt 1g	23.29	1.001	26.40	1.41E+03
R15-67	66.7	67	Cerro Toledo	31.06	1.001	26.44	1.41E+03
R15-69.5	69.3	69.5	Cerro Toledo	27.97	1.001	26.59	1.41E+03
R15-74.5	74.3	74.5	Cerro Toledo Pumice Fall	38.48	1.001	26.70	1.41E+03
R15-79.5	79.3	79.5	Cerro Toledo	11.49	1.001	26.68	1.41E+03
R15-84.5	84.3	84.5	Cerro Toledo	15.05	1.002	26.74	2.11E+03
R15-86.1	86	86.1	Cerro Toledo	25.23	1.001	26.79	1.41E+03
R15-87.5	87.4	87.5	Cerro Toledo	47.78	1.002	26.83	2.11E+03
R15-89.5	89.3	89.5	Cerro Toledo	38.01	1.002	26.79	2.82E+03
R15-94.5	94.3	94.5	Cerro Toledo	20.49	1.001	26.83	1.41E+03
R15-99.5	99.3	99.5	Cerro Toledo	19.07	1.001	26.83	7.05E+02
R15-104.5	104.3	104.5	Cerro Toledo	11.18	1.002	26.79	2.82E+03
R15-109.5	109.3	109.5	Cerro Toledo	15.48	1.003	25.48	3.50E+03
R15-114.5	114.3	114.5	Cerro Toledo	9.83	1.001	25.83	1.40E+03
R15-119.5	119.3	119.5	Cerro Toledo	14.17	1.000	25.82	-7.03E+02
R15-124.5	124.3	124.5	Otowi Member	18.16	1.001	25.83	7.02E+02
R15-129.5	129.3	129.5	Otowi Member	16.85	1.000	25.89	0.00E+00
R15-134.5	134.3	134.5	Otowi Member	16.96	1.000	25.89	-7.03E+02
R15-139.5	139.3	139.5	Otowi Member	17.93	1.000	25.95	-7.03E+02
R15-144.5	144.3	144.5	Otowi Member	19.06	1.001	25.90	1.40E+03
R15-149.5	149.3	149.5	Otowi Member	14.29	1.000	25.97	0.00E+00
R15-154.5	154.3	154.5	Otowi Member	15.99	1.000	26.07	-7.03E+02
R15-159.5	159.3	159.5	Otowi Member	16.10	1.000	25.74	-7.03E+02
R15-164.5	164.3	164.5	Otowi Member	16.38	1.000	26.03	-7.03E+02
R15-169.5	169.3	169.5	Otowi Member	14.88	1.001	26.05	7.03E+02
R15-174.5	174.3	174.5	Otowi Member	15.13	1.000	26.17	-7.04E+02
R15-179.5	179.3	179.5	Otowi Member	16.71	1.000	26.23	0.00E+00
R15-184.5	184.3	184.5	Otowi Member	16.89	1.000	26.25	0.00E+00

Sample ID*	Upper Depth (ft)	Lower Depth (ft)	Geologic Unit	Gravimetric Moisture (%)	Activity (H ₂ O)	Temperature (°C)	Matric Potential (cm)
R15-189.5	189.3	189.5	Otowi Member	16.78	1.000	26.38	0.00E+00
R15-194.5	194.3	194.5	Otowi Member	17.95	1.001	26.47	7.04E+02
R15-199.5	199.3	199.5	Otowi Member	17.74	1.000	26.50	-7.04E+02
R15-204.5	204.3	204.5	Otowi Member	16.73	1.000	26.49	0.00E+00
R15-209.5	209.3	209.5	Otowi Member	17.32	1.000	26.27	-7.04E+02
R15-214.5	214.3	214.5	Otowi Member	16.72	1.001	26.34	7.04E+02
R15-219.5	219.3	219.5	Otowi Member	17.52	1.002	26.31	2.11E+03
R15-224.5	224.3	224.5	Otowi Member	16.95	1.000	26.53	0.00E+00
R15-229.5	229.3	229.5	Otowi Member	16.46	0.999	26.59	-1.41E+03
R15-234.5	234.3	234.5	Otowi Member	17.25	1.000	26.67	-7.05E+02
R15-239.5	239.3	239.5	Otowi Member	17.17	1.000	26.58	-7.05E+02
R15-244.5	244.3	244.5	Otowi Member	16.44	1.000	26.73	-7.05E+02
R15-249.8	249.5	249.8	Otowi Member	14.96	1.000	26.72	0.00E+00
R15-254.5	254.3	254.5	Otowi Member	16.64	1.000	26.79	0.00E+00
R15-259.5	259.3	259.5	Otowi Member	16.78	1.000	26.81	0.00E+00
R15-264.8	264.5	264.8	Otowi Member	15.50	0.999	26.76	-1.41E+03
R15-269.5	269.3	269.5	Otowi Member	16.08	1.001	26.77	7.05E+02
R15-274.5	274.3	274.5	Otowi Member	16.03	0.999	26.80	-1.41E+03
R15-279.5	279.3	279.5	Otowi Member	17.71	1.000	26.80	0.00E+00
R15-284.5	284.3	284.5	Otowi Member	18.25	1.001	26.67	1.41E+03
R15-289.5	289.3	289.5	Otowi Member	18.86	1.001	26.75	1.41E+03
R15-294.5	294.3	294.5	Otowi Member	18.98	1.000	26.90	0.00E+00
R15-299.5	299.3	299.5	Otowi Member	18.62	1.001	26.82	7.05E+02
R15-304.5	304.3	304.5	Otowi Member	18.62	1.000	26.87	0.00E+00
R15-309.5	309.3	309.5	Otowi Member	18.69	1.000	25.60	0.00E+00
R15-314.5	314.3	314.5	Otowi Member	19.48	1.001	25.90	7.03E+02
R15-319.5	319.3	319.5	Otowi Member	19.67	1.001	26.06	7.03E+02
R15-324.5	324.3	324.5	Otowi Member	17.89	1.001	26.06	1.41E+03
R15-329.5	329.3	329.5	Otowi Member	19.79	1.002	26.11	2.11E+03
R15-334.5	334.3	334.5	Otowi Member	17.19	1.001	26.25	7.03E+02
R15-339.5	339.3	339.5	Otowi Member	14.46	0.999	26.27	-1.41E+03
R15-344.5	344.3	344.5	Otowi Member	19.71	1.001	26.36	7.04E+02
R15-349.5	349.3	349.5	Otowi Member	17.29	1.000	26.40	0.00E+00
R15-354.5	354.3	354.5	Otowi Member	19.27	1.000	26.34	0.00E+00
R15-359.5	359.3	359.5	Otowi Member	17.34	1.001	26.14	7.03E+02
R15-364.5	364.3	364.5	Otowi Member	19.46	1.001	26.36	7.04E+02
R15-369.5	369.3	369.5	Otowi Member	22.46	1.001	26.28	1.41E+03
R15-374.5	374.3	374.5	Otowi Member	22.33	1.001	26.36	7.04E+02
R15-379.5	379.3	379.5	Otowi Member	19.58	1.001	26.42	7.04E+02

Sample ID*	Upper Depth (ft)	Lower Depth (ft)	Geologic Unit	Gravimetric Moisture (%)	Activity (H ₂ O)	Temperature (°C)	Matric Potential (cm)
R15-384.5	384.3	384.5	Otowi Member	17.73	1.002	26.23	2.11E+03
R15-389.5	389.3	389.5	Otowi Member	18.91	1.002	24.27	2.79E+03
R15-394.2	394	394.2	Otowi Member	19.49	1.003	24.31	3.72E+03
R15-399.6	399.4	399.6	Otowi Member	19.13	1.001	24.51	6.99E+02
R15-404.2	404	404.2	Otowi Member	19.87	1.001	24.62	1.40E+03
R15-409.6	409.4	409.6	Otowi Member	19.85	1.001	24.58	6.99E+02
R15-414.2	414	414.2	Otowi Member	20.08	1.002	24.56	2.10E+03
R15-419.2	419	419.2	Otowi Member	20.23	1.002	24.50	2.10E+03

*See Appendix A, "Hydrologic Property," sample ID numbers (CAMO-9x-xxxx).